


Fall 12-2017

Water Chemistry Dynamics in Four Vernal Pools in Maine, USA

Lydia H. Kifner

University of Maine, lydia.kifner@maine.edu

Follow this and additional works at: <https://digitalcommons.library.umaine.edu/etd>

 Part of the [Biochemistry Commons](#), [Environmental Chemistry Commons](#), [Environmental Engineering Commons](#), [Natural Resources and Conservation Commons](#), and the [Water Resource Management Commons](#)

Recommended Citation

Kifner, Lydia H., "Water Chemistry Dynamics in Four Vernal Pools in Maine, USA" (2017). *Electronic Theses and Dissertations*. 2802.
<https://digitalcommons.library.umaine.edu/etd/2802>

This Open-Access Thesis is brought to you for free and open access by DigitalCommons@UMaine. It has been accepted for inclusion in Electronic Theses and Dissertations by an authorized administrator of DigitalCommons@UMaine. For more information, please contact um.library.technical.services@maine.edu.

**WATER CHEMISTRY DYNAMICS IN FOUR
VERNAL POOLS IN MAINE, USA**

By

Lydia Kifner

B.S. University of New Mexico, 2015

A THESIS

Submitted in Partial Fulfillment of the

Requirements for the Degree of

Master of Science

(in Civil Engineering)

The Graduate School

The University of Maine

December 2017

Advisory Committee:

Aria Amirbahman, Professor of Civil and Environmental Engineering, Co-
Advisor

Aram Calhoun, Professor of Wetland Ecology. Co-Advisor

Stephen Norton, Professor Emeritus of Earth and Climate Sciences

Copyright 2017 Lydia Kifner

WATER CHEMISTRY DYNAMICS IN FOUR VERNAL POOLS IN MAINE, USA

By Lydia Kifner

Thesis Co-Advisors: Dr. Aria Amirbahman & Dr. Aram Calhoun

An Abstract of the Thesis Presented
in Partial Fulfillment of the Requirements for the
Degree of Master of Science
(in Civil Engineering)

December 2017

Vernal pools are small seasonal wetlands that are a common landscape feature that contribute to biodiversity in northeastern North American forests. However, even basic information about their biogeochemical functions, such as carbon cycling, is limited. Dissolved gas concentrations (CH_4 , CO_2) and other water chemistry parameters were monitored weekly at the bottom and surface of four vernal pools in central and eastern Maine, USA, from April to August 2016. The vernal pools were supersaturated with respect to CH_4 and CO_2 at all sampling dates and locations. Concentrations of dissolved CH_4 and CO_2 ranged from 0.4 to $2.1 \times 10^2 \mu\text{mol L}^{-1}$ and 72 to $2.3 \times 10^3 \mu\text{mol L}^{-1}$, respectively. Evaporative fluxes of CH_4 and CO_2 into the atmosphere ranged from 0.2 to $73 \text{ mmol m}^{-2} \text{ d}^{-1}$, and 30 to $5.9 \times 10^2 \text{ mmol m}^{-2} \text{ d}^{-1}$, respectively. During the study period, the vernal pools emitted between 0.1 to 5.8 kgC m^{-2} and 9.6 to $1.2 \times 10^2 \text{ kgC m}^{-2}$ of CH_4 and CO_2 , respectively. This is a carbon export of up to $2.4 \times 10^2 \text{ kgC}$, which is less than the estimated carbon leaf litter input. The production rates of CH_4 and CO_2 ranged from 2.4×10^{-2} to 6.6×10^{-1} and 4.0×10^{-1} to $4.6 \text{ gC m}^{-2} \text{ d}^{-1}$, respectively, and increased significantly over the season. Concentrations of CH_4 and CO_2 covaried with alkalinity, temperature, and dissolved oxygen. Our study pools were characterized by large

concentrations and effluxes of CH₄ and CO₂ with respect to other permanently inundated wetlands, indicating vernal pools may be important contributors to the global carbon budget and are metabolically active sites.

In addition to dissolved gas concentrations, temperature, dissolved oxygen, pH, ortho-P, NO₃⁻, NH₄⁺, Cl⁻, SO₄²⁻, Na⁺, K⁺, Mg²⁺, Ca²⁺, DOC, alkalinity, chlorophyll *a*, speciated Al, speciated Fe, speciated Mn, and speciated Si were monitored from April to August 2016 to establish general temporal trends in pool biogeochemistry. The pH in the vernal pools generally decreased over the study period. Dissolved oxygen concentrations fluctuated throughout the season but were generally lower in benthic samples than in surface. The nutrients ortho-P and NH₄⁺ increased over the study period. Concentrations of NO₃⁻ were low throughout the study period, indicating denitrification was occurring. Dissolved organic carbon concentrations and alkalinity both increased over the study period. Concentrations of Cl⁻, and Na⁺ decreased over the season. Concentrations of K⁺ increased over the season. Concentrations of the metals Al, Fe, and Mn increased over the study period. The pools in this study are diverse in their biogeochemistry, but do exhibit trends in their aquatic chemistry during the open water season. These data can be used as a jumping off point for future studies on vernal pool biogeochemistry.

ACKNOWLEDGEMENTS

This research was funded by a National Science Foundation Coupled Natural Human Systems (CNH) grant #1313627 to Aram Calhoun et al., and by a Maine Space Grant Consortium Graduate Research Fellowship. We thank the CNH team, Carly Eakin, Kaci Fitzgibbon, Elizabeth Gorse, Thomas Hastings, Kristine Hoffmann, Jared Homola, Malcolm Hunter, Abigail Kaminski, Gregory McDonald, Anthony Pawlicki, Kelli Straka, Andy Reeve, and Sudheera Yaparante for help in the field, laboratory, friendly advice, and use of unpublished data.

TABLE OF CONTENTS

ACKNOWLEDGEMENTS	iii
LIST OF TABLES	vi
LIST OF FIGURES	viii
LIST OF EQUATIONS	x
CHAPTER 1 METHANE AND CARBON DIOXIDE FLUX WITHIN FOUR VERNAL POOLS IN ME, USA	1
1.1. Introduction.....	1
1.2. Methods.....	5
1.2.1. Study Area	5
1.2.2. Field Methods	8
1.2.3. Gas Flux Calculations.....	11
1.2.4. Net Production Calculations	12
1.2.5. Statistical Analysis.....	13
1.3. Results.....	14
1.3.1. Pool Chemistry	14
1.3.2. Greenhouse Gas Concentrations and Fluxes.....	17
1.3.3. Covariates of CH ₄ and CO ₂	18
1.3.4. Net Production of CH ₄ and CO ₂	23
1.4. Discussion	32
1.4.1. CH ₄ and CO ₂ Concentrations and Fluxes	32
1.4.2. Covariates of CH ₄ and CO ₂	35

1.4.3. Net Production of CH ₄ and CO ₂	38
1.4.4. The Role of Vernal Pools in Carbon Cycling	39
REFERENCES	42
APPENDIX A CH ₄ AND CO ₂	50
APPENDIX B TEMPORAL TRENDS IN WATER CHEMISTRY FOR FOUR VERNAL POOLS IN ME, USA	61
BIOGRAPHY OF THE AUTHOR.....	93

LIST OF TABLES

Table 1.1.	Geologic, forest, and hydrologic characteristics for four Maine vernal pools	7
Table 1.2.	Chemical characteristics for four Maine vernal pools.....	16
Table 1.3.	Pearson correlation coefficients between CH ₄ and CO ₂ flux and environmental variables.....	19
Table 1.4.	Multiple linear regression models for CH ₄ concentration.....	21
Table 1.5.	Linear mixed effect models for CH ₄ concentrations.....	21
Table 1.6.	Multiple linear regression models for CO ₂ concentration.....	21
Table 1.7.	Linear mixed effect models for CO ₂ concentrations.....	22
Table 1.8.	Mass accumulation, groundwater output, evaporative flux, net production, and zero order rates of CH ₄ and CO ₂	25
Table 1.9.	Reported surface water CH ₄ and CO ₂ concentrations and emissions for a selection of ponds, wetlands, and lakes.....	31
Table A.1.1.	Methane flux.....	50
Table A.1.2.	Carbon dioxide flux.....	52
Table A.1.3.	Net production of CH ₄ in P1.....	54
Table A.1.4.	Net production of CO ₂ in P1.....	54
Table A.1.5.	Net production of CH ₄ in P2.....	55
Table A.1.6.	Net production of CO ₂ in P2.....	56
Table A.1.7.	Net production of CH ₄ in P3.....	57
Table A.1.8.	Net production of CO ₂ in P3.....	58

Table A.1.9. Net production of CH ₄ in P4.....	59
Table A.1.10. Net production of CO ₂ in P4.....	60

LIST OF FIGURES

Figure 1.1.	Location of study area and vernal pool locations in Maine, USA.....	6
Figure 1.2.	CH ₄ average concentrations, fluxes, net production, and net production rates in 4 pools.....	26
Figure 1.3.	CO ₂ average concentrations, fluxes, net production, and net production rates in 4 pools.....	27
Figure 1.4.	Time-series of CH ₄ average concentrations, fluxes, net production, and net production rates in 4 pools.....	28
Figure 1.5.	Time-series of CO ₂ average concentrations, fluxes, net production, and net production rates in 4 pools.....	29
Figure 1.6.	Relationship between time and CH ₄ average concentrations, fluxes, net production, and net production rates in 4 pools.....	30
Figure 1.7.	Relationship between time and CO ₂ average concentrations, fluxes, net production, and net production rates in 4 pools.....	31
Figure B.2.1.	Surface temperature in four vernal pools.....	66
Figure B.2.2.	Dissolve oxygen concentrations in four vernal pools.....	67
Figure B.2.3.	The pH in four vernal pools.....	68
Figure B.2.4.	Ortho-P concentrations in four vernal pools.....	69
Figure B.2.5.	Nitrate concentrations in four vernal pools.....	70
Figure B.2.6.	Ammonium concentrations in four vernal pools.....	71
Figure B.2.7.	Chloride concentrations in four vernal pools.....	72
Figure B.2.8.	Sulfate concentrations in four vernal pools.....	73
Figure B.2.9.	Sodium concentrations in four vernal pools.....	74

Figure B.2.10. Potassium concentrations in four vernal pools.....	75
Figure B.2.11. Magnesium concentrations in four vernal pools.....	76
Figure B.2.12. Calcium concentrations in four vernal pools.....	77
Figure B.2.13. Dissolved organic carbon concentrations in four vernal pools.....	78
Figure B.2.14. Alkalinity in four vernal pools.....	79
Figure B.2.15. Chlorophyll <i>a</i> concentrations in four vernal pools.....	80
Figure B.2.16. Concentrations of total Al in four vernal pools	81
Figure B.2.17. Concentrations of organically bound Al in four vernal pools.....	82
Figure B.2.18. Concentrations of ionic Al in four vernal pools.....	83
Figure B.2.19. Concentrations of total Fe in four vernal pools	84
Figure B.2.20. Concentrations of organically bound Fe in four vernal pools	85
Figure B.2.21. Concentrations of ionic Fe in four vernal pools	86
Figure B.2.22. Concentrations of total Mn in four vernal pools	87
Figure B.2.23. Concentrations of organically bound Mn in four vernal pools	88
Figure B.2.24. Concentrations of ionic in four vernal pools	89
Figure B.2.25. Concentrations of total Si in four vernal pools	90
Figure B.2.26. Concentrations of organically bound Si in four vernal pools	91
Figure B.2.27. Concentrations of ionic Si in four vernal pools	92

LIST OF EQUATIONS

- Eq. 1.1. $CH_{4(gas)} \times K_H = CH_{4(aqueous)} \dots\dots\dots 11$
- Eq. 1.2. $F = k_{l,w}(C - C_s) \dots\dots\dots 11$
- Eq. 1.3. $k_{l,w} = \left(\frac{sc_i}{sc_{CO_2,20}} \right)^{-a} k_{CO_2,20} \dots\dots\dots 11$
- Eq. 1.4. $\frac{d(VC)}{dt} = Q_{in}C_{in} - Q_{out}C_{out} - R_{ef} + R_p \dots\dots\dots 12$

CHAPTER 1
METHANE AND CARBON DIOXIDE FLUX WITHIN
FOUR VERNAL POOLS IN ME, USA

1.1. Introduction

The increase in concentrations of atmospheric CH₄ and CO₂ since the Industrial Era (IPCC 2013) has highlighted the importance of understanding the global carbon budget. Inland waters release between 1.0 and 2.1 PgC of CO₂ per year, (~0.001% of total atmospheric CO₂; Cole et al. 2007; IPCC 2013; Raymond et al. 2013). Additionally, wetlands account for 20 to 25% of global methane emissions and ~75% of total natural emissions (Casper et al., 2000; Christensen et al., 2003; IPCC 2013; Mitsch et al., 2013; Whalen, 2005). Rice paddies account for an additional 6-20% of global methane emissions (Bloom et al. 2010; Whalen 2005), and reservoirs, such as those for aquaculture, water supply, and recreation account for 7% of global warming potential from anthropogenic sources (St. Louis et al. 2000).

Globally, small water bodies are estimated to comprise more surface area than large lakes; ponds and lakes < 0.01 km² constitute ~31% of total lake and pond area in the world (Downing et al. 2006), and small ponds < 0.001 km², make up ~8.6% of all freshwater surface area (Holgerson and Raymond 2016). Additionally, small water bodies have relatively large contributions of CH₄ and CO₂ emissions with respect to their size (Bastviken et al. 2004; Holgerson 2015, Holgerson and Raymond, 2016; Kankaala et al. 2013; Raymond et al. 2013). Holgerson and Raymond (2016) estimate that although

small ponds $< 0.001 \text{ km}^2$ make up $< 10\%$ of all freshwater surface area, they emit about 40% of total freshwater CH_4 and about 15% of total freshwater CO_2 . Small ponds have a large impact on global carbon emissions, but as a result of their size they can be difficult to quantify and map, and are commonly excluded from global carbon budgets (Holgerson and Raymond 2016; Tiner et al. 2015; Verpoorter et al. 2014). Temporary wetlands are a subset of small ponds that do not have permanent standing water and are often ephemeral in nature (also called seasonal wetlands, vernal pools, gilgais, or temporary pools; Calhoun et al. 2017).

Temporarily inundated wetlands have varied hydrologic regimes that result in unique wetland ecosystem functions such as increasing biodiversity by providing habitat for species adapted to waters with temporary hydroperiods (Calhoun et al. 2014; 2017; Zedler 2003). Additionally, intermittently inundated wetlands are biogeochemical hotspots for organic matter decomposition, denitrification, and water quality improvement through sediment retention and absorption of aquatic pollutants. Temporary wetlands have higher rates of these biogeochemical processes compared to adjacent upland ecosystems, primarily because they have disproportionately large wetland edges with respect to their size, which enhance the rate of biogeochemical transformations (Calhoun et al. 2017; Capps et al. 2014; Marton et al. 2015; McLain et al. 2003). Water table fluctuations in temporary wetlands stimulate microbial activity, resulting in faster mineralization of organic matter (Corstanje and Reddy 2004; Rezanezhad et al. 2014). Although they are difficult to quantify and map, temporary wetlands are a common wetland globally (Calhoun et al. 2017).

In glaciated northeastern North America, vernal pools are a type of temporary, ephemeral wetland, which are relatively small (generally < 0.002 km²; Calhoun et al. 2003). They occur in forested landscapes and range from open water wetlands to forested wetlands (Campbell Grant 2005; Zedler 2003). Reported densities in New England range from 0.1 to 49.5 pools per km² (Brooks et al. 1998; Calhoun et al. 2003; Faccio et al. 2013). Based on these densities, and using an average size of 0.001 km², vernal pools could comprise up to 4,536 km² of the area in the State of Maine. This is approximately 39% of the 11,750 km² of surface water, and approximately 5% of the total Maine area of 91,633 km² (United States Geological Survey, 2016). Vernal pools occur in a wide range of surficial glacial deposits and range in hydrogeomorphic setting from perched, precipitation-fed pools to pools strongly influenced by groundwater input and discharge (Calhoun et al. 2014; Wingham and Jordan 2003; Zedler 2003). They are typically at their highest water level in the spring, dry down by mid-summer, and re-fill in the autumn, while some dry on cycles longer than a year (Calhoun et al., 2014).

Vernal pools are amphibian breeding habitat and seasonal habitat for other wildlife. They have been widely studied as specialized breeding sites for species adapted to life in temporary waters (Colburn et al. 2007; Faccio 2003; Regosin et al. 2005; Semlitsch and Skelly 2007; Williams 1996). However, their biogeochemistry, including carbon dynamics, is not widely quantified. Carbon cycling and greenhouse gas emissions have been evaluated in peatlands, lakes, and ponds (Bastviken 2004; Holgerson and Raymond 2016; Huttunen et al. 2003; Lansdown et al. 1992; Rask et al. 2002), however, the role of seasonal wetlands, including vernal pools, in carbon dynamics is less known.

Consequently, they have been largely excluded in biogeochemical studies and global carbon emission estimates.

Capps et al. (2014) focused on decomposition and denitrification in vernal pools and found that material in seasonally flooded sections of vernal pools decomposed faster than in the surrounding upland area. The inputs and outputs of carbon from vernal pools in relation to pool hydrology were studied in Rhode Island (Ross 2017) by examining different carbon pools throughout the vernal pool basin as well as CO₂ and CH₄ flux from the soil. Saturated zones of vernal pools emit CH₄, while aerobic vernal pool environments emit CO₂ and metabolize CH₄ in the water column. The potential CH₄ and CO₂ production from Massachusetts vernal pools with wet and dry conditions were explored in a laboratory experiment (Kuhn 2015). Wetter conditions produced less organic matter content but higher potential CH₄ and CO₂ production rates than drier conditions. Additionally, the environmental predictors of CH₄ and CO₂ concentrations were studied in small temporary ponds in Connecticut, where the main environmental predictors for CH₄ and CO₂ concentrations were found to be precipitation and dissolved oxygen (DO), respectively (Holgerson 2015). These small temporary wetlands have different characteristics than large lakes, such as high terrestrial carbon content, more complete mixing, high perimeter to area ratio, and varying seasonal dynamics that may influence unique carbon cycling (Calhoun et al. 2017; Holgerson 2015).

Vernal pool carbon emissions may play a significant role in global carbon transformations, especially when considering their broad distribution across the North American landscape. Carbon cycling in vernal pools needs further study in the context of their water chemistry and surrounding ecosystem in order to understand the pools'

cumulative contributions to the global carbon budget. In this study, we examined dissolved carbon dynamics in four Maine vernal pools with different geologic substrates from ice-off until dry down in 2016. The specific objectives of this study were to (i) quantify the dissolved concentrations and diffusive fluxes of CH₄ and CO₂, (ii) identify environmental covariates of CH₄ and CO₂ emissions in vernal pools, and (iii) estimate the carbon turnover by comparing leaf litter carbon inputs to carbon emissions.

1.2. Methods

1.2.1. Study Area

We studied four vernal pools in Maine, USA (Figure 1.1.). P1 and P2 are located on the Presumpscot Formation (Table 1.1.), a low permeability glacio-marine silt/clay. P1 and P2 are in Bangor, Maine, ~200 m from surrounding areas of human activity and moderate landscape modification. P1 is in a closed canopy, dominantly deciduous forest. P2 has an open canopy, with shrubs and emergent aquatic vegetation as the dominant cover. Part of the P2 watershed was in open fields and is now regenerating to forest. P3 is located on a sand and gravel esker in a minimally modified landscape located ~100 m from a gravel road used by logging trucks. P3 is very large and so is open canopy with a mixed deciduous and coniferous forest surrounding the pool. P4 is located on thin till and is in a managed forest ~1 km from routine human activity or development, but ~10 m from a logging road. This site has closed canopy with dominantly deciduous forest cover. All sites have been logged but P1, P2, and P3 have not been cut for at least 25 years.

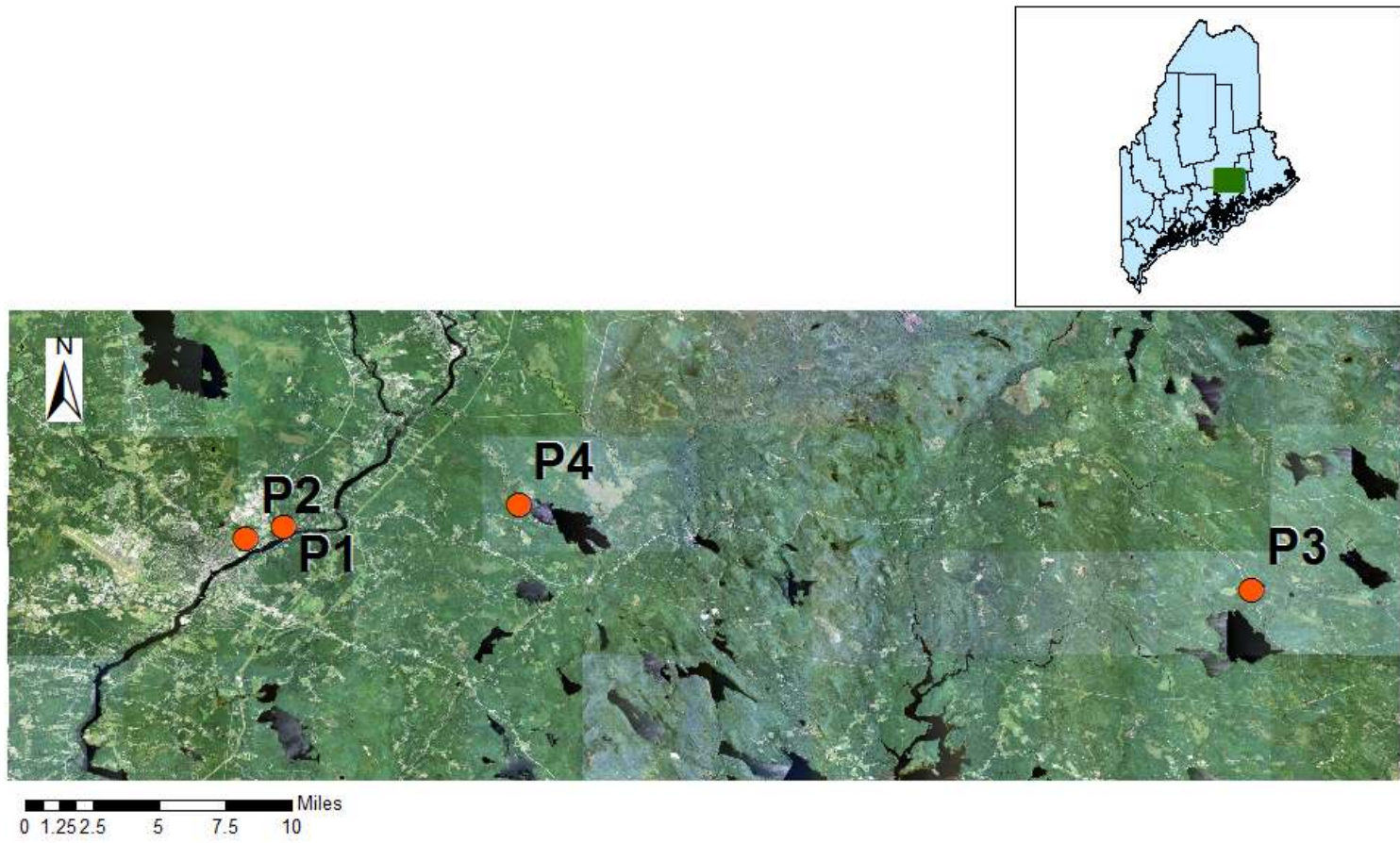


Figure 1.1. Location of study area and vernal pool locations in Maine, USA

Table 1.1. Geologic, forest, and hydrologic characteristics for four Maine vernal pools. Concentrations are reported as means with range in parentheses. Maximum surface area, maximum volume, groundwater recharge rates, and benthic temperature from Straka (2017). Groundwater recharge rate, temperature and benthic temperature are from the study period, April 2016-August 2016.

Pool	underlying geology	dominant forest type	canopy cover	dry down (Julian day)	max depth (m)	max surf area (m ²)	max vol (m ³)	groundwater recharge rate (m/s)	temp (°C)	benthic temp (°C)
P1	Presumpscot Formation	deciduous	closed	173	0.3	325	31	1.3×10 ⁻⁶ (1.1×10 ⁻⁶ – 1.5×10 ⁻⁶)	17.4 (14–22)	12.3 (8–16)
P2	Presumpscot Formation	shrub	open	216	0.3	260	58	0	21.0 (15–30)	15.7 (10–21)
P3	sand and gravel esker	mixed	open	209	1.5	2930	1930	4.6×10 ⁻⁷ (3.4×10 ⁻⁷ – 6.4×10 ⁻⁷)	20.9 (10–31)	16.7 (8–26)
P4	thin glacial till	deciduous	closed	209	0.5	510	126	2.2×10 ⁻⁷ (9.9×10 ⁻⁸ – 3.0×10 ⁻⁷)	14.3 (8–19)	11.5 (7–17)

Spring 2016 was a relatively dry year. During the study period, Bangor, ME (near P1, P2, and P4) and Osborn, ME (near to P3) received 6.1, 6.1, 9.2, and 13.2 cm of precipitation in April, May, June, and July, respectively. The 1981 to 2010 normal monthly precipitation is 9.2, 9.2, 9.6, and 8.8 cm in April, May, June, and July, respectively (National Weather Service 2017). The four pools had varying hydroperiods. In 2016, P1 had a maximum volume of 31 m³ and P2 had a maximum volume of 58 m³ (Table 1.1.). P3 was the largest of the pools, with an estimated maximum high water volume of 2930 m³. P4 had a maximum volume of 126 m³ (Table 1.1.; Straka, 2017). All four pools were at their greatest extent in March. P1 was dry by Julian day 173, P2 was dry by Julian day 216, and P3 and P4 were dry by Julian day 209.

1.2.2. Field Methods

Water in all pools was sampled at the deepest point, with the exception of P3, which was sampled at a depth of 1.25 m until later in the season when the deepest section was more accessible. Sampling locations were marked with a stake. Two lengths of Tygon™ tubing were attached to each stake, one fixed at ~5 cm from the bottom sediment of the pool, and one floating ~5 cm below the water surface. The floating tube was attached to a fishing bobber so that the tube inlet would fluctuate with the water level. These two tubes allowed for sampling of benthic and surface waters of the pools. Water was sampled through the tubes using a hand held vacuum pump to avoid disturbing the pool sediments and water chemistry. Sample tubing was purged of any sitting water prior to taking samples for analysis.

We collected samples from each pool at minimum every 10 days from ice-out in late April until the pools dried completely in June or July. Aqueous samples for dissolved

carbon dioxide (CO₂), dissolved methane (CH₄), and dissolved nitrous oxide (N₂O) were collected every week. Additional samples collected included chlorophyll *a* (chl *a*), dissolved organic carbon (DOC), sulfate (SO₄²⁻), dissolved oxygen (DO), ortho-phosphate (ortho-P), nitrate (NO₃⁻), ammonium (NH₄⁺), closed cell pH, and alkalinity. Samples from each pool were taken at approximately the same time of day to minimize variation caused by diurnal fluctuations. Immediately after collection, all samples were placed on ice in the dark prior to laboratory analysis.

We collected aqueous samples for CH₄, CO₂ and N₂O directly from the tubing into a 60 mL syringe to prevent atmospheric air contamination. We extracted gases by injecting 30 mL of helium (He) gas into 30 mL of each water sample and shaking the sample vigorously for 5 min. The gas was then injected into a 25 mL crimp-sealed gas vial that had been previously flushed with He and then evacuated. We analyzed gas samples using gas chromatography on a Shimadzu GC-2014 with CTC AOC-5000 autoinjector and three detectors (FID, ECD, TCD) at the University of New Hampshire Water Quality Analysis Laboratory.

We sampled dissolved oxygen (DO) directly from the tubing with a 100 mL syringe preventing air contact. The 100 mL DO sample was transferred into a 60 mL BOD bottle via a tube that extended to the bottom of the bottle. We measured DO using a YSI 5100 Dissolved Oxygen Meter the same day as sample collection. We also sampled pH directly from the tubing using a 60 mL syringe. These samples were measured by passing them through a Cole-Parmer 800 µL closed flow-through cell equipped with a Cole-Parmer combination, double junction pH electrode.

We collected ortho-P, NO_3^- and NH_4^+ sampled in 50 mL centrifuge tubes. All were filtered through a 0.45 μm membrane (Whatman Puradisc 0.45 μm polypropylene). Samples were analyzed at the Analytical Laboratory and Maine Soil Testing Service at the University of Maine. Ortho-P concentration was determined by colorimetric ascorbic acid method using ammonium molybdate and potassium antimonyl tartrate (O'Dell 1993). NO_3^- concentration was analyzed conductimetrically by ion chromatography (Dionex 2000i Ion Chromatograph). NH_4^+ concentration was determined colorimetrically by ion analyzer using the hypochlorite/salicylate method (Eaton et al. 1995).

We collected alkalinity samples in 125 mL Nalgene bottles and analyzed them using the Inflection Point method. Samples for chl *a* were collected in 125mL glass amber bottles, filtered through a glass fiber pre-filter (Sartorius, 13400 grade) and frozen until analysis by hot ethanol extraction followed by spectrophotometric analysis (Thermo Scientific Genesys 10UV).

We filtered samples for SO_4^{2-} and DOC (Whatman Puradisc 0.45 μm polypropylene filters) into 60 mL Nalgene™ bottles. SO_4^{2-} was analyzed using ion chromatography (Dionex ICS1100), and DOC by high temperature catalytic combustion with NDIR detection (Shimadzu TOC-L and NM-1 with ASI-L Autosampler). SO_4^{2-} , DOC, alkalinity and chl *a* were analyzed at the University of New Hampshire Water Quality Analysis Laboratory.

Hydrologic data were provided by Straka (2017). Precipitation data were collected from NOAA radar data (National Weather Service 2017). Precipitation for the two weeks preceding the sampling day was considered.

1.2.3. Gas Flux Calculations

We calculated dissolved gas concentrations in the samples by summing the extracted gas concentration in He and the residual dissolved gas following extraction; the latter value was calculated using Henry's Law:

$$CH_{4(gas)} \times K_H = CH_{4(aqueous)} \quad \text{Eq. 1.1}$$

where K_H is Henry's constant (Weisenberg and Guinasso, 1979; Weiss, 1974) and was temperature adjusted.

The dissolved gas concentrations immediately below the water surface were then used to calculate the evaporative flux to the atmosphere:

$$F = k_{l,w}(C - C_s) \quad \text{Eq. 1.2.}$$

where F is the flux ($\text{mol L}^{-1} \text{d}^{-1}$), $k_{l,w}$ is the mass transfer velocity across the water boundary layer (m d^{-1}), C is the gas concentration (mol L^{-1}) in the surface water sample, and C_s is the saturation gas concentration (mol L^{-1}) calculated using Henry's Law with the atmospheric partial pressures (National Weather Service 2017) and the K_H values for the ambient water temperature (Weisenberg and Guinasso, 1979; Weiss, 1974). $k_{l,w}$ was calculated using the equation (Schwarzenbach et al. 2003):

$$k_{l,w} = \left(\frac{Sc_i}{Sc_{CO_2,20}} \right)^{-a} k_{CO_2,20} \quad \text{Eq. 1.3.}$$

where Sc_i , the dimensionless Schmidt number, is the ratio of the water kinematic viscosity to the diffusion coefficient of a gas in water, both of which vary directly with temperature; a is the constant that varies with wind velocity and is equal to 0.67 for a smooth water surface; and $Sc_{CO_2,20}$ and $k_{CO_2,20}$ are the Schmidt number and the mass transfer velocity across the water boundary layer for CO_2 at 20 °C, respectively. A value of 0.56 m d^{-1} was used for $k_{CO_2,20}$ as the recommended value for the case where wind

velocity 10m above the surface is $< 4.2 \text{ m s}^{-1}$ (Schwarzenbach et al., 2003). We assumed the wind velocity at all four sites to be negligible, because the recorded average daily wind speed at nearby weather stations was generally $< 9.4 \text{ m s}^{-1}$ (Weather Underground 2017), and the closed canopy of the pools provided dampening of the wind. The range of $k_{l,w}$ values for CO_2 and CH_4 were $0.36\text{--}0.80 \text{ m d}^{-1}$ and $0.36\text{--}0.79 \text{ m d}^{-1}$, respectively, for a water temperature range of $8\text{--}31 \text{ }^\circ\text{C}$. Holgerson and Raymond (2016) used a $k_{l,w}$ value of 0.36 m d^{-1} to estimate CO_2 and CH_4 fluxes for pools with a surface area $< 0.001 \text{ km}^2$.

1.2.4. Net Production Calculations

We used a mass balance approach to estimate the net production of CH_4 and CO_2 in each pool over the sampling period. Equation 4 expresses mass balance for a species in water by assuming a well-mixed pool (e.g., Schnoor, 1996) and that the calculated instantaneous fluxes are representative of fluxes between consecutive samplings:

$$\frac{d(VC)}{dt} = Q_{in}C_{in} - Q_{out}C_{out} - R_{ef} + R_P \quad \text{Eq. 1.4.}$$

where V is the average pool volume between two consecutive samples; Q ($\text{m}^3 \text{ d}^{-1}$) is the flow rate of water in and out of the pool; R_{ef} (gC d^{-1}) is the mass evaporation rate of each gas into the atmosphere (obtained by multiplying the average weekly flux from Eq. 2 by the average weekly pool surface area); and R_P (gC d^{-1}) is the net mass production rate of each gas. The left hand side of Eq. 4 expresses the mass accumulated in the pool water between two consecutive sampling periods. Zero order mass production rates ($\text{gC m}^2 \text{ d}^{-1}$) were calculated by dividing R_P by the average area of the period between samplings.

In Eq. 4, the influence of overland and groundwater flow on the mass of gases carried into the pool ($Q_{in}C_{in}$) is neglected. We are assuming that the concentrations of CH_4 and CO_2 brought into the pools by groundwater are much less than the

concentrations produced in the pools. Keeley and Zedler 1996 and Rains et al. 2008 showed that groundwater does not have large influence on the hydrology of vernal pools. We are able to account for the CH₄ and CO₂ export through groundwater ($Q_{out}C_{out}$) using groundwater discharge velocities and bottom surface area data from Straka (2017). During our sampling period, P1, P3, and P4 had downflow from the vernal pool into the groundwater, but P2 did not.

1.2.5. Statistical Analysis

We log-transformed variables that were not normally distributed, such as CH₄ and CO₂ concentration, flux, net production, and production rate. Ortho-P, NH₄⁺, SO₄²⁻, DOC, surface area, depth, volume, surface temperature, benthic temperature, and chl *a* (as 1 + chl *a*) were also log transformed prior to analyses. Precipitation and alkalinity were square root-transformed. We performed linear regression and analysis of variance (R version 3.3.3, R Core Team) to examine trends and variation among pools. Methane and CO₂ concentrations were checked for autocorrelation using the timeSeries package in R (Wuertz et al. 2015), and were determined not to be autocorrelated. Multiple linear regression models were generated using the gmulti package in R (Calcagno 2013). Response variables were assessed for collinearity using $r > 0.35$ or < -0.35 as a disqualifier; if variables were collinear, they were selected based on simple linear regression models and by previous findings in the literature (Badiou et al. 2011; Bastviken et al. 2004; Holgerson 2015; Pennock et al. 2010; Rantakari and Kortelainen 2005; Roehm et al. 2009). The data were scaled using the scale() function in R. The top models with ΔAIC values ≤ 2 were selected for inclusion. Linear mixed effect models were generated using the lme4 package in R (Bates et al. 2014), using pool as a random

effect for further examination of the significant response variables. We used the MuMIn package (Barton 2016) package to estimate marginal (associated with fixed effects) and conditional (associated with fixed and random effects) R^2 values (Nakagawa and Schielzeth 2013). Significance was considered to be $p \leq 0.05$.

1.3. Results

1.3.1. Pool Chemistry

The water chemistry of the four vernal pools in this study varied throughout the season and among pools (Table 1.2). Benthic water temperature in the four pools ranged from 6.6 to 26.1°C (Straka 2017), and surface water temperature ranged from 8 to 31°C. The temperature increased in benthic ($R^2 = 0.65$, $p < 0.001$) and surface water ($R^2 = 0.39$, $p < 0.001$) samples over the season. There were significant differences in benthic ($p < 0.001$) and surface temperatures ($p < 0.001$) among pools. The pH of the four pools ranged from 4.4 to 6.0, and decreased from April to August ($R^2 = 0.17$, $p < 0.001$), and varied significantly among the four pools ($p < 0.001$). The DO concentrations ranged from 0.6 to 10.3 mg L⁻¹, with a mean of 4.85 ± 0.26 mg L⁻¹. The DO concentrations among pools were significantly different ($p < 0.001$), as well as the concentrations between benthic and surface samples ($p < 0.001$), with the benthic samples almost always lower than the surface samples. The chl *a* concentrations ranged from 0 to 189 µg L⁻¹, with a mean of 15.3 ± 31.1 µg L⁻¹, suggesting trophic level ranging from oligotrophic to hypereutrophic throughout the wet season in 2016. The chl *a* concentrations varied significantly among pools ($p < 0.001$). Nitrate concentrations were near or below the detection limit (0.002 mgN L⁻¹) for the duration of sampling. Ammonium concentrations ranged from below the

detection limit (0.02 mgN L^{-1}) to 2.9 mg L^{-1} , increased during the season ($R^2 = 0.45$, $p < 0.001$), and did not vary significantly among pools. Ortho-P concentrations ranged from below the detection limit (0.016 mg L^{-1}) to 0.76 mgP L^{-1} , increased throughout the season ($R^2 = 0.39$, $p < 0.001$), and varied significantly among pools ($p < 0.05$).

Table 1.2. Chemical characteristics for four Maine vernal pools. Samples collected April 2016-August 2016. Concentrations are reported as means with range in parentheses.

Pool	pH	DO (mg L ⁻¹)	ortho-P (µgP L ⁻¹)	NH ₄ ⁺ (µgN L ⁻¹)	SO ₄ ²⁻ (µgS L ⁻¹)	DOC (mgC L ⁻¹)	alk (µeq L ⁻¹)	chl <i>a</i> (µg L ⁻¹)
P1	5.1	2.3	54.1	130.1	1113.7	13.4	88.6	10.3
benthic	(4.8–5.4)	(0.6–4.1)	(18–85)	(1–631)	(25–4933)	(89–20)	(37–169)	(0–35)
P1	5.1	3.8	40.5	31.0	1225	13.0	65.5	12.6
surface	(4.8–5.3)	(2.9–4.9)	(15–62)	(1–62)	(45–4989)	(8–20)	(36–90)	(0–43)
P2	5.2	4.6	38.6	44.4	64.6	20.9	172.3	4.4
benthic	(4.9–5.9)	(0.7–7.3)	(15–107)	(4–222)	(12–171)	(14–29)	(56–296)	(0–20)
P2	5.3	6.7	38.1	58.6	61.8	20.6	170.6	2.9
surface	(4.9–5.9)	(3.6–10.3)	(11–121)	(11–314)	(9–181)	(13–29)	(99–261)	(0–8)
P3	4.9	5.8	121.5	345.1	187.0	12.7	83.7	38.0
benthic	(4.6–5.5)	(1.2–10.2)	(8–757)	(16–2944)	(28–330)	(6–20)	(23–339)	(0–190)
P3	4.9	7.0	109.9	296.5	170.0	14.1	71.2	42.3
surface	(4.4–5.7)	(3.3–10.2)	(9–229)	(6–882)	(64–298)	(6–29)	(24–328)	(1–176)
P4	5.0	2.4	96.1	121.7	209.5	33.0	357.2	8.3
benthic	(4.4–5.7)	(0.8–8.5)	(12–201)	(8–469)	(36–488)	(16–148)	(235–482)	(0–29)
P4	5.3	4.4	73.3	99.6	244.5	19.3	271.5	4.5
surface	(4.6–6.0)	(1.1–8.9)	(10–189)	(9–434)	(69–377)	(10–28)	(212–333)	(0–17)

1.3.2. Greenhouse Gas Concentrations and Fluxes

Dissolved CH₄ concentrations ranged from 3.9×10^{-7} to 2.1×10^{-4} mol L⁻¹, with an overall mean of $2.7 \times 10^{-5} \pm 4.6 \times 10^{-6}$ mol L⁻¹ (Figure. 1.2.). Methane was highly supersaturated, with 75% of the samples > 787-fold, and 25% > 5,394-fold. There were significant variations in dissolved CH₄ concentrations among sites ($p < 0.05$). The CH₄ concentrations had a weak but significant, positive relationship with time ($R^2 = 0.09$, $p < 0.01$).

Dissolved CO₂ concentrations ranged from 7.2×10^{-5} to 2.3×10^{-3} mol L⁻¹, with an overall mean of $4.2 \times 10^{-4} \pm 4.2 \times 10^{-5}$ mol L⁻¹ (Figure. 1.3.). Carbon dioxide supersaturation was > 10-fold for 75% of the samples and > 25-fold for 25%. There were significant variations in dissolved CO₂ concentrations among sites ($p < 0.001$). The CO₂ concentrations had a weak but significant, positive relationship with time ($R^2 = 0.05$, $p < 0.05$).

Dissolved N₂O concentrations were near or below the detection limit (2.3×10^{-7} mol L⁻¹) at each of the four pools throughout the entire sampling period.

The evaporative CH₄ flux in all pools ranged from 2.5×10^{-1} to 73.1 mmol m⁻² d⁻¹, with a seasonal average of 10.8 ± 2.9 mmol m⁻² d⁻¹ (Figure. 1.2.). There were no significant variations in CH₄ flux among pools. The evaporative CO₂ flux in all pools ranged from 30.1 to 5.9×10^2 mmol m⁻² d⁻¹, with a seasonal average of $1.7 \times 10^2 \pm 18.6$ mmol m⁻² d⁻¹ (Figure. 1.3.). There were no significant variations in CO₂ flux among pools. The fluxes of both CH₄ and CO₂ increased over the season ($R^2 = 0.34$, $p < 0.001$; and $R^2 = 0.35$, $p < 0.001$, respectively).

1.3.3. Covariates of CH₄ and CO₂

To identify environmental covariates of carbon fluxes, multiple linear regression models were created for CH₄ and CO₂ flux. Terms were removed if they demonstrated correlation with an $|r| > 0.35$ to other inputs to the model. The final response variables used for multiple linear regression model generation in both CH₄ and CO₂ were DO, alkalinity, precipitation, chl a, and water temperature. The models selected by $\Delta AIC \leq 2$ criterion were then used for linear mixed effects models, so that the variation with respect to pool could be separated and examined.

Methane was significantly positively correlated to surface temperature, ortho-P, NH₄⁺, DOC, alkalinity, and precipitation, and significantly negatively correlated with SO₄²⁻, pool volume, surface area and depth (Table 1.3). Alkalinity + temperature was the best predictive model for CH₄ concentrations (Tables 1.4., Table 1.5.). The other top models included precipitation and chl a. Alkalinity and temperature explained 34% of the variance in CH₄ concentrations in the linear mixed effect model. Between-pool variation did not explain any additional variance in CH₄ concentrations (Table 1.5.).

Table 1.3. Pearson correlation coefficients between CH₄ and CO₂ flux and environmental variables. Significance is shown as: $p < 0.05$ *, $p < 0.01$ **, $p < 0.001$ ***.

	pH	DO	log (temp)	log (ben temp)	log (ortho-P)	log (NH ₄)	log (SO ₄)	log (DOC)	sqrt (alk)	log (1+chl a)	sqrt (precip)	log (vol)	log (SA)	log (CH ₄)	log (CO ₂)
pH	1	0.04	-0.54***	-0.62***	-0.44***	-0.40***	0.02	-0.11	0.25	-0.33***	-0.26	0.28*	0.22	-0.23	-0.14
DO		1	-0.06	-0.03	-0.28**	-0.09	-0.25	-0.13*	-0.27***	0.09	-0.04	0.45**	0.44**	-0.02*	-0.24***
log (temp)			1	0.90***	0.45***	0.48***	-0.42***	0.54	0.06	0.23**	0.19	-0.49***	-0.48***	0.46*	0.18
log (ben temp)				1	0.55***	0.66***	-0.34**	0.53**	0.12	0.19*	0.28	-0.55***	-0.54***	0.47	0.19
log (ortho-P)					1	0.82***	-0.08	0.32***	0.44***	0.21**	0.29*	-0.56***	-0.53***	0.36***	0.38***
log (NH ₄)						1	-0.04	0.40***	0.40***	0.17	0.43**	-0.52***	-0.51***	0.46***	0.40**
log (SO ₄)							1	-0.44***	-0.24	0.02	0.28***	-0.02	0.02	-0.21*	0.05
log (DOC)								1	0.59***	-0.04	0.16	-0.48***	-0.51***	0.54***	0.48***
sqrt (alk)									1	-0.31*	0.11	-0.37**	-0.42***	0.47***	0.55***
log (1+chl a)										1	0.05	-0.07	0.01	0.14	0.05
sqrt (precip)											1	-0.19	-0.18	0.32*	0.36*

Table 1.3. continued.

	pH	DO	log (temp)	log (ben temp)	log (ortho- P)	log (NH4)	log (SO4)	log (DOC)	sqrt (alk)	log (1+chl a)	sqrt (precip)	log (vol)	log (SA)	log (CH4)	log (CO2)
log (SA)													1	-0.40***	-0.40***
log (CH4)														1	0.77***
log (CO2)															1

Table 1.4. Multiple linear regression models for CH₄ concentration. $\Delta\text{AIC} < 2$. Significance is shown as: $p < 0.05$ *, $p < 0.01$ **, $p < 0.001$ ***.

Model	AIC	ΔAIC	Weight	R ²
alk + temp	211.35	0	0.34	0.32***
alk + temp + precip	212.56	1.21	0.19	0.32***
alk + temp + chl a	213.08	1.73	0.14	0.32***

Table 1.5. Linear mixed effect models for CH₄ concentrations.

Model	AIC	ΔAIC	R ² marg	R ² cond	Pool variance	Residual variance	Est intercept	Est alk	Est temp	Est precip	Est chl a
alk + temp	285.5	0	0.34	0.34	3.83×10^{-16}	1.56	-17.25	0.17	1.27	--	--
alk + temp + precip	286.5	1.0	0.35	0.35	0	1.54	-17.52	0.16	1.23	0.24	--
alk + temp + chl a	287.0	1.5	0.35	0.35	0	1.54	-17.16	0.17	1.18	--	0.08

Table 1.6. Multiple linear regression models for CO₂ concentration, $\Delta\text{AIC} < 2$. Significance is shown as: $p < 0.05$ *, $p < 0.01$ **, $p < 0.001$ ***.

Model	AIC	ΔAIC	Weight	R ²
alk + temp + DO	198.64	0	0.20	0.45***
alk + temp	199.08	0.44	0.16	0.44***
alk + temp + DO + precip	199.14	0.50	0.15	0.45***
alk + temp + DO + chl a	199.70	1.06	0.12	0.45***
alk + temp + precip	199.80	1.16	0.11	0.44***
alk + temp + DO + precip + chl a	200.22	1.58	0.09	0.45***
alk + temp + chl a	200.36	1.72	0.08	0.44***

Table 1.7. Linear mixed effect models for CO₂ concentrations.

Model	AIC	ΔAIC	R ² marg	R ² cond	Pool variance	Residual variance	Est intercept	Est alk	Est temp	Est DO	Est precip	Est chl a
alk + temp	143.9	0	0.45	0.48	0.02	0.28	-9.36	0.10	0.05	--	--	--
alk + temp + DO	144.0	0.1	0.47	0.47	0	0.28	-8.82	0.09	-0.04	-0.04	--	--
alk + temp + precip	144.1	0.2	0.46	0.49	0.02	0.27	-9.54	0.10	0.04	--	0.13	--
alk + temp + DO + precip	144.2	0.3	0.48	0.48	0	0.28	-8.95	0.09	-0.07	-0.04	0.13	--
alk + temp + DO + chl a	144.7	0.8	0.48	0.48	0	0.28	-8.74	0.10	-0.10	-0.04	--	0.05
alk + temp + chl a	144.8	0.9	0.45	0.49	0.04	0.27	-9.28	0.10	-0.01	--	--	0.05
alk + temp + DO + precip + chl a	144.9	1.0	0.49	0.49	0	0.27	-8.87	0.09	-0.13	-0.05	0.13	0.05

Carbon dioxide was significantly positively correlated with ortho-P, NH_4^+ , DOC, alkalinity, and precipitation, and significantly negatively correlated with DO, pool volume, surface area and depth (Table 1.3). Alkalinity + temperature + DO was the best multiple linear regression and linear mixed effect model for CO_2 concentrations (Table 1.6., 1.7.). Precipitation, DO, and chl a were also important in the models with $\Delta\text{AIC} < 2$. Alkalinity, temperature, and DO explained 45% of the variance in CO_2 concentrations (Table 1.6.) in the top linear mixed effect model. Between-pool variation explained an additional 3% of the variation in CO_2 concentrations in the top linear mixed effects model (Table 1.7.).

1.3.4. Net Production of CH_4 and CO_2

We calculated the net production and the rate of production of CH_4 and CO_2 in the vernal pools by Eq. 4, using the calculated fluxes, the change in mass over time within the pools, and the export through groundwater. This is a way to quantify the production and release of CH_4 and CO_2 in the pools while accounting for the changing water levels that are characteristic of vernal pools. The mass accumulated in the pool ($\Delta m/\Delta t$) could be either positive or negative. The concentration of CH_4 and CO_2 leaving through groundwater ($Q_{\text{out}}C_{\text{out}}$) values were always positive in P1, P3, and P4, and were zero in P2 because of the lack of downflow. Emissions of CH_4 and CO_2 were always positive, a result of the supersaturation of the pools. Net production in the four pools ranged from -3.5 to 1.5×10^2 gC d^{-1} and 8.5×10 to 8.2×10^2 gC d^{-1} for CH_4 and CO_2 , respectively (Table 1.8.). The rates of production varied from -2.4×10^{-2} to 9.9×10^{-1} $\text{gC m}^{-2} \text{d}^{-1}$ and 4.0×10^{-1} to 4.6 $\text{gC m}^{-2} \text{d}^{-1}$ for CH_4 and CO_2 , respectively. $Q_{\text{out}}C_{\text{out}}$ was always smaller than R_{ef} and $\Delta m/\Delta t$ was almost always smaller than R_{ef} . The majority of the CH_4 and CO_2 that was produced left

the pools through evaporative flux; it did not leave through groundwater or stay within the pools.

There were significant differences in CH₄ and CO₂ net production among sites (Figure 1.2., Figure 1.3.; $p < 0.01$, $p < 0.001$, respectively). The net production of CH₄ increased significantly over the season ($R^2 = 0.19$, $p < 0.01$), but the net production of CO₂ did not. The rates of CH₄ and CO₂ production, increased significantly over the season ($R^2 = 0.57$, $p < 0.001$, $R^2 = 0.49$, $p < 0.001$, respectively). There were no significant differences among pools in production rates of CH₄ and CO₂ (Figure 1.2., Figure 1.3.).

Table 1.8. Mass accumulation, groundwater output, evaporative flux, net production, and zero order rates of CH₄ and CO₂. Average values are reported with ranges in parentheses over the sampling season.

	dm/dt [gC d ⁻¹]	$Q_{out}C_{out}$ [gC d ⁻¹]	R_{ef} [gC d ⁻¹]	R_p [gC d ⁻¹]	R_p rate [gC m ⁻² d ⁻¹]
CH₄					
P1	1.1×10 ⁻¹ (-1.1–8.6×10 ⁻¹)	7.4×10 ⁻¹ (1.2×10 ⁻¹ –1.4)	2.3 (9.1×10 ⁻¹ –4.1)	3.2 (9.7×10 ⁻¹ –4.7)	3.0×10 ⁻² (1.9×10 ⁻² –5.6×10 ⁻²)
P2	6.0×10 ⁻¹ (-3.9×10–2.9×10)	--	3.1×10 (1.1–1.2×10 ²)	3.1×10 (-3.5–1.5×10 ²)	2.0×10 ⁻¹ (-2.4×10 ⁻² –9.9×10 ⁻¹)
P3	-3.0×10 ⁻¹ (-2.8–2.6)	3.5×10 ⁻¹ (9.3×10 ⁻² –1.2)	3.8×10 (8.8–1.4×10 ²)	3.8×10 (7.3–1.4×10 ²)	1.5×10 ⁻¹ (3.0×10 ⁻³ –6.6×10 ⁻¹)
P4	3.6×10 ⁻¹ (-3.0–5.4)	2.8×10 ⁻¹ (2.4×10 ⁻² –7.9×10 ⁻¹)	2.2×10 (5.3–6.5×10)	2.3×10 (5.2–6.4×10)	8.5×10 ⁻² (1.3×10 ⁻² –2.3×10 ⁻¹)
CO₂					
P1	9.8×10 ⁻³ (-4.0–6.6)	8.0 (4.1–1.0×10)	1.5×10 ² (7.9×10–2.6×10 ²)	1.6×10 ² (8.5×10–2.7×10 ²)	1.4 (1.0–2.0)
P2	-8.9×10 ⁻¹ (-1.4×10–8.3)	--	3.6×10 ² (1.5×10 ² –6.9×10 ²)	3.6×10 ² (1.4×10 ² –7.0×10 ²)	2.2 (9.7×10 ⁻¹ –4.6)
P3	-3.8×10 (-1.4×10 ² –2.2×10)	9.6 (4.5–1.7×10)	9.9×10 ² (1.4×10 ² –2.1×10 ³)	9.6×10 ² (1.4×10 ² –2.2×10 ³)	1.8 (4.0×10 ⁻¹ –4.4)
P4	-2.0 (-5.4×10–8.4×10)	5.8 (1.3–1.2×10)	6.2×10 ² (3.5×10 ² –8.4×10 ²)	6.2×10 ² (3.5×10 ² –8.2×10 ²)	2.4 (1.1–3.8)

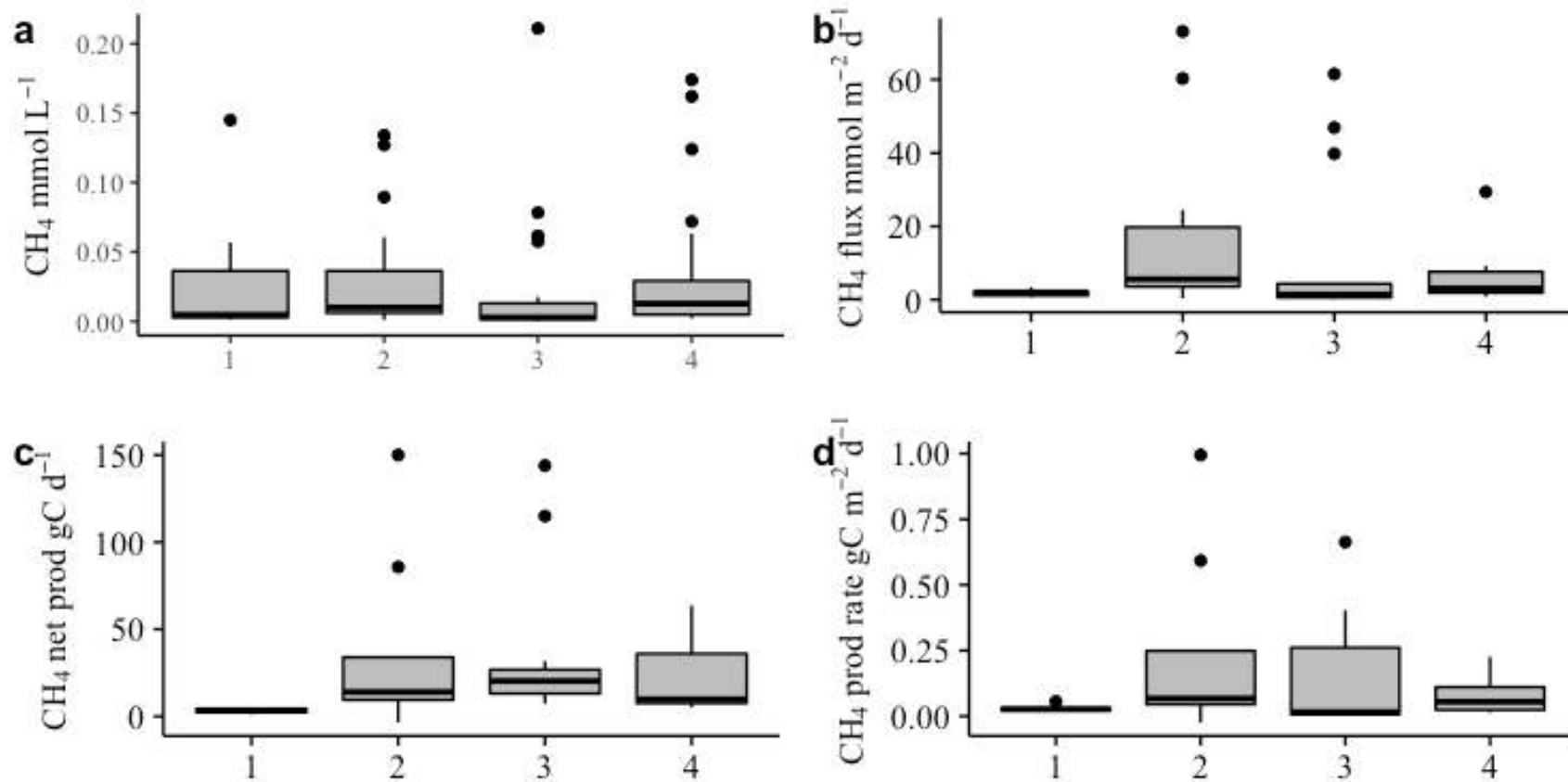


Figure 1.2 CH₄ average concentrations, fluxes, net production, and net production rates in 4 pools. Samples collected from April to August 2016.

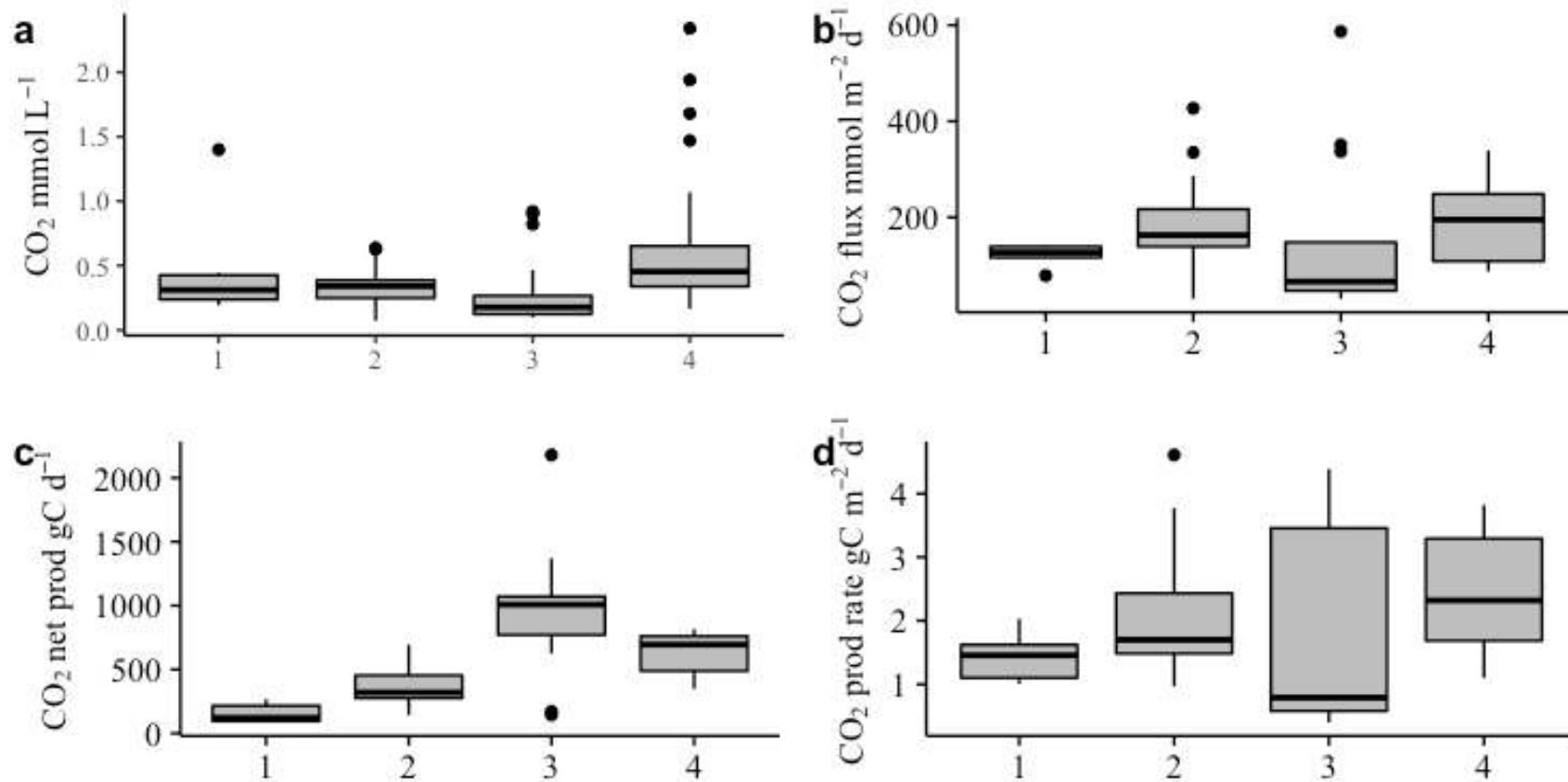


Figure 1.3. CO_2 average concentrations, fluxes, net production, and net production rates in 4 pools. Samples collected from April to August 2016.

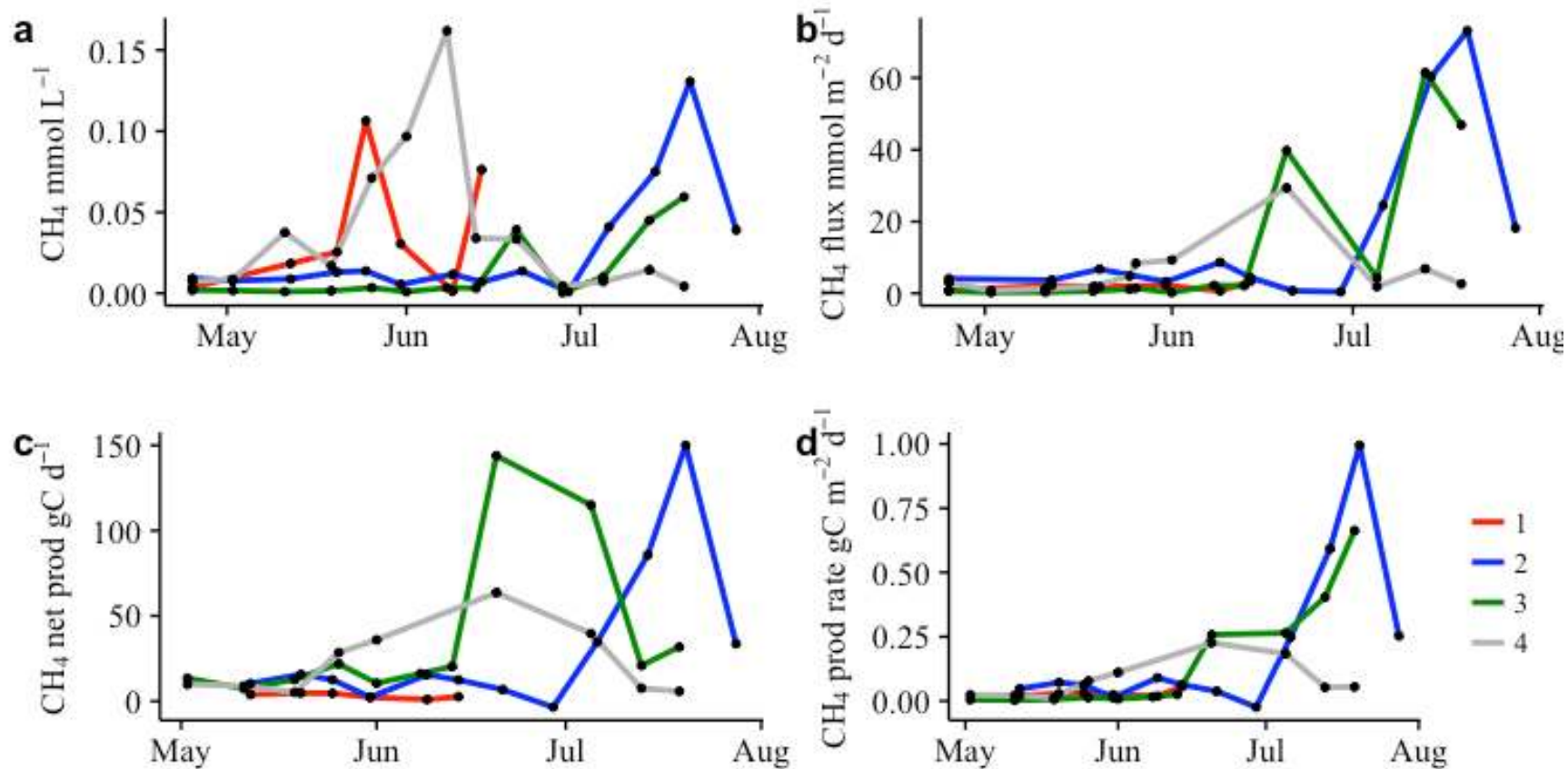


Figure 1.4. Time-series of CH₄ average concentrations, fluxes, net production, and net production rates in 4 pools. Samples collected from April to August 2016.

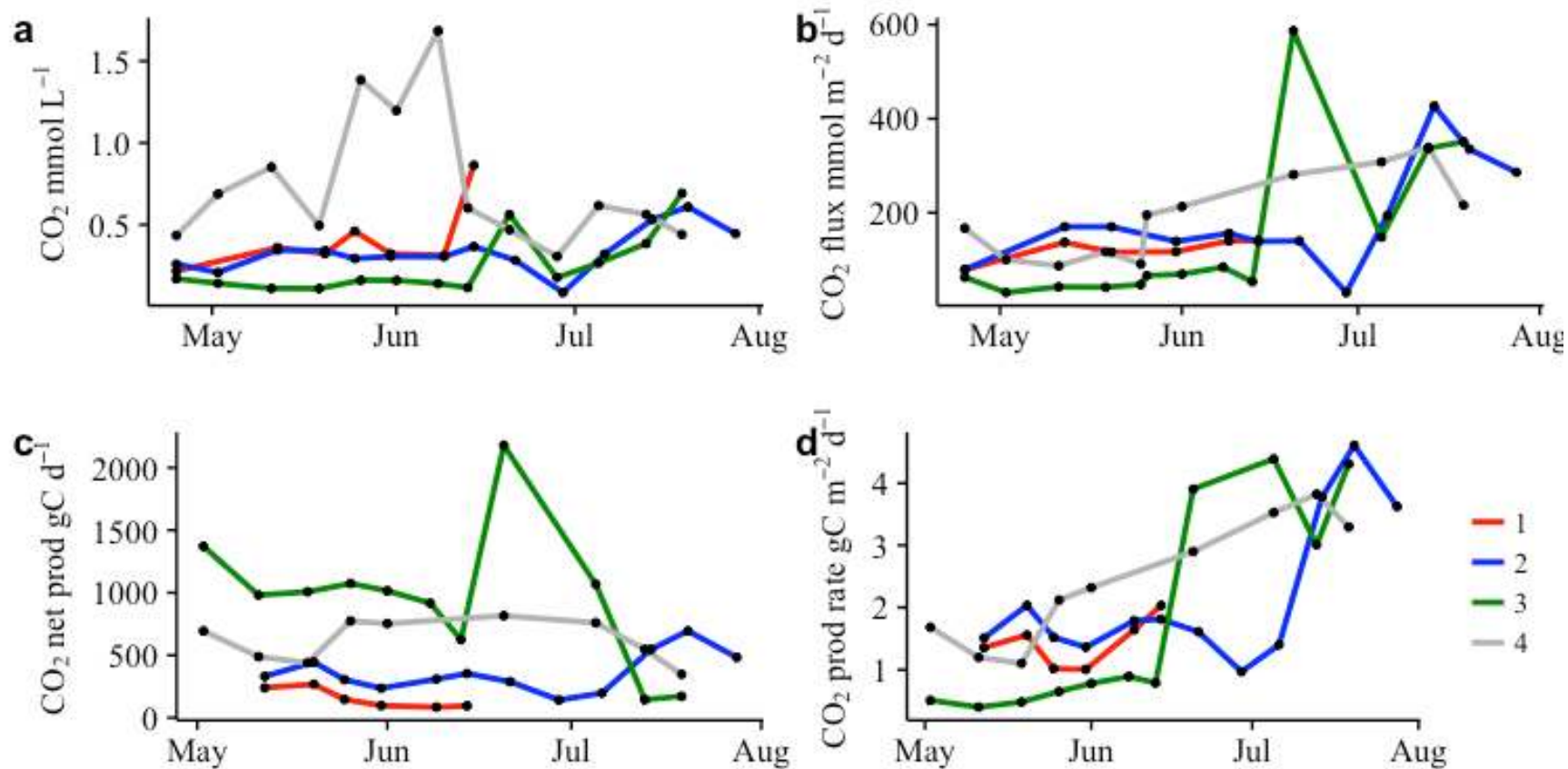


Figure 1.5. Time-series of CO₂ average concentrations, fluxes, net production, and net production rates in 4 pools. Samples collected from April to August 2016.

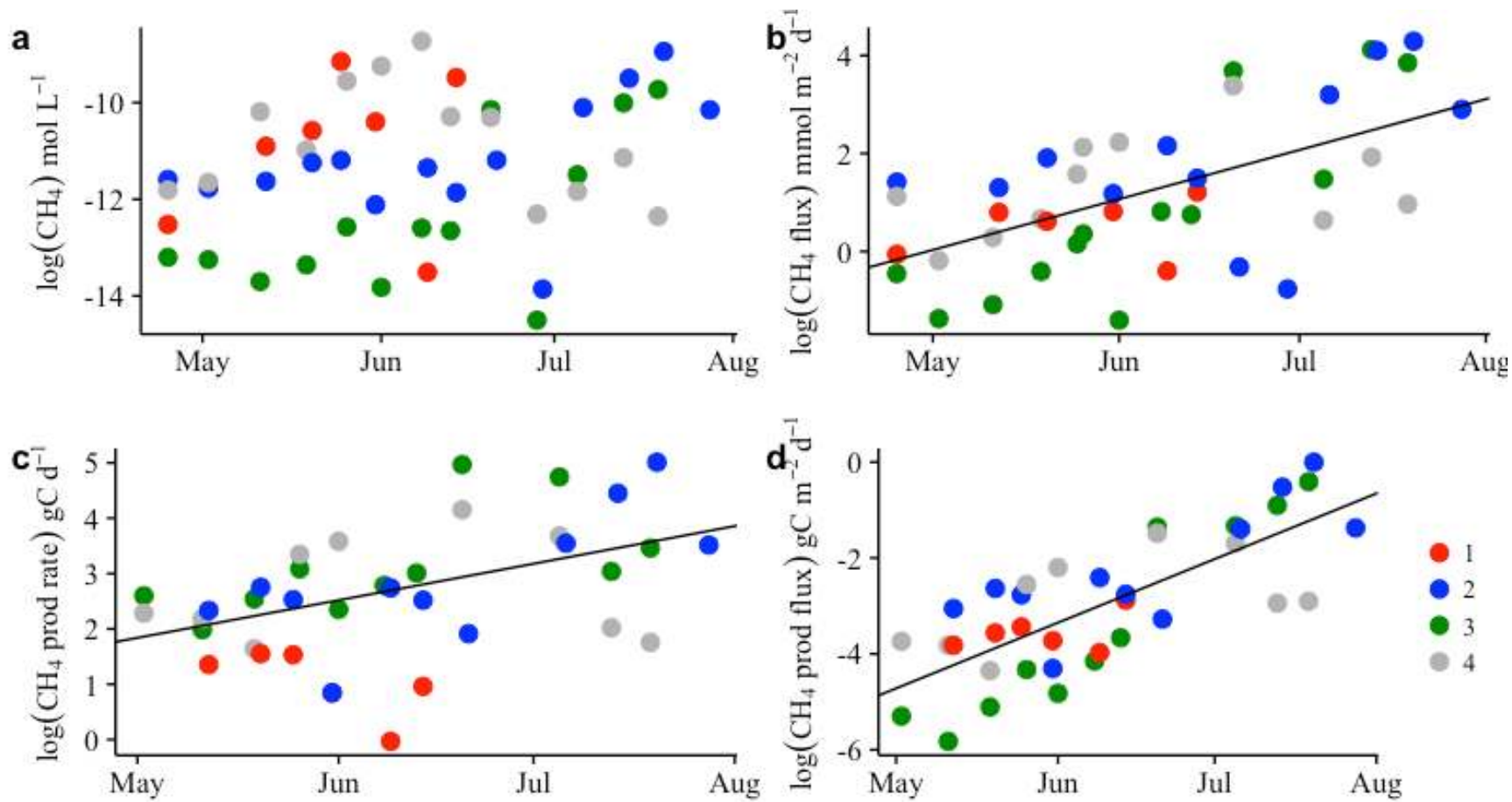


Figure 1.6. Relationship between time and CH₄ average concentrations, fluxes, net production, and net production rates in 4 pools.

Samples collected from April to August 2016.

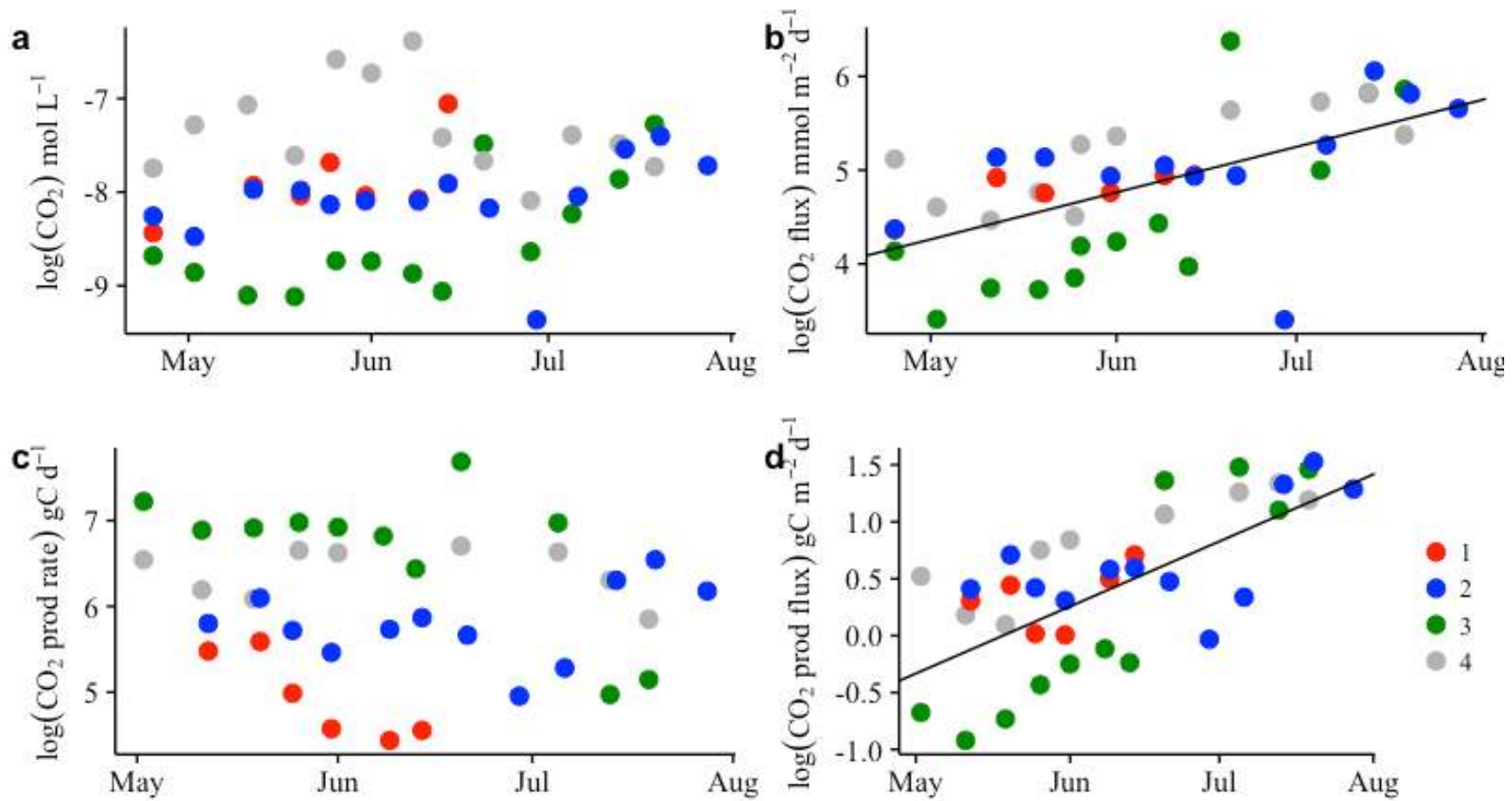


Figure 1.7. Relationship between time and CO₂ average concentrations, fluxes, net production, and net production rates in 4 pools.

Samples collected from April to August 2016.

1.4. Discussion

1.4.1. CH₄ and CO₂ Concentrations and Fluxes

The CH₄ and CO₂ concentrations and fluxes in this study are of similar magnitude to those in a study in Connecticut on small, temporary ponds with similar sampling design (Holgerson, 2015), but higher CH₄ than in a study of vernal pools in Massachusetts (Kuhn 2015). Vernal pools in Rhode Island emitted similar amounts of CH₄ during May and June, and similar amounts of CO₂ (Ross 2017). The fluxes of CH₄ and CO₂ from the vernal pools were 1-2 orders of magnitude larger than those from lakes (Bastviken et al. 2004; Casper et al. 2000; Huttunen et al. 2003; Kankaala et al. 2013; Rantakari and Kortelainen 2005). Salt marshes have CH₄ and CO₂ fluxes in the same order of magnitude as our study pools (Chmura et al. 2011; Magenheimer et al. 1996). These vernal pools have some of the highest documented concentrations and fluxes of CH₄ and CO₂ for ponds, lakes, and wetlands (Table 1.9.).

Table 1.9. Reported surface water CH₄ and CO₂ concentrations and emissions for a selection of ponds, wetlands, and lakes. Concentrations and fluxes are reported as means with range in parentheses when more than one location was included or multiple samplings of a location occurred. When fluxes are presented on a per year basis, they were converted to a per day basis, assuming equal flux for all 365 days.

Location	# sites	CH ₄ conc (μmol L ⁻¹)	CO ₂ conc (μmol L ⁻¹)	CH ₄ emission (mmol m ⁻² d ⁻¹)	CO ₂ emission (mmol m ⁻² d ⁻¹)	Source
Vernal pools, ME, USA	4	27.0 (0.4–211)	424 (71.8–2340)	10.8 (0.2–73.1)	167 (30.1–587)	Present study
Vernal pools, RI, USA	4			(-1.4×10 ⁻² –4.6×10 ⁻²)	(7.2–31.7)	Ross 2017
Vernal pools, MA, USA	2	(2.0×10 ⁻² –0.1)				Kuhn 2015
Small temporary ponds, CT, USA	6	33.4 (21.0–58.9)	353.2 (273.3–553.4)	10.6±0.13	100.6±0.51	Holgerson 2015
Prairie potholes, SK, CA	62			(0.1–3.8)		Badiou et al. 2011
Lakes, ponds, & reservoirs, FI	9			(9.0×10 ⁻² –8.3)	(-1.8–73.0)	Huttunen et al. 2003
Lakes, WI, USA & Sweden	24	(0.1–2.32)		(2.2×10 ⁻² –4.1)		Bastviken et al. 2004
Small lake, U.K.	1	1.3 (0.31–4.8)	132 (27–326)	(0–108.4)	(3.9–101.6)	Casper et al. 2000
Lakes, FI	12	(5.0×10 ⁻³ –1787)	(11–2394)	(8.2×10 ⁻³ –1.1)	(5.8–65.2)	Kankaala et al. 2013
Boreal lakes, FI	37				(5.5–19)	Rantakari and Kortelainen 2005
Microtidal, macrotidal salt marsh NB and NS, CA	2			2.9×10 ⁻² ±8.7×10 ⁻² , 5.3×10 ⁻² ±0.1	264.5±138.0, 217.1±109.6	Chmura et al. 2011
Salt marsh, NB, CA	52			0.1 (1.3×10 ⁻² –0.7)	56.8 (6.8–84.1)	Magenheimer et al. 1996
Temperate bog, WA, USA	1			6.1 (0.1–31.7)	216.7(16.7–2000)	Lansdown et al. 1992
Coastal meadow, fen, DK	2			8.0×10 ⁻³ , 0.4		Priemé 1994
Boreal fen, SK, CA	1			(0.5–6.2)		Rask et al. 2002
Drained, flooded rice paddy canopy, JP (nocturnal)	1				805.1±137.5, 373.1±117.8	Miyata et al. 2000
Afternoon, night rice paddy canopy, JP (drained)	1			(6.5–7.0), (1.6–2.2)		Miyata et al. 2000

The pools were supersaturated with CH₄ and CO₂ across all surface samples and dates, indicating that the pools were emitting CH₄ and CO₂ across the air-water interface at all pools and times. The atmospheric fluxes in this study were estimated using Eqs. 2 and 3 which consider only diffusion across the water boundary layer. Due to the low solubility of CH₄ in water, ebullition can also be an important mechanism for its atmospheric emission. CH₄ ebullition can be especially important in water bodies with relatively shallow depths, such as vernal pools, because of the relatively low hydrostatic pressure (Bastviken et al. 2004; Casper et al. 2000; Coulthard et al. 2009; Fendinger et al. 1992; Huttunen et al. 2003; Whalen 2005). Methane can also be released from the sediment into the atmosphere through transport in plants (Bastviken et al. 2004; Sebacher et al. 1985; Segers 1998; Whalen 2005). Therefore, the evaporative fluxes estimated in this study are minimum values, especially for CH₄.

Further, in this study CH₄ and CO₂ evaporative fluxes were estimated only during periods of inundation. When the pools dry down and the previously inundated sediment is exposed to air, carbon dynamics do not halt. Water table fluctuations in wetlands influence CH₄ and CO₂ production zones (Boon et al. 1997; Fromin et al. 2010; Kettunen et al. 1999; Nykänen et al. 1998; Rezanezhad et al. 2014). A higher water level generally leads to higher CH₄ emissions (Kettunen et al. 1996; Moore and Knowles 1989; Nykänen et al. 1998; Rask et al. 2002), and a lower one leads to higher CO₂ emissions (Fromin et al. 2010; Moore and Knowles 1989; Rezanezhad et al. 2014). Though influence of water level on CH₄ and CO₂ fluxes has been studied previously, there is little information on emissions from a dried vernal pool basin. Ross (2017) found that vernal pools emitted CO₂ continuously, but their soils absorbed CH₄ for the ten months out of the year when

they were dry. Methanogenesis may only occur in the wet areas of the pools, and only during certain times of the wet-dry cycle. Vernal pools are dry and/or frozen for the majority of the year, and CH₄ and CO₂ emissions (positive or negative) during these times should be considered in an annual budget.

1.4.2. Covariates of CH₄ and CO₂

The primary covariates of CH₄ and CO₂ concentrations in this study were alkalinity and temperature. They appeared in every multiple linear regression model (Table 1.4., Table 1.6.). The best model explaining CH₄ concentration using both multiple linear regression and linear mixed effects was alkalinity + DO (Table 4, Table 5). The best model explaining CO₂ concentration using multiple linear regression was alkalinity + temp + DO (Table 6), and using linear mixed effect it was alkalinity + temperature (Table 1.7.). Using linear mixed effects changed the best model for CO₂ concentrations because it accounts for the random effect of pool. Including the random effect of pool did not increase the conditional R² value for CH₄, because the variance among pools was negligible (Table 1.5.). However, for CO₂ the between pool variation was not negligible for the top model and two other models, and therefore including the random effect of the pool did increase the conditional R² value (Table 1.7.), and did alter the models by reducing the variation in the residual. Similarly to this study, Holgerson (2015) found that the random effect of temporary pond increased the conditional R² by 0.03 for CH₄, and by 0.37 for CO₂ in their best model.

Alkalinity is significantly positively correlated with DOC, ortho-P, and NH₄⁺, and significantly negatively correlated with DO (Table 1.3.). In general, aerobic respiration has little effect on alkalinity, but the anaerobic processes of denitrification, nitrate

reduction to NH_4^+ , and iron (Fe), manganese (Mn), and SO_4^{2-} reduction all increase alkalinity. Although methanogenesis does not affect alkalinity, an increase in other anaerobic activities occurring in the sediments of the vernal pools can affect alkalinity. In addition to generating CH_4 and CO_2 , anaerobic reactions result in the production of DOC, NH_4^+ , and release of P from the sediment (Stumm and Morgan, 1996). DOC has a positive relationship with CO_2 in lakes (Bastviken et al. 2004; Roehm et al. 2009; Striegl et al. 2001), and a negative relationship to CH_4 (Bastviken et al. 2004). Total P and total N have also been shown to have positive correlations with greenhouse gas fluxes (Bastviken et al. 2004; Huttunen et al. 2003; Rantakari and Kortelainen 2005).

Sulfate had a weak, but significant negative relationship with CH_4 concentrations (Table 1.3.). In addition to contributing to alkalinity, SO_4^{2-} serves as an alternative electron acceptor to the SO_4^{2-} reducing microbes that compete for organic substrate with the methanogens, suppressing methanogenesis (Chmura et al. 2011; Segers 1998). As a result of low SO_4^{2-} concentrations in freshwater (typically $3.2\text{-}6.4 \text{ mgS L}^{-1}$), methanogenesis is typically unaffected by SO_4^{2-} as an alternative electron acceptor (Liu and Whitman 2008). However, a negative relationship between SO_4^{2-} and CH_4 occurs in prairie potholes and lakes (Badiou et al. 2011; Bansal et al. 2016; Liikanen 2002; Pennock et al. 2010).

CH_4 and CO_2 production are influenced by temperature (Bergman et al. 1998; Liikanen 2002; Marotta et al. 2014; Ross 2017; Whalen 2005), and CH_4 and CO_2 emission generally increase as soil temperature increases and microbial activity increases (Allen et al. 2005; Bansal et al. 2016; Bastviken et al., 2004; Brinson et al. 1981; Christiansen et al., 2016; Christensen et al., 2003; Huttunen et al., 2003; Kettunen et al.

1996; Mitsch et al., 2013; Rask et al., 2002; Yavitt et al. 1997; Yvon-Durocher et al. 2017). The increasing concentrations and evaporative fluxes of both CH₄ and CO₂ over the 2016 field season can also be attributed to increasing temperature.

Dissolved oxygen was a covariate of, and was negatively related to, CO₂ concentrations (Table 1.4.). Holgerson (2015) found that DO best predicted CO₂ concentrations in small temporary pools, and also found a significant negative linear relationship between CO₂ and DO. Similarly, in our study, the negative relationship between CO₂ and DO was significant (Table 1.3.). A correlation between CO₂ and DO indicates high rates of respiration and organic matter decomposition in the sediment (Holgerson 2015; Jonsson et al. 2003; Rantakari and Kortelainen 2005). Methanogenesis is an anaerobic process, but DO was not found to be a predictor for CH₄ concentrations, similar to Holgerson (2015).

Another covariate of CH₄ and CO₂ emissions in this study was precipitation (Table 1.4., Table 1.6.). Other studies have documented that CH₄ and CO₂ increased with precipitation (Einola et al. 2011; Kettunen et al. 1996; Natchimuthu et al. 2014; Rantakari and Kortelainen 2005; Roehm et al. 2009). In lakes, precipitation is related to increased carbon inputs from the watershed, which can increase substrate for CO₂ (Einola et al. 2011; Rantakari and Kortelainen 2005; Roehm et al. 2009) and possibly CH₄ production. In contrast to our study and those of others, Holgerson (2015) found that precipitation was an environmental predictor of CH₄ concentrations in small, temporary ponds. They attributed the finding to dilution of biological and chemical parameters and increasing the gas exchange rate at the surface of the pool.

Chlorophyll *a* was a covariate in one of the CH₄ (Table 1.4.) and in three of the CO₂ (Table 1.6.) multiple linear regression models. A positive relationship between CH₄ and chl *a* has been found in other studies (Bastviken et al. 2004; Holgerson 2015), has been attributed to the enhanced growth of periphyton and phytoplankton chl *a* with increasing temperature (Holgerson 2015). Similarly, in our study chl *a* is significantly positively correlated with temperature (Table 1.4.). It was also hypothesized that chl *a* can provide organic substrate for methanogenesis, which could increase production (Holgerson 2015). Chl *a* has been found to negatively correlate with CO₂ concentrations (Holgerson 2015; Roehm et al. 2009). However, we did not observe this in our study; chl *a* does not have a significant relationship to CO₂ concentrations (Table 1.3.).

1.4.3. Net Production of CH₄ and CO₂

The net production in the four vernal pools was almost always positive, meaning that CH₄ and CO₂ were being generated in the pools. The amount of CH₄ and CO₂ transported through groundwater flow was generally negligible compared to that transported through evaporative flux. Total net production is dependent on pool area, but the production rates are not. Thus differing pool area explains the differences in net production among pools. For instance, a pool the size of P3 will produce more CH₄ and CO₂ than a pool the size of P1, but the production rates were not statistically different among the pools. The increase in production rates as the summer progresses can be attributed to rising temperatures and higher rates of decomposition within the pools.

1.4.4. The Role of Vernal Pools in Carbon Cycling

It is difficult to determine a representative system of vernal pools in Maine; the only commonality among these sites is that they all have seasonal hydroperiod; the other characteristics are challenging to generalize. If we view these pools as representative in Maine because of their diversity in hydroperiod, geology, and forest type, we can examine the potential large-scale impacts of vernal pools. The density of vernal pools across Maine ranges from 1.4 to 49.5 pools per km² (Calhoun et al. 2003). Combining the range of calculated evaporative fluxes in this study with the range of pool densities in Maine, we calculate that vernal pools could potentially emit between 1.4×10^{-4} and 1.2×10 TgC of CH₄ and between 1.7×10^{-2} and 5.3×10^4 TgC of CO₂ per year in Maine. These estimates have a large range because of the variation in pool densities in Maine and the variation of the calculated emissions of CH₄ and CO₂ (Figure 1.2., Figure 1.3.), but they indicate that vernal pools are important as biogeochemical reactors in Maine. Vernal pools and other temporary wetlands are widely distributed across northeastern landscapes (DiBello et al. 2016; Faccio et al. 2013; Wu et al. 2014; Van Meter et al. 2008), and globally (Keeley and Zedler 1998; Calhoun et al. 2017), so these evaporative fluxes can potentially constitute a large contribution to inland waters' carbon emissions. Small water bodies tend to have higher concentrations of CH₄ and CO₂ than larger bodies of freshwater (Bastviken et al. 2004; Holgerson, 2015; Holgerson and Raymond, 2016; Kankaala et al. 2013), and therefore they can have a disproportionate effect with respect to their size on carbon emissions.

Carbon is the energy currency that moves through ecosystems (Fernandez 2008), and vernal pools are important for carbon transformations from leaf litter into nutrient

forms that can be transferred to upland ecosystems. In order to understand the balance between carbon emissions and carbon inputs to vernal pool systems, we must know the carbon inputs to vernal pool systems. Leaf litter is the primary source of carbon for undisturbed vernal pools (Capps et al. 2014; Earl and Semlitsch 2013). Simmons et al. (1996) found annual mean litter mass ranging from 2.38×10^2 to 3.87×10^2 g m⁻² in different regions of Maine, with an overall mean of 2.99×10^2 g m⁻². They also found an average carbon flux in litter of between 1.14×10^2 and 1.43×10^2 gC m⁻², with an overall mean of 1.25×10^2 gC m⁻². The total input from litter mass was 3.01×10^2 g m⁻² and the input from leaf litter carbon flux was 1.24×10^2 gC m⁻² in the region where our four vernal pool sites are located (Simmons et al. 1996). These leaf litter fluxes were higher than those found in Acadia National Park, ME (Sheehan et al. 2006), but lower than others in other temperate deciduous forests (Morrison 1991; Nadelhoffer et al. 1983).

Applying the Simmons et al. (1996) mean estimate for litter flux, and assuming the maximum recorded surface area of our four vernal pools in 2016, we estimate that 1.4×10^6 g of leaf litter fell into our study sites in 2016, and of that leaf litter, 5.6×10^5 gC was carbon input into the four vernal pools. During the study period, each vernal pool emitted between 1.4×10^2 to 5.8×10^3 gC and 9.6×10^3 to 1.2×10^5 gC of CH₄ and CO₂, respectively, for a total carbon export of maximum 2.4×10^5 gC from the four pools during the study period. Therefore, the estimated carbon flux from leaf litter into the pools is approximately twice as large as the maximum evaporative carbon flux from the pools. This disparity between carbon input and outputs from the pools may be explained by the immense amount of energy being transferred from wetlands to terrestrial environments in the form of vertebrates (Gibbons et al. 2006). Additionally, wetlands

have been shown to sequester carbon in soil and plant matter (Mitsch et al. 2013; Mitsch and Gosselink 2015; Lal 2008).

Demonstrated by their high rates of CH₄ and CO₂ production these vernal pools have higher rates of decomposition, carbon mineralization, and nutrient cycling than ponds and other permanently inundated wetlands. High CH₄ and CO₂ emissions are a measure of a very metabolically active system. Vernal pools are important in the biogeochemical transformation of leaf litter into usable nutrient forms for aquatic and terrestrial fauna. As a result of the broad distribution of these vernal pools and other temporary wetlands across the world, their contributions to carbon emissions are not insignificant. More research is needed to examine the carbon emissions in these pools after dry down and during ice cover, and to further quantify the amounts of terrestrial carbon outputs and carbon storage.

REFERENCES

- Allen AP, Gillooly JF, Brown JH (2005) Linking the global carbon cycle to individual metabolism. *Funct. Ecol.* 19:202-213
- Badiou P, McDougal R, Pennock D, Clark B (2011) Greenhouse gas emissions and carbon sequestration potential in restored wetlands of the Canadian prairie pothole region. *Wetlands Ecol. Manage.* 19:237-256
- Bansal S, Tangen B, Finocchiaro R (2016) Temperature and hydrology affect methane emissions from Prairie Pothole wetlands. *Wetlands* 36 (Suppl 2):S371-S381
- Barton K (2016) MuMIn: Multi-model inference. Package in R 1.15.6
- Bastviken D, Cole J, Pace M, Tranvik L (2004) Methane emissions from lakes: Dependence of lake characteristics, two regional assessments, and a global estimate. *Global Biogeochem. Cy.* 18
- Bates D, Maechler M, Bolker B, Walker S (2014) lme4: Linear mixed effects models using Eigen and S4.R package version 1.0.7
- Bergman I, Svensson BH, Nilsson M (1998) Regulation of methane production in a Swedish acid mire by pH, temperature and substrate. *Soil Biol. Biochem.* 30:729-741
- Bloom AA, Palmer PI, Fraser A, Reay DS, Frankenberg C (2010) Large-scale controls of methanogenesis inferred from methane and gravity spaceborne data. *Science* 327:322-325
- Boon PI, Mitchell A, Lee K (1997) Effects of wetting and drying on methane emissions from ephemeral floodplain wetlands in south-eastern Australia. *Hydrobiologia* 357:73-87
- Brinson MM, Lugo AE, Brown S (1981) Primary productivity, decomposition and consumer activity in freshwater wetlands. *Ann. Rev. Ecol. Syst.* 12:123-161
- Brooks RT, Stone J, Lyons P (1998) An inventory of seasonal forest ponds on the Quabbin Reservoir Watershed, Massachusetts. *Northeast Nat.* 5:219-230
- Calcagno V (2013) gmulti: Model selection and multimodel inference made easy. R package version 1.0.7
- Calhoun AJK, Arrigoni J, Brooks RP, Hunter ML, Ritcher SC (2014) Creating successful vernal pools: A literature review and advice for practitioners. *Wetlands* 34:1027-1038

- Calhoun AJK, Mushet DM, Bell KP, Boix D, Fitzsimons JA, Isselin-Nondedeu F (2017) Temporary wetlands: challenges and solutions to conserving a ‘disappearing’ ecosystem. *Biol. Conserv.* 211:3-11
- Calhoun AJK, Walls TE, Stockwell SS, McCollough M (2003) Evaluating vernal pools as a basis for conservation strategies: A Maine case study. *Wetlands* 23:70-81
- Campbell Grant, EH (2005) Correlates of vernal pool occurrence in the Massachusetts, USA landscape. *Wetlands* 25:480-487
- Capps KA, Rancatti R, Tomczyk N, Parr TB, Calhoun AJK, Hunter M (2014) Biogeochemical hotspots in forested landscapes: The role of vernal pools in denitrification and organic matter processing. *Ecosystems* 17:1455-1468
- Casper P, Maberly SC, Hall GH, Finlay BJ (2000) Fluxes of methane and carbon dioxide from a small productive lake to the atmosphere. *Biogeochemistry* 49:1-19.
- Chmura GL, Kellman L, Guntenspergen GR (2011) The greenhouse gas flux and potential global warming feedbacks of a northern macrotidal and microtidal salt marsh. *Environ. Res. Lett.* 6
- Christensen TR, Ekberg A, Ström L, Mastepanov M, Panikov N, Öquist M, Svensson BH, Nykänen H, Martikainen PJ, Oskarsson H (2003) Factors controlling large scale variations in methane emissions from wetlands. *Geophys. Res. Lett.* 30
- Christiansen JR, Levy-Booth D, Prescott CE, Grayton SJ (2016) Microbial and environmental controls of methane fluxes along a soil moisture gradient in a Pacific coastal temperate rainforest. *Ecosystems* 19:1255-1270
- Colburn EA, Weeks SC, Reed SK (2007) Diversity and ecology of vernal pool invertebrates. In: Calhoun AJK, DeMaynadier PG (eds) *Science and conservation of vernal pools in northeastern North America*. CRC Press, Boca Raton, pp 105-126
- Cole JJ, Prairie YT, Caraco NF, McDowell WH, Tranvik LJ, Striegl RG, Duarte CM, Kortelainen P, Downing JA, Middelburg JJ, Melack J (2007) Plumbing the global carbon cycle: Integrating inland waters into the terrestrial carbon budget. *Ecosystems* 110:171-184
- Corstanje R, Reddy KR (2004) Response of biogeochemical indicators to a drawdown and subsequent reflood. *J. Environ. Qual.* 33:2357-2366
- Coulthard TJ, Baird AJ, Ramirez J, Waddington JM (2009) Methane dynamics in peat: Importance of shallow peats and a novel reduced-complexity approach for modeling ebullition. *Carbon Cycling in Northern Peatlands*:173-185

- DiBello F, Calhoun AJK, Morgan DE, Shearin AF (2016) Efficiency and detection accuracy using print and digital stereo aerial photography for remotely mapping vernal pools in New England landscapes. *Wetlands* 36:505-514
- Downing JA, Prairie YT, Cole JJ, Duarte CM, Tranvik LJ, Striegl RG, McDowell WH, Kortelainen P, Caraco NF, Melack JM, Middelburg JJ (2006) The global abundance and size distribution of lakes, ponds, and impoundments. *Limnol. Oceanogr.* 51:2388-2397
- Earl JE, Semlitsch RD (2013) Spatial subsidies, trophic state, and community structure: Examining the effects of leaf litter input on ponds. *Ecosystems* 16:639-651
- Eaton AD, Clesceri LS, Greenberg AE, Franson MAH (eds), American Public Health association, American Water Works Association, Water Environment Federation (1995) Standard methods for the examination of water and wastewater, 19th edition. American Public Health Association, Washington, DC
- Einola E, Rantakari M, Kankaala P, Kortelainen P, Ojala A, Pajunen H, Mäkelä S, Arvola L (2011) Carbon pools and fluxes in a chain of five boreal lakes: A dry and wet year comparison. *J Geophys Res Biogeosci* 116:G03009
- Faccio SD (2003) Postbreeding Emigration and habitat use by Jefferson and Spotted Salamanders in Vermont. *J. Herpetol.* 37:479-489
- Faccio SD, Lew-Smith M, Worthley A (2013) Vermont vernal pool mapping project.
- Fendinger NJ, Adams DD, Glotfelty DE. (1992) The role of gas ebullition in the transport of organic contaminants from sediments. *Sci. Total Environ.* 112:189-201
- Fernandez IJ (2008) Carbon and nutrients in Maine forest soils. Station MAaFE (ed.) Technical Bulletin. Orono: Maine Agricultural and Forest Experiment Station
- Fromin N, Pinay G, Montuelle B, Landais D, Ourcival JM, Joffre R, Lensi R (2010) Impact of seasonal sediment desiccation and rewetting on microbial processes involved in greenhouse gas emissions. *Ecohydrol* 3:339-348
- Gibbons JW, Winne CT, Scott DE, Willson JD, Glaudas X, Andrews KM, Todd BD, Fedewa LA, Wilkinson L, Tsaliagos RN, Harper SJ, Greene JL, Tuberville TD, Metts BS, Dorcas ME, Nestor JP, Young CA, Akre T, Reed RN, Buhlmann KA, Norman J, Croshaw DA, Hagen C, Rothermel BB (2006). Remarkable amphibian biomass and abundance in an isolated wetland: Implications for wetland conservation. *Conserv. Biol.* 20:1457-1465
- Holgerson MA (2015) Drivers of carbon dioxide and methane supersaturation in small, temporary ponds. *Biogeochemistry* 124:305-318

- Holgerson MA, Raymond PA (2016) Large contribution to inland water CO₂ and CH₄ emissions from very small ponds. *Nat. Geosci.* 9:222-226
- Huttunen JT, Alm J, Liikanen A, Juutinen S, Larmola T, Hammar T, Silvola J, Martikainen PJ (2003) Fluxes of methane, carbon dioxide and nitrous oxide in boreal lakes and potential anthropogenic effects on the aquatic greenhouse gas emissions. *Chemosphere* 52:609-621
- IPCC (2013) *Climate change 2013: the physical science basis*. Cambridge University Press, Cambridge
- Jonsson A, Karlsson J, Jansson M (2003) Sources of carbon dioxide supersaturation in Clearwater and humic lakes in Northern Sweden. *Ecosystems* 6:224-235
- Kankaala P, Huotari J, Tulonen T, Ojala A (2013) Lake-size dependent physical forcing drives carbon dioxide and methane effluxes from lakes in a boreal landscape. *Limnol. Oceanogr.* 58:1915-1930
- Keeley JE, Zedler PH (1998) Characterization and global distribution of vernal pools. Ecology, conservation, and management of vernal pool ecosystems, *Proceedings from 1996 conference*. 1:1-14
- Kettunen A, Kaitala V, Lehtinen A, Lohila A, Alm J, Silvola J, Martikainen PJ (1999) Methane production and oxidation potentials in relation to water table fluctuations in two boreal mires. *Soil Biol. Biochem.* 31:1741-1749
- Kettunen A, Kaitala V, Alm J, Silvola J, Nykänen H, Martikainen PJ (1996). Cross-correlation analysis of the dynamics of methane emissions from a boreal peatland. *Global Biogeochem. Cy.* 10:457-471
- Kuhn M (2015) Methane dynamics in vernal pools. Honor's Thesis, Wheaton College.
- Lal R (2008) Carbon Sequestration. *Phil Trans R Soc B* 363:815-830
- Lansdown JM, Quay PD, King SL (1992) CH₄ production via CO₂ reduction in a temperate bog: A source of ¹³C-depleted CH₄. *Geochim. Cosmochim. Acta* 56:3493-3503
- Liikanen A (2002) Greenhouse gas and nutrient dynamics in lake sediment and water column in changing environment. Dissertation, in: *Natural and Environmental Sciences* vol. 147. Kuopio University Publications C, Kuopio, Finland.
- Lui Y, Whitman WB (2008) Metabolic, phylogenetic, and ecological diversity of the methanogenic archaea. *Ann. N.Y. Acad. Sci.* 1125:171-189

- Magenheimer JF, Moore TR, Chmura GL, Daoust RJ (1996) Methane and carbon dioxide flux from a macrotidal salt marsh, Bay of Fundy, New Brunswick. *Estuaries* 19:139-145
- Marotta H, Pinho L, Gudasz C, Bastviken D, Tranvik LJ, Enrich Prast A (2014) Greenhouse gas production in low-latitude lake sediments responds strongly to warming. *Nat. Clim. Change* 4:467-470
- Marton JM, Creed I, Lewis D, Lane C, Basu N, Cohen M, Craft C (2015) Geographically isolated wetlands are important biogeochemical reactors on the landscape. *Bioscience* 65:408-418
- McClain ME, Boyer EW, Dent CL, Gergel SE, Grimm NB, Groffman PM, Hart SC, Harvey JW, Johnston CA, Mayorga E, McDowell WH, Pinay G (2003) Biogeochemical hot spots and hot moments at the interface of terrestrial and aquatic ecosystems. *Ecosystems* 6:301-312
- Mitsch WJ, Bernal B, Nahlik AM, Mander Ü, Zhang L, Anderson CJ, Jørgensen SE, Brix H (2013) Wetlands, carbon, and climate change. *Landscape Ecol.* 28:583-597
- Mitsch WJ, Gosselink JG (2015) *Wetlands*, 5th edn. Wiley, Hoboken
- Miyata A, Leuning R, Denmead OT, Kim J, Harazono Y (2000) Carbon dioxide and methane fluxes from an intermittently flooded paddy field. *Agr. Forest. Meteorol.* 102:287-303
- Morrison IK (1991) Addition of organic matter and elements to the forest floor of an old-growth *Acersaccharum* forest in the annual litter fall. *Can. J. For. Res.* 21:462-468
- Moore TR, Knowles R (1989) The influence of water table levels on methane and carbon dioxide emissions from peatland soils. *Can. J. Soil. Sci.* 69:33-38
- Nadelhoffer KJ, Aber JD, Melillo JM (1983) Leaf-litter production and soil organic matter dynamics along a nitrogen-availability gradient in Southern Wisconsin (U.S.A.). *Can. J. For. Res.* 13:12-21
- Nakagawa S, Schielzeth H (2013) A general and simple method for obtaining R^2 from generalized linear mixed effect models. *Methods Ecol. Evol.* 4:133-142
- Natchimuthu S, Selvam BP, Bastviken D (2014) Influence of weather variables on methane and carbon dioxide flux from a shallow pond. *Biogeochemistry* 119:403-413
- National Weather Service (2017) Daily Precip Accumulation. http://www.srh.noaa.gov/ridge2/RFC_Precip/ Cited 21 August 2016

- Nykänen H, Alm J, Silvola J, Tolonen K, Martikainen PJ (1998) Methane fluxes on boreal peatlands of different fertility and the effect of long-term experimental lowering of the water table on flux rates. *Global Biogeochem. Cy.* 12:53-69
- O'Dell JW (ed) (1993) Method 365.1: Determination of phosphorus by semi-automated colorimetry. Environmental Monitoring Systems Laboratory Office of Research and Development U.S. Environmental Protection Agency, Cincinnati
- Pennock D, Yates T, Bedard-Haughn A, Phipps K, Farrell R, McDougal R (2010) Landscape controls on N₂O and CH₄ emissions from freshwater mineral soil wetlands of the Canadian Prairie Pothole region. *Geoderma* 155:308-319
- Priemé A (1994) Production and emission of methane in a brackish and a freshwater wetland. *Soil Biol. Biochem.* 26:7-18
- Rains MC, Dahlgren RA, Fogg GE, Harter T, Williamson (2008) Geological control of physical and chemical hydrology in California vernal pools. *Wetlands* 28:347-362
- Rantakari M, Kortelainen P (2005) Interannual variation and climatic regulation of the CO₂ emission from large boreal lakes. *Glob. Change Biol.* 11:1368-1380
- Rask H, Schoenau J, Anderson D (2002) Factors influencing methane flux from a boreal forest wetland in Saskatchewan, Canada. *Soil Biol. Biochem.* 34:435-443
- Raymond PA, Hartmann J, Lauerwald R, Sobek S, McDonald C, Hoover M, Butman D, Striegl R, Mayorga E, Humborg C, Kortelainen P, Dürr H, Meybeck M, Ciais P, Guth P (2013) Global carbon dioxide emissions from inland waters. *Nature* 503:355-359
- Regosin JV, Windmiller BS, Homan RN, Reed JM (2005) Variation in terrestrial habitat use by four pool-breeding amphibian species. *J. Wildl. Manag.* 69:1481-1493
- Rezanezhad F, Couture RM, Kovac R, O'Connell D, Van Cappellen P (2014) Water table fluctuations and soil biogeochemistry: An experimental approach using an automated soil column system. *J. Hydrol.* 509:245-256
- Roehm CL, Prairie YT, del Giorgio PA (2009) The pCO₂ dynamics in lakes in the boreal region of northern Québec, Canada. *Glob. Biogeochem. Cy.* 23
- Ross BN (2017) Assessing hydrology, carbon flux, and soil spatial variability within vernal pool wetlands. Master's Theses, University of Rhode Island
- Schnoor JL (1996) Environmental Modeling. Wiley-Interscience. New York, NY

- Schwarzenbach RP, Gschwend PM, Imboden DM (2003) Environmental Organic Chemistry 2nd edn. Wiley-Interscience. Hoboken, NJ
- Sebacher DI, Harriss RC, Bartlett KB (1985) Methane emissions to the atmosphere through aquatic plants. *J Environ. Qual.* 14:40-46
- Segers R (1998) Methane production and methane consumption: a review of processes underlying wetland methane fluxes. *Biogeochemistry* 41:23-51
- Semlitsch RD and Skelly DK (2007) Ecology and conservation of pool-breeding amphibians. In: Calhoun AJK, deMaynadier PG (eds) Science and Conservation of Vernal Pools in Northeastern North America. CRC Press, Boca Raton, pp 127-148
- Sheehan KD, Fernandez IJ, Kahl JS, Amirbahman A (2006) Litterfall mercury in two forested watersheds at Acadia National Park, Maine, USA. *Water Air Soil Pollut.* 170:249-265
- Simmons JA, Fernandez IJ, Briggs RD, Delaney MT (1996) Forest floor carbon pools and fluxes along a regional climate gradient in Maine, USA. *Forest Ecol. Manag.* 84:81-95
- St. Louis VL, Kelly CA, Duchemin É, Rudd JWM, Rosenberg DM (2000) Reservoir surfaces as sources of greenhouse gases to the atmosphere: A global estimate. *BioScience* 50:766-775
- Straka KM (2017) Characterizing hydrologic fluxes in six Central Maine vernal pools with a focus on groundwater flow. Master's Theses, University of Maine
- Striegl RG, Kortelainen P, Chanton JP, Wickland KP, Bugna GC, Rantakari M (2001) Carbon dioxide partial pressure and ¹³C content of north temperate and boreal lakes at spring ice melt. *Limnol. Oceanogr.* 46:941-945
- Stumm W, Morgan JJ (1996) Aquatic Chemistry, 3rd edn. John Wiley & Sons, Inc., New York
- Tiner RW, Lang MW, Klemas VV (eds) (2015) Remote sensing of wetlands: Applications and advances. CRC Press, Boca Raton
- United States Geological Survey (2016) How much of your state is wet? <https://water.usgs.gov/edu/wetstates.html> Cited 21 October, 2017
- Van Meter R, Bailey LL, Campbell Grant, EH (2008) Methods for estimating the amount of vernal pool habitat in the Northeastern United States. *Wetlands* 28:585-593
- Verpoorter C, Kutser T, Seekell DA, Tranvik L (2014) A global inventory of lakes based on high-resolution satellite imagery. *Geophys. Res. Lett.* 41:6396-6402

- Weather Underground (2017) Historical Weather.
<https://www.wunderground.com/history/> Cited June 15 2017
- Weisenberg DA, Guinasso NL (1979) Equilibrium solubilities of methane, carbon monoxide, and hydrogen in water and sea water. *J. Chem. Eng. Data* 24:356-360
- Weiss RF (1974) Carbon dioxide in water and seawater: the solubility of a non-ideal gas. *Mar. Chem.* 2:203-215
- Whalen SC (2005) Biogeochemistry of methane exchange between natural wetlands and the atmosphere. *Environ. Eng. Sci.* 22:73-94
- Williams DD (1996) Environmental constraints in temporary fresh waters and their consequences for the insect fauna. *J. N. Am. Benthol. Soc.* 15:634-650
- Wingham DF, Jordan TE (2003) Isolated wetlands and water quality. *Wetlands* 23:541-549
- Wu Q, Lane C, Liu H (2014) An effective method for detecting potential woodland vernal pools using high-resolution LiDAR data and aerial imagery. *Remote Sens.* 6:11444-11467
- Wuertz D, Setz T, Chalabi Y (2015) timeSeries: R-metrics-financial time series objects. R package version 3022.202.2
- Yavitt JB, Williams CJ, Wieder RK (1997). Production of methane and carbon dioxide in peatland ecosystems across North America: Effects of temperature, aeration, and organic chemistry of peat. *Geomicrobiol J.* 14:299-316
- Yvon-Durocher G, Hulatt CJ, Woodward G, Trimmer M (2017) Long-term warming amplifies shifts in the carbon cycle of experimental ponds. *Nat. Clim. Change* 7:209-213
- Zedler PH (2003) Vernal pools and the concept of “isolated wetlands”. *Wetlands* 23:597-607

APPENDIX A

CH₄ AND CO₂

Table A.1.1. Methane flux. Table of methane flux calculations including the sampled methane in the gaseous and aqueous phase, the Henry's constant for the field temperature, and the supersaturation of CH₄ with respect to the atmosphere.

ID	Date (2016)	CH ₄ meas (ppm)	CH ₄ aq (mol L ⁻¹)	n (mol)	CH ₄ g (mol L ⁻¹)	CH ₄ T (mol L ⁻¹)	K _H (mol L ⁻¹ atm ⁻¹)	Sc _{CH4}	K _{iw}	C _s (mol L ⁻¹)	C (mol L ⁻¹)	flux (mmol m ² d ⁻¹)	super sat
P1	4/25	4.98E+01	6.48E-08	6.15E-08	2.05E-06	2.11E-06	1.76E-03	8.44E+02	5.17E-04	3.24E-09	2.11E-06	9.43E-01	6.52E+02
P2	4/25	2.02E+02	2.63E-07	2.49E-07	8.31E-06	8.58E-06	1.68E-03	7.58E+02	5.56E-04	3.10E-09	8.58E-06	4.12E+00	2.77E+03
P3	4/25	3.48E+01	4.53E-08	4.30E-08	1.43E-06	1.48E-06	1.80E-03	8.91E+02	4.99E-04	3.32E-09	1.48E-06	6.36E-01	4.45E+02
P4	4/25	1.75E+02	2.27E-07	2.16E-07	7.20E-06	7.42E-06	1.84E-03	9.41E+02	4.81E-04	3.40E-09	7.42E-06	3.08E+00	2.18E+03
P3	5/2	1.59E+01	2.06E-08	1.96E-08	6.53E-07	6.74E-07	1.94E-03	1.08E+03	4.39E-04	3.57E-09	6.74E-07	2.54E-01	1.89E+02
P4	5/2	5.47E+01	7.11E-08	6.76E-08	2.25E-06	2.32E-06	2.04E-03	1.17E+03	4.15E-04	3.76E-09	2.32E-06	8.32E-01	6.18E+02
P3	5/11	1.55E+01	2.01E-08	1.91E-08	6.37E-07	6.57E-07	1.61E-03	6.78E+02	5.99E-04	2.97E-09	6.57E-07	3.38E-01	2.21E+02
P4	5/11	7.84E+01	1.02E-07	9.68E-08	3.23E-06	3.33E-06	1.89E-03	9.94E+02	4.63E-04	3.48E-09	3.33E-06	1.33E+00	9.55E+02
P1	5/12	1.01E+02	1.32E-07	1.25E-07	4.16E-06	4.30E-06	1.61E-03	6.78E+02	5.99E-04	2.97E-09	4.30E-06	2.22E+00	1.45E+03
P2	5/12	1.68E+02	2.18E-07	2.07E-07	6.90E-06	7.12E-06	1.61E-03	6.78E+02	5.99E-04	2.97E-09	7.12E-06	3.68E+00	2.40E+03
P3	5/19	3.27E+01	4.25E-08	4.03E-08	1.34E-06	1.39E-06	1.68E-03	7.58E+02	5.56E-04	3.10E-09	1.39E-06	6.65E-01	4.48E+02
P4	5/19	1.15E+02	1.49E-07	1.42E-07	4.72E-06	4.87E-06	1.89E-03	9.94E+02	4.63E-04	3.48E-09	4.87E-06	1.95E+00	1.40E+03
P1	5/20	7.34E+01	9.54E-08	9.06E-08	3.02E-06	3.11E-06	1.49E-03	5.53E+02	6.87E-04	2.74E-09	3.11E-06	1.85E+00	1.14E+03
P2	5/20	3.07E+02	4.00E-07	3.80E-07	1.27E-05	1.31E-05	1.61E-03	6.79E+02	5.99E-04	2.97E-09	1.31E-05	6.75E+00	4.40E+03
P1	5/25	4.99E+01	6.49E-08	6.16E-08	2.05E-06	2.12E-06	1.55E-03	6.10E+02	6.43E-04	2.85E-09	2.12E-06	1.17E+00	7.44E+02
P2	5/25	1.92E+02	2.50E-07	2.37E-07	7.91E-06	8.16E-06	1.49E-03	5.53E+02	6.87E-04	2.74E-09	8.16E-06	4.84E+00	2.98E+03
P3	5/26	6.28E+01	8.16E-08	7.75E-08	2.58E-06	2.66E-06	1.58E-03	6.43E+02	6.21E-04	2.91E-09	2.66E-06	1.43E+00	9.16E+02
P4	5/26	4.27E+02	5.55E-07	5.27E-07	1.76E-05	1.81E-05	1.72E-03	8.00E+02	5.36E-04	3.17E-09	1.81E-05	8.39E+00	5.72E+03
P1	5/31	9.60E+01	1.25E-07	1.19E-07	3.95E-06	4.08E-06	1.55E-03	6.10E+02	6.43E-04	2.85E-09	4.08E-06	2.26E+00	1.43E+03
P2	5/31	1.17E+02	1.53E-07	1.45E-07	4.83E-06	4.98E-06	1.41E-03	4.80E+02	7.55E-04	2.59E-09	4.98E-06	3.25E+00	1.92E+03

Table A.1.1. continued.

P3	6/1	9.22E+00	1.20E-08	1.14E-08	3.79E-07	3.91E-07	1.43E-03	5.03E+02	7.32E-04	2.63E-09	3.91E-07	2.46E-01	1.49E+02
P4	6/1	4.56E+02	5.92E-07	5.62E-07	1.87E-05	1.93E-05	1.68E-03	7.58E+02	5.56E-04	3.09E-09	1.93E-05	9.29E+00	6.26E+03
P3	6/8	8.68E+01	1.13E-07	1.07E-07	3.57E-06	3.68E-06	1.46E-03	5.27E+02	7.09E-04	2.68E-09	3.68E-06	2.26E+00	1.37E+03
P1	6/9	3.55E+01	4.62E-08	4.39E-08	1.46E-06	1.51E-06	1.76E-03	8.44E+02	5.17E-04	3.23E-09	1.51E-06	6.72E-01	4.66E+02
P2	6/9	4.41E+02	5.73E-07	5.44E-07	1.81E-05	1.87E-05	1.72E-03	8.00E+02	5.36E-04	3.16E-09	1.87E-05	8.66E+00	5.92E+03
P3	6/13	1.08E+02	1.40E-07	1.33E-07	4.44E-06	4.58E-06	1.72E-03	8.00E+02	5.36E-04	3.16E-09	4.58E-06	2.12E+00	1.45E+03
P1	6/14	1.77E+02	2.30E-07	2.19E-07	7.29E-06	7.52E-06	1.76E-03	8.44E+02	5.17E-04	3.23E-09	7.52E-06	3.36E+00	2.33E+03
P2	6/14	2.27E+02	2.95E-07	2.80E-07	9.34E-06	9.64E-06	1.72E-03	8.00E+02	5.36E-04	3.16E-09	9.64E-06	4.46E+00	3.05E+03
P3	6/20	1.44E+03	1.87E-06	1.78E-06	5.92E-05	6.11E-05	1.41E-03	4.80E+02	7.55E-04	2.59E-09	6.11E-05	3.98E+01	2.36E+04
P4	6/20	1.49E+03	1.94E-06	1.84E-06	6.15E-05	6.34E-05	1.72E-03	8.00E+02	5.36E-04	3.16E-09	6.34E-05	2.94E+01	2.01E+04
P2	6/21	2.90E+01	3.77E-08	3.58E-08	1.19E-06	1.23E-06	1.49E-03	5.53E+02	6.87E-04	2.73E-09	1.23E-06	7.28E-01	4.50E+02
P2	6/29	2.05E+01	2.67E-08	2.53E-08	8.45E-07	8.71E-07	1.58E-03	6.43E+02	6.21E-04	2.90E-09	8.71E-07	4.66E-01	3.00E+02
P3	7/5	1.48E+02	1.93E-07	1.83E-07	6.11E-06	6.30E-06	1.36E-03	4.37E+02	8.04E-04	2.49E-09	6.30E-06	4.38E+00	2.53E+03
P4	7/5	8.32E+01	1.08E-07	1.03E-07	3.42E-06	3.53E-06	1.58E-03	6.43E+02	6.21E-04	2.89E-09	3.53E-06	1.89E+00	1.22E+03
P2	7/6	8.58E+02	1.12E-06	1.06E-06	3.53E-05	3.64E-05	1.38E-03	4.58E+02	7.79E-04	2.53E-09	3.64E-05	2.45E+01	1.44E+04
P3	7/13	1.84E+03	2.40E-06	2.28E-06	7.59E-05	7.83E-05	1.29E-03	3.64E+02	9.09E-04	2.37E-09	7.83E-05	6.15E+01	3.30E+04
P4	7/13	3.01E+02	3.92E-07	3.72E-07	1.24E-05	1.28E-05	1.58E-03	6.43E+02	6.21E-04	2.89E-09	1.28E-05	6.86E+00	4.42E+03
P2	7/14	2.11E+03	2.74E-06	2.60E-06	8.68E-05	8.95E-05	1.38E-03	4.58E+02	7.79E-04	2.53E-09	8.95E-05	6.03E+01	3.53E+04
P3	7/19	1.45E+03	1.88E-06	1.79E-06	5.96E-05	6.15E-05	1.29E-03	3.80E+02	8.83E-04	2.37E-09	6.15E-05	4.69E+01	2.59E+04
P4	7/19	1.20E+02	1.56E-07	1.48E-07	4.94E-06	5.10E-06	1.61E-03	6.79E+02	5.99E-04	2.95E-09	5.10E-06	2.63E+00	1.73E+03
P2	7/20	3.00E+03	3.90E-06	3.70E-06	1.23E-04	1.27E-04	1.52E-03	5.80E+02	6.65E-04	2.78E-09	1.27E-04	7.31E+01	4.58E+04
P2	7/28	5.63E+02	7.31E-07	6.95E-07	2.32E-05	2.39E-05	1.29E-03	3.80E+02	8.83E-04	2.37E-09	2.39E-05	1.82E+01	1.01E+04

Table A.1.2. Carbon dioxide flux. Table of CO₂ flux calculations including the sampled methane in the gaseous and aqueous phase, the Henry's constant for the field temperature, and the supersaturation of CO₂ with respect to the atmosphere.

ID	Date (2016)	CO ₂ meas (ppm)	CO ₂ aq (mol L ⁻¹)	n (mol)	CO ₂ g (mol L ⁻¹)	CO ₂ T (mol L ⁻¹)	K _H (mol L ⁻¹ atm ⁻¹)	S _{cCO2}	K _{lw}	C _s (mol L ⁻¹)	C (mol L ⁻¹)	flux (mmol m ⁻² d ⁻¹)	super sat
P1	4/25	2.53E+03	8.84E-05	3.12E-06	1.04E-04	1.92E-04	4.70E-02	8.25E+02	5.25E-04	1.91E-05	1.92E-04	7.86E+01	1.00E+01
P2	4/25	2.37E+03	8.29E-05	2.92E-06	9.75E-05	1.80E-04	4.41E-02	7.39E+02	5.65E-04	1.80E-05	1.80E-04	7.93E+01	1.00E+01
P3	4/25	2.14E+03	7.49E-05	2.64E-06	8.81E-05	1.63E-04	4.86E-02	8.74E+02	5.05E-04	1.98E-05	1.63E-04	6.26E+01	8.24E+00
P4	4/25	5.70E+03	1.99E-04	7.03E-06	2.34E-04	4.34E-04	5.02E-02	9.82E+02	4.67E-04	2.04E-05	4.34E-04	1.67E+02	2.12E+01
P3	5/2	1.33E+03	4.65E-05	1.64E-06	5.47E-05	1.01E-04	5.34E-02	1.07E+03	4.41E-04	2.18E-05	1.01E-04	3.03E+01	4.65E+00
P4	5/2	3.96E+03	1.39E-04	4.89E-06	1.63E-04	3.02E-04	5.75E-02	1.17E+03	4.16E-04	2.34E-05	3.02E-04	1.00E+02	1.29E+01
P3	5/11	1.28E+03	4.48E-05	1.58E-06	5.27E-05	9.75E-05	4.15E-02	6.65E+02	6.07E-04	1.69E-05	9.75E-05	4.22E+01	5.76E+00
P4	5/11	3.11E+03	1.09E-04	3.83E-06	1.28E-04	2.37E-04	5.19E-02	9.82E+02	4.67E-04	2.12E-05	2.37E-04	8.70E+01	1.12E+01
P1	5/12	3.65E+03	1.28E-04	4.50E-06	1.50E-04	2.78E-04	4.15E-02	6.65E+02	6.07E-04	1.69E-05	2.78E-04	1.37E+02	1.64E+01
P2	5/12	4.48E+03	1.57E-04	5.53E-06	1.84E-04	3.41E-04	4.15E-02	6.65E+02	6.07E-04	1.69E-05	3.41E-04	1.70E+02	2.02E+01
P3	5/19	1.35E+03	4.73E-05	1.67E-06	5.56E-05	1.03E-04	4.41E-02	7.39E+02	5.65E-04	1.80E-05	1.03E-04	4.15E+01	5.72E+00
P4	5/19	4.07E+03	1.42E-04	5.02E-06	1.67E-04	3.10E-04	5.19E-02	9.82E+02	4.67E-04	2.12E-05	3.10E-04	1.17E+02	1.46E+01
P1	5/20	2.74E+03	9.58E-05	3.38E-06	1.13E-04	2.09E-04	3.91E-02	5.43E+02	6.95E-04	1.59E-05	2.09E-04	1.16E+02	1.31E+01
P2	5/20	4.49E+03	1.57E-04	5.54E-06	1.85E-04	3.42E-04	4.15E-02	6.65E+02	6.07E-04	1.69E-05	3.42E-04	1.70E+02	2.02E+01
P1	5/25	1.31E+03	4.59E-05	1.62E-06	5.39E-05	9.98E-05	3.91E-02	6.00E+02	6.50E-04	1.59E-05	9.98E-05	4.71E+01	6.26E+00
P2	5/25	2.18E+03	7.64E-05	2.69E-06	8.98E-05	1.66E-04	3.69E-02	5.43E+02	6.95E-04	1.50E-05	1.66E-04	9.07E+01	1.10E+01
P3	5/26	1.81E+03	6.35E-05	2.24E-06	7.46E-05	1.38E-04	4.03E-02	6.31E+02	6.28E-04	1.64E-05	1.38E-04	6.61E+01	8.41E+00
P4	5/26	5.68E+03	1.99E-04	7.01E-06	2.34E-04	4.32E-04	4.56E-02	7.80E+02	5.45E-04	1.86E-05	4.32E-04	1.95E+02	2.33E+01
P1	5/31	2.93E+03	1.02E-04	3.62E-06	1.21E-04	2.23E-04	3.49E-02	6.00E+02	6.50E-04	1.42E-05	2.23E-04	1.17E+02	1.57E+01
P2	5/31	2.95E+03	1.03E-04	3.64E-06	1.21E-04	2.25E-04	3.40E-02	4.70E+02	7.66E-04	1.39E-05	2.25E-04	1.39E+02	1.62E+01
P3	6/1	1.61E+03	5.63E-05	1.98E-06	6.62E-05	1.22E-04	3.49E-02	4.93E+02	7.41E-04	1.42E-05	1.22E-04	6.93E+01	8.62E+00
P4	6/1	5.97E+03	2.09E-04	7.37E-06	2.46E-04	4.54E-04	4.41E-02	7.39E+02	5.65E-04	1.79E-05	4.54E-04	2.13E+02	2.53E+01

Table A.1.2. continued.

P3	6/8	1.97E+03	6.89E-05	2.43E-06	8.11E-05	1.50E-04	3.55E-02	5.18E+02	7.18E-04	1.44E-05	1.50E-04	8.41E+01	1.04E+01
P1	6/9	4.29E+03	1.50E-04	5.29E-06	1.76E-04	3.27E-04	4.70E-02	8.25E+02	5.25E-04	1.91E-05	3.27E-04	1.40E+02	1.71E+01
P2	6/9	4.60E+03	1.61E-04	5.68E-06	1.89E-04	3.50E-04	4.56E-02	7.80E+02	5.45E-04	1.85E-05	3.50E-04	1.56E+02	1.89E+01
P3	6/13	1.72E+03	6.03E-05	2.13E-06	7.09E-05	1.31E-04	4.56E-02	7.80E+02	5.45E-04	1.85E-05	1.31E-04	5.31E+01	7.08E+00
P1	6/14	4.32E+03	1.51E-04	5.33E-06	1.78E-04	3.29E-04	4.70E-02	8.25E+02	5.25E-04	1.91E-05	3.29E-04	1.41E+02	1.72E+01
P2	6/14	4.11E+03	1.44E-04	5.07E-06	1.69E-04	3.13E-04	4.56E-02	7.80E+02	5.45E-04	1.85E-05	3.13E-04	1.39E+02	1.69E+01
P3	6/20	1.18E+04	4.14E-04	1.46E-05	4.87E-04	9.01E-04	3.40E-02	4.70E+02	7.66E-04	1.38E-05	9.01E-04	5.87E+02	6.52E+01
P4	6/20	8.08E+03	2.83E-04	9.97E-06	3.32E-04	6.15E-04	4.56E-02	7.80E+02	5.45E-04	1.85E-05	6.15E-04	2.81E+02	3.32E+01
P2	6/21	3.26E+03	1.14E-04	4.02E-06	1.34E-04	2.48E-04	3.69E-02	5.43E+02	6.95E-04	1.50E-05	2.48E-04	1.40E+02	1.65E+01
P2	6/29	9.43E+02	3.30E-05	1.16E-06	3.88E-05	7.18E-05	4.03E-02	6.31E+02	6.28E-04	1.64E-05	7.18E-05	3.01E+01	4.38E+00
P3	7/5	2.93E+03	1.02E-04	3.61E-06	1.20E-04	2.23E-04	3.22E-02	4.27E+02	8.17E-04	1.30E-05	2.23E-04	1.48E+02	1.71E+01
P4	7/5	7.66E+03	2.68E-04	9.46E-06	3.15E-04	5.83E-04	4.03E-02	6.31E+02	6.28E-04	1.63E-05	5.83E-04	3.08E+02	3.58E+01
P2	7/6	3.90E+03	1.37E-04	4.82E-06	1.61E-04	2.97E-04	3.31E-02	4.48E+02	7.91E-04	1.34E-05	2.97E-04	1.94E+02	2.22E+01
P3	7/13	5.69E+03	1.99E-04	7.03E-06	2.34E-04	4.33E-04	2.91E-02	3.54E+02	9.26E-04	1.18E-05	4.33E-04	3.37E+02	3.68E+01
P4	7/13	8.41E+03	2.94E-04	1.04E-05	3.46E-04	6.41E-04	4.03E-02	6.31E+02	6.28E-04	1.63E-05	6.41E-04	3.39E+02	3.93E+01
P2	7/14	8.37E+03	2.93E-04	1.03E-05	3.45E-04	6.38E-04	3.31E-02	4.48E+02	7.91E-04	1.34E-05	6.38E-04	4.27E+02	4.77E+01
P3	7/19	6.10E+03	2.14E-04	7.53E-06	2.51E-04	4.65E-04	2.98E-02	3.70E+02	8.99E-04	1.21E-05	4.65E-04	3.51E+02	3.85E+01
P4	7/19	5.63E+03	1.97E-04	6.94E-06	2.31E-04	4.28E-04	4.15E-02	6.65E+02	6.07E-04	1.68E-05	4.28E-04	2.16E+02	2.55E+01
P2	7/20	7.78E+03	2.72E-04	9.60E-06	3.20E-04	5.92E-04	3.80E-02	5.71E+02	6.72E-04	1.54E-05	5.92E-04	3.35E+02	3.85E+01
P2	7/28	4.99E+03	1.75E-04	6.17E-06	2.06E-04	3.80E-04	2.98E-02	3.70E+02	8.99E-04	1.21E-05	3.80E-04	2.86E+02	3.15E+01

Table A.1.3. Net production of CH₄ in P1. Production was calculated using the mass of carbon in the pool, the surface area, groundwater area, pool volume, and groundwater velocity. Change in mass in the vernal pool, mass leaving through groundwater, mass lost to evaporative flux, and net production was calculated.

date	CH ₄ pool avg (g C)	flux week avg (mmol m ⁻² d ⁻¹)	SA week avg (m ²)	GW area week avg (m ²)	V week avg (m ³)	velocity week avg (m s ⁻¹)	dm/dt (gC d ⁻¹)	QC _{out} (gC d ⁻¹)	R _{ef} (gC d ⁻¹)	R _p (gC d ⁻¹)	prod rate (gC m ⁻² d ⁻¹)
4/25	6.86E-01										
5/12	3.23E+00	1.58E+00	1.77E+02	2.24E+01	1.52E+01	-1.47E-06	1.50E-01	3.69E-01	3.36E+00	3.88E+00	2.19E-02
5/20	3.29E+00	2.03E+00	1.67E+02	2.04E+01	1.27E+01	-1.44E-06	7.38E-03	6.55E-01	4.06E+00	4.73E+00	2.84E-02
5/25	7.01E+00	1.51E+00	1.44E+02	1.64E+01	8.13E+00	-1.41E-06	7.44E-01	1.27E+00	2.61E+00	4.62E+00	3.21E-02
5/31	6.01E-01	1.72E+00	9.62E+01	1.17E+01	3.57E+00	-1.31E-06	-1.07E+00	1.41E+00	1.98E+00	2.32E+00	2.41E-02
6/9	7.28E-02	1.47E+00	5.15E+01	1.12E+01	3.06E+00	-1.15E-06	-5.87E-02	1.22E-01	9.06E-01	9.70E-01	1.88E-02
6/14	4.38E+00	2.02E+00	4.67E+01	1.33E+01	4.62E+00	-1.13E-06	8.61E-01	6.26E-01	1.13E+00	2.62E+00	5.60E-02

Table A.1.4. Net production of CO₂ in P1. Production was calculated using the mass of carbon in the pool, the surface area, groundwater area, pool volume, and groundwater velocity. Change in mass in the vernal pool, mass leaving through groundwater, mass lost to evaporative flux, and net production was calculated.

date	CO ₂ pool avg (g C)	flux week avg (mmol m ⁻² d ⁻¹)	SA week avg (m ²)	GW area week avg (m ²)	V week avg (m ³)	velocity week avg (m s ⁻¹)	dm/dt (gC d ⁻¹)	QC _{out} (gC d ⁻¹)	R _{ef} (gC d ⁻¹)	R _p (gC d ⁻¹)	prod rate (gC m ⁻² d ⁻¹)
4/25	4.09E+01										
5/12	6.32E+01	1.08E+02	1.77E+02	2.24E+01	1.52E+01	-1.46E-06	1.32E+00	9.71E+00	2.29E+02	2.40E+02	1.35E+00
5/20	4.17E+01	1.26E+02	1.72E+02	2.04E+01	1.27E+01	-1.41E-06	-2.68E+00	1.03E+01	2.60E+02	2.68E+02	1.56E+00
5/25	3.04E+01	8.13E+01	1.44E+02	1.64E+01	8.13E+00	-1.31E-06	-2.28E+00	8.23E+00	1.41E+02	1.47E+02	1.02E+00
5/31	6.38E+00	8.22E+01	9.62E+01	1.17E+01	3.57E+00	-1.15E-06	-4.00E+00	5.98E+00	9.49E+01	9.69E+01	1.01E+00
6/9	1.67E+01	1.28E+02	5.15E+01	1.12E+01	3.06E+00	-1.13E-06	1.15E+00	4.12E+00	7.93E+01	8.45E+01	1.64E+00
6/14	4.95E+01	1.40E+02	4.67E+01	1.33E+01	4.62E+00	-1.21E-06	6.56E+00	9.93E+00	7.85E+01	9.50E+01	2.03E+00

Table A.1.5. Net production of CH₄ in P2. Production was calculated using the mass of carbon in the pool, the surface area, groundwater area, pool volume, and groundwater velocity. Change in mass in the vernal pool, mass leaving through groundwater, mass lost to evaporative flux, and net production was calculated.

date	CH ₄ pool avg (g C)	flux week avg (mmol m ⁻² d ⁻¹)	SA week avg (m ²)	GW area week avg (m ²)	V week avg (m ³)	velocity week avg (m s ⁻¹)	dm/dt (gC d ⁻¹)	QC _{out} (gC d ⁻¹)	R _{ef} (gC d ⁻¹)	R _p (gC d ⁻¹)	prod rate (gC m ⁻² d ⁻¹)
4/25	4.28E+01										
5/12	4.40E+01	3.90E+00	2.19E+02	2.54E+01	3.85E+01	0	6.98E-02	0.00E+00	1.02E+01	1.03E+01	4.71E-02
5/20	5.99E+01	5.21E+00	2.19E+02	2.54E+01	4.12E+01	0	2.00E+00	0.00E+00	1.37E+01	1.57E+01	7.17E-02
5/25	5.30E+01	5.80E+00	2.00E+02	2.43E+01	3.97E+01	0	-1.38E+00	0.00E+00	1.39E+01	1.25E+01	6.26E-02
5/31	1.67E+01	4.05E+00	1.73E+02	2.25E+01	3.51E+01	0	-6.06E+00	0.00E+00	8.39E+00	2.34E+00	1.35E-02
6/9	4.52E+01	5.96E+00	1.73E+02	2.25E+01	2.87E+01	0	3.17E+00	0.00E+00	1.23E+01	1.55E+01	8.98E-02
6/14	3.04E+01	6.56E+00	1.95E+02	2.40E+01	2.86E+01	0	-2.97E+00	0.00E+00	1.54E+01	1.24E+01	6.36E-02
6/21	3.87E+01	2.60E+00	1.79E+02	2.29E+01	3.38E+01	0	1.19E+00	0.00E+00	5.59E+00	6.78E+00	3.78E-02
6/29	2.20E+00	5.97E-01	1.46E+02	2.06E+01	2.96E+01	0	-4.57E+00	0.00E+00	1.05E+00	-3.52E+00	-2.41E-02
7/6	9.80E+01	1.25E+01	1.40E+02	2.02E+01	2.12E+01	0	1.37E+01	0.00E+00	2.11E+01	3.48E+01	2.47E-01
7/14	1.95E+02	4.24E+01	1.45E+02	2.05E+01	1.95E+01	0	1.21E+01	0.00E+00	7.36E+01	8.57E+01	5.92E-01
7/20	3.70E+02	6.67E+01	1.51E+02	2.10E+01	2.08E+01	0	2.93E+01	0.00E+00	1.21E+02	1.50E+02	9.94E-01
7/28	5.57E+01	4.57E+01	1.33E+02	1.96E+01	2.26E+01	0	-3.93E+01	0.00E+00	7.30E+01	3.37E+01	2.53E-01

Table A.1.6. Net production of CO₂ in P2. Production was calculated using the mass of carbon in the pool, the surface area, groundwater area, pool volume, and groundwater velocity. Change in mass in the vernal pool, mass leaving through groundwater, mass lost to evaporative flux, and net production was calculated.

date	CO ₂ pool avg (g C)	flux week avg (mmol m ⁻² d ⁻¹)	SA week avg (m ²)	GW area week avg (m ²)	V week avg (m ³)	velocity week avg (m s ⁻¹)	dm/dt (gC d ⁻¹)	QC _{out} (gC d ⁻¹)	R _{ef} (gC d ⁻¹)	R _p (gC d ⁻¹)	prod rate (gC m ⁻² d ⁻¹)
4/25	1.20E+02										
5/12	1.70E+02	1.25E+02	2.19E+02	2.54E+01	3.85E+01	0	2.96E+00	0.00E+00	3.28E+02	3.31E+02	1.51E+00
5/20	1.57E+02	1.70E+02	2.19E+02	2.54E+01	3.98E+01	0	-1.69E+00	0.00E+00	4.46E+02	4.45E+02	2.03E+00
5/25	1.13E+02	1.31E+02	2.00E+02	2.43E+01	3.97E+01	0	-8.84E+00	0.00E+00	3.13E+02	3.05E+02	1.52E+00
5/31	9.31E+01	1.15E+02	1.73E+02	2.25E+01	3.51E+01	0	-3.25E+00	0.00E+00	2.39E+02	2.36E+02	1.36E+00
6/9	1.17E+02	1.48E+02	1.73E+02	2.25E+01	2.87E+01	0	2.61E+00	0.00E+00	3.06E+02	3.09E+02	1.79E+00
6/14	1.58E+02	1.47E+02	1.95E+02	2.40E+01	2.86E+01	0	8.26E+00	0.00E+00	3.45E+02	3.54E+02	1.81E+00
6/21	7.94E+01	1.39E+02	1.79E+02	2.29E+01	3.38E+01	0	-1.12E+01	0.00E+00	3.00E+02	2.89E+02	1.61E+00
6/29	1.96E+01	8.50E+01	1.46E+02	2.06E+01	2.96E+01	0	-7.47E+00	0.00E+00	1.49E+02	1.42E+02	9.69E-01
7/6	7.67E+01	1.12E+02	1.40E+02	2.02E+01	2.12E+01	0	8.16E+00	0.00E+00	1.89E+02	1.97E+02	1.40E+00
7/14	1.38E+02	3.10E+02	1.45E+02	2.05E+01	1.95E+01	0	7.62E+00	0.00E+00	5.39E+02	5.46E+02	3.77E+00
7/20	1.73E+02	3.81E+02	1.51E+02	2.10E+01	2.08E+01	0	5.81E+00	0.00E+00	6.89E+02	6.95E+02	4.61E+00
7/28	6.35E+01	3.10E+02	1.33E+02	1.96E+01	2.26E+01	0	-1.36E+01	0.00E+00	4.96E+02	4.83E+02	3.62E+00

Table A.1.7. Net production of CH₄ in P3. Production was calculated using the mass of carbon in the pool, the surface area, groundwater area, pool volume, and groundwater velocity. Change in mass in the vernal pool, mass leaving through groundwater, mass lost to evaporative flux, and net production was calculated.

date	CH ₄ pool avg (g C)	flux week avg (mmol m ⁻² d ⁻¹)	SA week avg (m ²)	GW area week avg (m ²)	V week avg (m ³)	velocity week avg (m s ⁻¹)	dm/dt (gC d ⁻¹)	QC _{out} (gC d ⁻¹)	R _{ef} (gC d ⁻¹)	R _p (gC d ⁻¹)	prod rate (gC m ⁻² d ⁻¹)
4/25	3.54E+01										
5/2	2.81E+01	4.45E-01	2.69E+03	1.81E+02	1.46E+03	-3.74E-07	-1.04E+00	1.27E-01	1.44E+01	1.35E+01	5.00E-03
5/11	1.39E+01	2.96E-01	2.46E+03	1.73E+02	1.18E+03	-4.14E-07	-1.58E+00	1.10E-01	8.75E+00	7.28E+00	2.96E-03
5/19	1.38E+01	5.02E-01	2.09E+03	1.59E+02	8.81E+02	-4.31E-07	-1.02E-02	9.29E-02	1.26E+01	1.27E+01	6.06E-03
5/26	2.04E+01	1.05E+00	1.65E+03	1.41E+02	6.09E+02	-4.42E-07	9.42E-01	1.51E-01	2.08E+01	2.19E+01	1.32E-02
6/1	3.93E+00	8.37E-01	1.30E+03	1.25E+02	4.10E+02	-4.78E-07	-2.75E+00	1.53E-01	1.31E+01	1.05E+01	8.05E-03
6/8	8.53E+00	1.25E+00	1.03E+03	1.10E+02	2.70E+02	-5.77E-07	6.58E-01	1.27E-01	1.54E+01	1.62E+01	1.58E-02
6/13	4.92E+00	2.19E+00	7.92E+02	9.64E+01	1.69E+02	-6.42E-07	-7.22E-01	2.13E-01	2.08E+01	2.03E+01	2.56E-02
6/20	2.34E+01	2.10E+01	5.58E+02	8.01E+01	8.89E+01	-6.42E-07	2.64E+00	7.07E-01	1.41E+02	1.44E+02	2.58E-01
7/5	3.29E-01	2.21E+01	4.35E+02	4.66E+01	2.62E+01	-6.42E-07	-1.54E+00	1.17E+00	1.15E+02	1.15E+02	2.64E-01
7/13	1.15E+00	3.29E+01	5.17E+01	2.14E+01	2.41E+00	-6.42E-07	1.03E-01	3.64E-01	2.04E+01	2.09E+01	4.04E-01
7/19	1.08E+00	5.42E+01	4.79E+01	1.92E+01	1.82E+00	-6.42E-07	-1.28E-02	6.52E-01	3.12E+01	3.18E+01	6.63E-01

Table A.1.8. Net production of CO₂ in P3. Production was calculated using the mass of carbon in the pool, the surface area, groundwater area, pool volume, and groundwater velocity. Change in mass in the vernal pool, mass leaving through groundwater, mass lost to evaporative flux, and net production was calculated.

date	CO ₂ pool avg (g C)	flux week avg (mmol m ⁻² d ⁻¹)	SA week avg (m ²)	GW area week avg (m ²)	V week avg (m ³)	velocity week avg (m s ⁻¹)	dm/dt (gC d ⁻¹)	QC _{out} (gC d ⁻¹)	R _{ef} (gC d ⁻¹)	R _p (gC d ⁻¹)	prod rate (gC m ⁻² d ⁻¹)
4/25	3.25E+03										
5/2	2.27E+03	4.64E+01	2.69E+03	1.81E+02	1.46E+03	-3.74E-07	-1.40E+02	1.10E+01	1.50E+03	1.37E+03	5.09E-01
5/11	1.38E+03	3.62E+01	2.46E+03	1.73E+02	1.18E+03	-4.14E-07	-9.89E+01	9.54E+00	1.07E+03	9.81E+02	3.99E-01
5/19	9.59E+02	4.19E+01	2.09E+03	1.59E+02	8.81E+02	-4.31E-07	-5.24E+01	7.85E+00	1.05E+03	1.01E+03	4.81E-01
5/26	9.46E+02	5.38E+01	1.65E+03	1.41E+02	6.09E+02	-4.42E-07	-1.86E+00	8.41E+00	1.07E+03	1.07E+03	6.49E-01
6/1	6.33E+02	6.77E+01	1.30E+03	1.25E+02	4.10E+02	-4.78E-07	-5.22E+01	9.92E+00	1.06E+03	1.02E+03	7.80E-01
6/8	3.54E+02	7.67E+01	1.03E+03	1.10E+02	2.70E+02	-5.77E-07	-3.99E+01	1.01E+01	9.46E+02	9.16E+02	8.91E-01
6/13	1.79E+02	6.86E+01	7.92E+02	9.64E+01	1.69E+02	-6.42E-07	-3.51E+01	8.42E+00	6.52E+02	6.25E+02	7.89E-01
6/20	3.35E+02	3.20E+02	5.58E+02	8.01E+01	8.89E+01	-6.42E-07	2.23E+01	1.28E+01	2.14E+03	2.18E+03	3.90E+00
7/5	8.57E+00	3.67E+02	2.43E+02	4.66E+01	2.62E+01	-6.42E-07	-2.18E+01	1.69E+01	1.07E+03	1.07E+03	4.39E+00
7/13	9.86E+00	2.43E+02	4.79E+01	2.14E+01	2.41E+00	-6.42E-07	1.62E-01	4.53E+00	1.40E+02	1.44E+02	3.01E+00
7/19	1.25E+01	3.44E+02	3.99E+01	1.92E+01	1.82E+00	-6.42E-07	4.43E-01	6.54E+00	1.65E+02	1.72E+02	4.31E+00

Table A.1.9. Net production of CH₄ in P4. Production was calculated using the mass of carbon in the pool, the surface area, groundwater area, pool volume, and groundwater velocity. Change in mass in the vernal poop, mass leaving through groundwater, mass lost to evaporative flux, and net production was calculated.

date	CH ₄ pool avg (g C)	flux week avg (mmol m ⁻² d ⁻¹)	SA week avg (m ²)	GW area week avg (m ²)	V week avg (m ³)	velocity week avg (m s ⁻¹)	dm/dt (gC d ⁻¹)	QC _{out} (gC d ⁻¹)	R _{ef} (gC d ⁻¹)	R _p (gC d ⁻¹)	prod rate (gC m ⁻² d ⁻¹)
4/25	8.09E+00										
5/2	8.52E+00	1.96E+00	4.12E+02	3.52E+01	8.63E+01	-2.40E-07	6.16E-02	7.02E-02	9.68E+00	9.82E+00	2.38E-02
5/11	3.93E+01	1.08E+00	4.07E+02	3.50E+01	8.44E+01	-2.52E-07	3.42E+00	2.16E-01	5.28E+00	8.92E+00	2.19E-02
5/19	1.56E+01	1.64E+00	4.00E+02	3.46E+01	8.17E+01	-2.51E-07	-2.96E+00	2.53E-01	7.86E+00	5.16E+00	1.29E-02
5/26	5.33E+01	5.17E+00	3.65E+02	3.31E+01	6.95E+01	-2.76E-07	5.38E+00	3.91E-01	2.27E+01	2.84E+01	7.79E-02
6/1	5.77E+01	8.84E+00	3.24E+02	3.11E+01	5.61E+01	-2.96E-07	7.35E-01	7.88E-01	3.44E+01	3.59E+01	1.11E-01
6/20	1.53E+01	1.93E+01	2.81E+02	2.89E+01	4.39E+01	-2.96E-07	-2.23E+00	6.15E-01	6.53E+01	6.37E+01	2.26E-01
7/5	1.78E+00	1.56E+01	2.16E+02	2.51E+01	2.94E+01	-1.98E-07	-9.03E-01	1.25E-01	4.04E+01	3.96E+01	1.84E-01
7/13	1.90E+00	4.38E+00	1.43E+02	2.03E+01	1.58E+01	-1.18E-07	1.57E-02	2.41E-02	7.51E+00	7.55E+00	5.28E-02
7/19	4.29E-01	4.75E+00	1.06E+02	1.74E+01	9.64E+00	-1.37E-07	-2.46E-01	2.49E-02	6.01E+00	5.79E+00	5.49E-02

Table A.1.10. Net production of CO₂ in P4 Production was calculated using the mass of carbon in the pool, the surface area, groundwater area, pool volume, and groundwater velocity. Change in mass in the vernal pool, mass leaving through groundwater, mass lost to evaporative flux, and net production was calculated.

date	CO ₂ pool avg (g C)	flux week avg (mmol m ⁻² d ⁻¹)	SA week avg (m ²)	GW area week avg (m ²)	V week avg (m ³)	velocity week avg (m s ⁻¹)	dm/dt (gC d ⁻¹)	QC _{out} (gC d ⁻¹)	R _{ef} (gC d ⁻¹)	R _p (gC d ⁻¹)	prod rate (gC m ⁻² d ⁻¹)
4/25	4.73E+02										
5/2	6.75E+02	1.34E+02	4.12E+02	3.52E+01	8.63E+01	-2.40E-07	2.89E+01	4.85E+00	6.61E+02	6.95E+02	1.68E+00
5/11	8.90E+02	9.36E+01	4.07E+02	3.50E+01	8.44E+01	-2.52E-07	2.38E+01	7.06E+00	4.57E+02	4.88E+02	1.20E+00
5/19	4.55E+02	1.02E+02	4.00E+02	3.46E+01	8.17E+01	-2.51E-07	-5.43E+01	6.19E+00	4.88E+02	4.40E+02	1.10E+00
5/26	1.04E+03	1.56E+02	3.65E+02	3.31E+01	6.95E+01	-2.76E-07	8.35E+01	8.48E+00	6.82E+02	7.74E+02	2.12E+00
6/1	7.13E+02	2.04E+02	3.24E+02	3.11E+01	5.61E+01	-2.96E-07	-5.44E+01	1.24E+01	7.95E+02	7.53E+02	2.32E+00
6/20	2.15E+02	2.47E+02	2.81E+02	2.89E+01	4.39E+01	-2.96E-07	-2.62E+01	7.82E+00	8.35E+02	8.16E+02	2.90E+00
7/5	1.52E+02	2.94E+02	2.16E+02	2.51E+01	2.94E+01	-1.98E-07	-4.19E+00	2.68E+00	7.61E+02	7.60E+02	3.53E+00
7/13	7.40E+01	3.23E+02	1.43E+02	2.03E+01	1.58E+01	-1.18E-07	-9.79E+00	1.48E+00	5.55E+02	5.47E+02	3.82E+00
7/19	4.39E+01	2.77E+02	1.06E+02	1.74E+01	9.64E+00	-1.37E-07	-5.03E+00	1.26E+00	3.51E+02	3.47E+02	3.29E+00

APPENDIX B

TEMPORAL TRENDS IN WATER CHEMISTRY FOR

FOUR VERNAL POOLS IN ME, USA

B2.1. Methods

B2.1.1. Study Area

We studied four vernal pools in Maine, USA (Figure 1.1). P1 and P2 are located on the Presumpscot Formation (Table 1.1), a low permeability glacio-marine silt/clay. P1 and P2 are in Bangor, Maine, ~200 m from surrounding areas of human activity and moderate landscape modification. P1 is in a closed canopy, dominantly deciduous forest. P2 has an open canopy, with shrubs and emergent aquatic vegetation as the dominant cover. Part of the P2 watershed was in open fields and is now regenerating to forest. P3 is located on a sand and gravel esker in a minimally modified landscape located ~100 m from a gravel road used by logging trucks. P3 is very large and so is open canopy with a mixed deciduous and coniferous forest surrounding the pool. P4 is located on thin glacial till and is in a managed forest ~1 km from routine human activity or development, but ~10 m from a logging road. This site has closed canopy with dominantly deciduous forest cover. All sites have been logged but P1, P2, and P3 have not been cut for at least 25 years.

Spring 2016 was a relatively dry year. During the study period, Bangor, ME (near to P1, P2, and P4) and Osborn, ME (near to P3) received 6.1, 6.1, 9.2, and 13.2 cm of precipitation in April, May, June, and July, respectively. The 1981 to 2010 normal monthly precipitation is 9.2, 9.2, 9.6, and 8.8 cm in April, May, June, and July, respectively (National Weather Service 2017). The four pools had varying hydroperiods. In 2016, P1 had a maximum volume of 31 m³ and P2 had a maximum volume of 58 m³

(Table 1.1.). P3 was the largest of the pools, with an estimated maximum high water volume of 2930 m³. P4 had a maximum volume of 126 m³ (Table 1.1.; Straka, 2017). All four pools were at their greatest extent in March. P1 was dry by Julian day 173, P2 was dry by Julian day 216, and P3 and P4 were dry by Julian day 209.

B2.1.2. Field Methods

Water in all pools was sampled at the deepest point, with the exception of P3, which was sampled at a depth of 1.25 m until later in the season when the deepest section was more accessible. Sampling locations were marked with a stake. Two lengths of Tygon™ tubing were attached to each stake, one fixed at ~5 cm from the bottom sediment of the pool, and one floating ~5 cm below the water surface. The floating tube was attached to a fishing bobber so that the tube inlet would fluctuate with the water level. These two tubes allowed for remote sampling of benthic and surface waters of the pools. Water was sampled through the tubes using a hand held vacuum pump to avoid disturbing the pool sediments and water chemistry.

We sampled from each pool at a minimum of every 10 days from ice-out in late April until the pools dried completely in June or July. Temperature was measured by a glass thermometer from the edge of the pool. The measurements were taken at the shore, progressing into the center of the pool as the water level decreased. Aqueous samples for dissolved oxygen (DO), closed cell pH, ortho-phosphate (ortho-P), nitrate (NO₃⁻), ammonium (NH₄⁺), chloride (Cl⁻), sulfate (SO₄²⁻), sodium (Na⁺), potassium (K⁺), magnesium (Mg²⁺), calcium (Ca²⁺), dissolved organic carbon (DOC), alkalinity, chlorophyll *a* (chl *a*), speciated aluminum (Al), speciated iron (Fe), speciated manganese (Mn), and speciated silicon (Si) were obtained from the surface and benthic tubes.

Samples from each pool were taken at approximately the same time of day to minimize variation caused by diurnal fluctuations. Immediately after collection, all samples were placed on ice in the dark prior to their laboratory analysis.

We sampled dissolved oxygen (DO) directly from the tubing with a 100 mL syringe with no air contact. The 100 mL DO sample was flushed into a 60 mL BOD bottle via a tube that extended to the bottom of the bottle. We measured DO using a YSI 5100 Dissolved Oxygen Meter the same day as sample collection. We also sampled pH directly from the tubing using a sealable 60 mL syringe. These samples were passed through a Cole-Parmer 800 μ L closed flow-through cell equipped with a Cole-Parmer combination, double junction pH electrode.

Samples for ortho-P, NO_3^- and NH_4^+ were filtered through a 0.45 μ m membrane (Whatman Puradisc 0.45 μ m polypropylene) into a 50 mL centrifuge tube. Samples were analyzed at the Analytical Laboratory and Maine Soil Testing Service at the University of Maine. Ortho-P concentration was determined by colorimetric ascorbic acid method using ammonium molybdate and potassium antimonyl tartrate (O'Dell 1993). NO_3^- concentration was analyzed conductimetrically by ion chromatography (Dionex 2000i Ion Chromatograph). NH_4^+ concentration was determined colorimetrically by ion analyzer using the hypochlorite/salicylate method (Eaton et al. 1995).

We filtered samples for Cl^- , SO_4^{2-} , Na^+ , K^+ , Mg^{2+} , Ca^{2+} , and DOC (Whatman Puradisc 0.45 μ m polypropylene filters) into 60 mL NalgeneTM bottles. Anions (Cl^- , SO_4^{2-}) and cations (Na^+ , K^+ , Mg^{2+} , Ca^{2+}) were analyzed using ion chromatography (Dionex ICS1100), and DOC by high temperature catalytic combustion with NDIR detection (Shimadzu TOC-L and NM-1 with ASI-L Autosampler).

We collected alkalinity samples in 125 mL Nalgene bottles and analyzed them using the Inflection Point method. Samples for chl *a* were collected in 125 mL glass amber bottles, filtered through a glass fiber pre-filter (Sartorius, 13400 grade) and frozen until analysis by hot ethanol extraction followed by spectrophotometric analysis (Thermo Scientific Genesys 10UV). Anions, cations, DOC, alkalinity and chl *a* were analyzed at the University of New Hampshire Water Quality Analysis Laboratory.

Three types of trace metal samples were taken: total, dissolved, and organically bound. The total metals sample was not filtered and includes particulate metals. Dissolved metals samples were collected by filtering through a Whatman Puradisc 0.45 μm polypropylene syringe filter. Subtraction of dissolved metals from total metals yields particulate metals. Lastly, raw sample was filtered through a Whatman Puradisc .45 micron polypropylene syringe filter and passed through a Dowex HCR-W2 cation exchange to determine organically bound metals. The metals that were captured by the ion exchange resin (organically bound metals subtracted from the dissolved metals) are ionic metals. If the ionic metals were calculated to be negative, this meant that either dissolved, organically bound values exceed dissolved metals (an impossibility), or some particulate passed through the filter prior to ion exchange and passed through the resin, or there were analytical errors. Such cases were rare. Metal samples were acidified with 1 drop of 50% HNO_3 per 20 ml, put on ice, and transported to the Sawyer Water Research Laboratory for analysis using ICP-MS (Thermo Element 2 high resolution).

B2.1.3. Statistical Analysis

Before statistical analysis, we transformed variables that were not normally distributed, so that they more closely resembled a normal distribution curve. Temperature, ortho-P,

NH_4^+ , Cl^- , SO_4^{2-} , Na^+ , K^+ , Ca^{2+} , DOC, unbound Al, total Fe, DOC bound Fe, unbound Fe, total Mn, DOC bound Mn, and unbound Mn were log transformed. Chlorophyll a and NO_3^- , were log transformed (as $1 + \text{variable value}$) to account for zero values in the datasets. Alkalinity and unbound Si were square root transformed. We performed linear regression and analysis of variance (R version 3.3.3, R Core Team) to examine trends and variation among pools. Significance was considered to be $p \leq 0.05$.

B2.2. Results

B2.2.1 Temperature

In P1, the water temperature in the four pools from ice off until dry down ranged from 14 to 22 °C. P2's temperature ranged from 15 to 30 °C. The water temperature in P3 ranged from 9.5 to 31°C. The temperature in P4 ranged from 8 to 19 °C. The temperature of the four pools combined increased over the season ($R^2 = 0.39, p < 0.001$). There were significant differences in temperature among pools ($p < 0.001$).

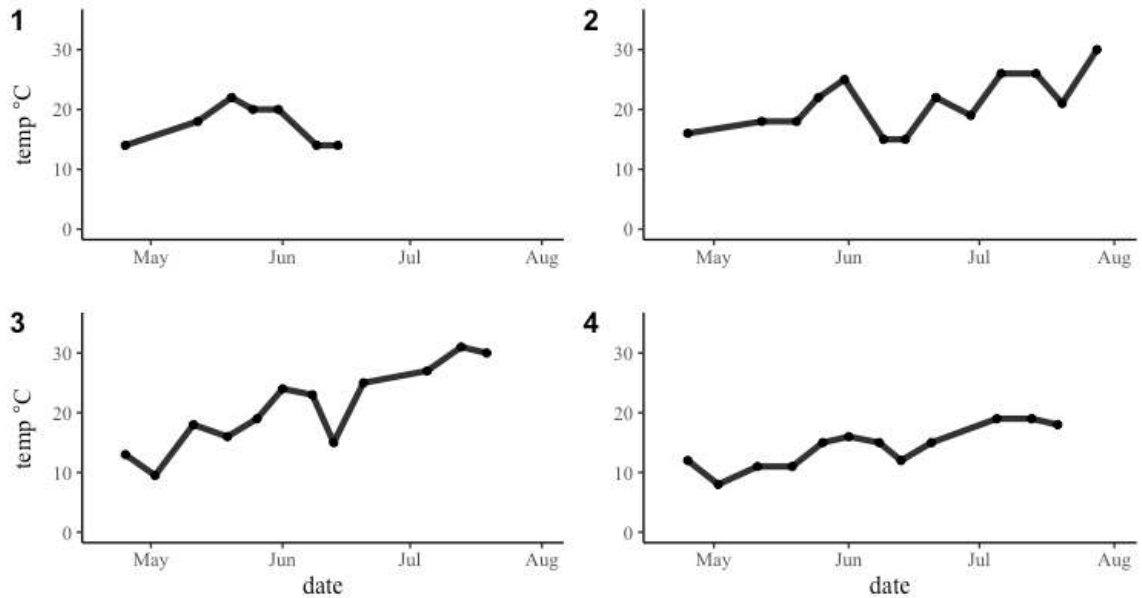


Figure B.2.1. Surface temperature in four vernal pools. Samples collected from April to August 2016.

B2.2.2 Dissolved oxygen

The DO concentrations in the four pools ranged from 0.6 to 10.3 mg L⁻¹, with a mean of 4.85 ± 0.26 mg L⁻¹ for the four pools. The DO ranged from 0.6 to 4.9 mg L⁻¹ in P1, from 0.7 to 10.3 mg L⁻¹ in P2, from 1.2 to 10.2 mg L⁻¹ in P3, and from 0.8 to 8.9 mg L⁻¹ in P4. The DO concentrations among pools were significantly different ($p < 0.001$), as well as the concentrations between benthic and surface samples ($p < 0.001$), with the benthic samples almost always lower than the surface samples. DO concentrations were hypothesized to decrease over the season as they do in lakes, because of temperature increased and they became more metabolically active. There was no relationship between DO and time. This could be a result of the changing water level of the vernal pools and the shallow water level that allows oxygen to be mixed throughout the basin.

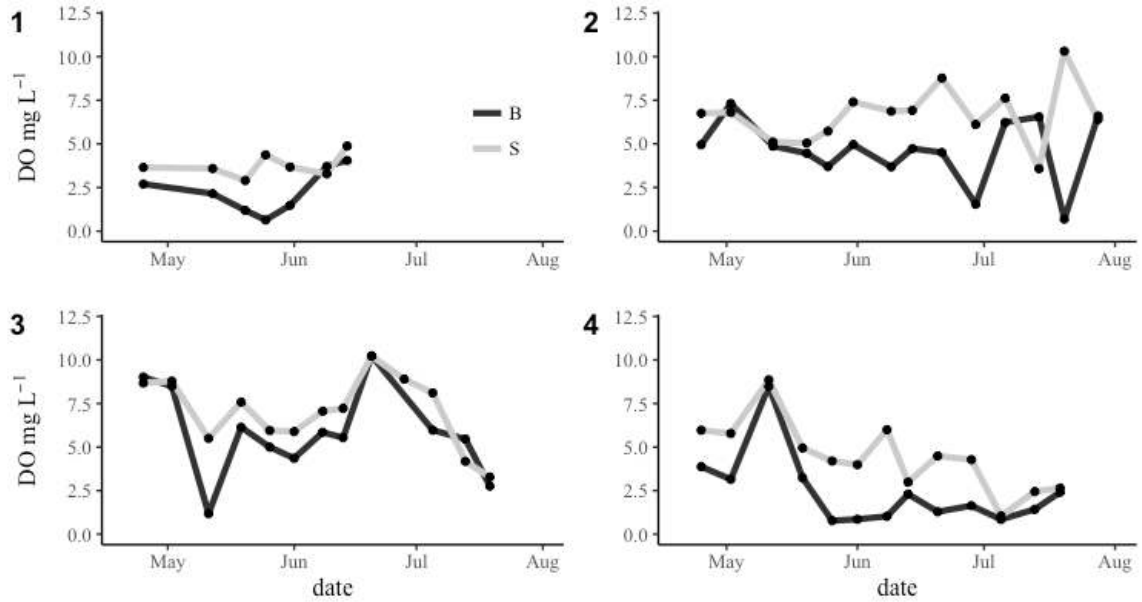


Figure B.2.2. Dissolved oxygen concentrations in four vernal pools. Samples collected from April to August 2016.

B2.2.3. pH

The pH in the four pools ranged from 4.4 to 6.0 within the four pools with an average of 5.1 ± 0.3 . The pH ranged from 4.8 to 5.4 in P1, from 4.9 to 5.9 in P2, from 4.4 to 5.7 in P3, and from 4.4 to 6.0 in P4. The pH in the four pools combined generally decreased over the season ($R^2 = 0.17, p < 0.001$). There were significant variations in pH among the four pools ($p < 0.001$), but not between the benthic and surface samples.

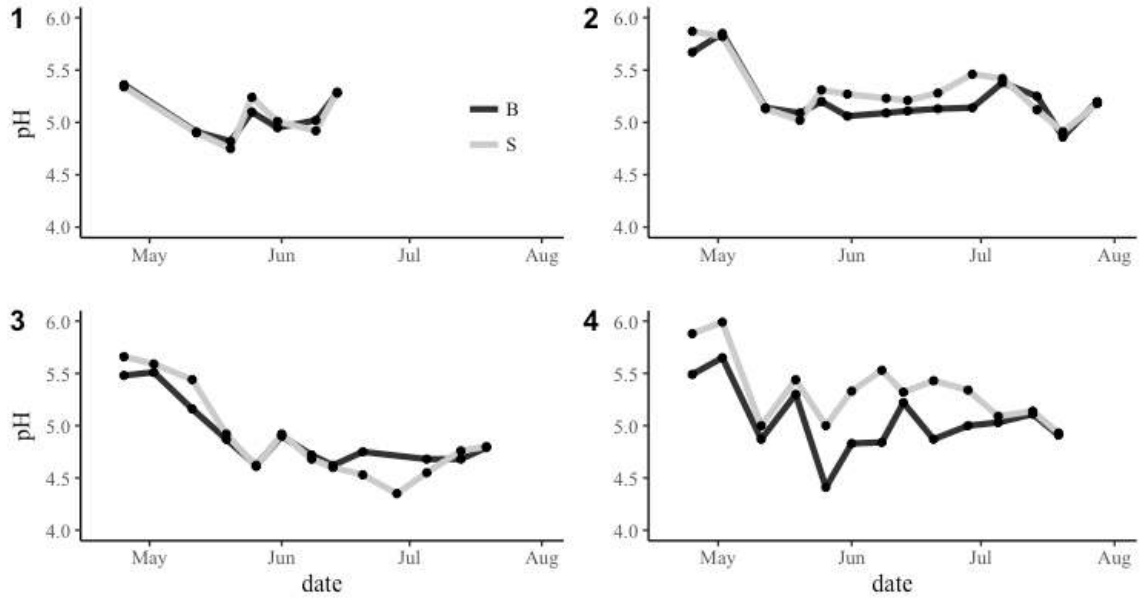


Figure B.2.3. The pH in four vernal pools. Samples collected from April to August 2016.

B2.2.4. Nutrients

B2.2.4.1. Ortho-P

Ortho-P concentrations in the four pools ranged from below the detection limit ($0.016 \text{ mg P L}^{-1}$) to 0.76 mg P L^{-1} , with an average of $0.07 \pm 0.1 \text{ mg P L}^{-1}$. The ortho-P concentration ranged from below detection to 0.09 mg P L^{-1} in P1, from below detection to 0.12 mg P L^{-1} in P2, from below detection to 0.76 mg P L^{-1} in P3, and from below detection to 0.20 mg P L^{-1} in P4. The concentrations combined increased throughout the season ($R^2 = 0.39$, $p < 0.001$), and varied significantly among pools ($p < 0.05$), but not between benthic and surface samples.

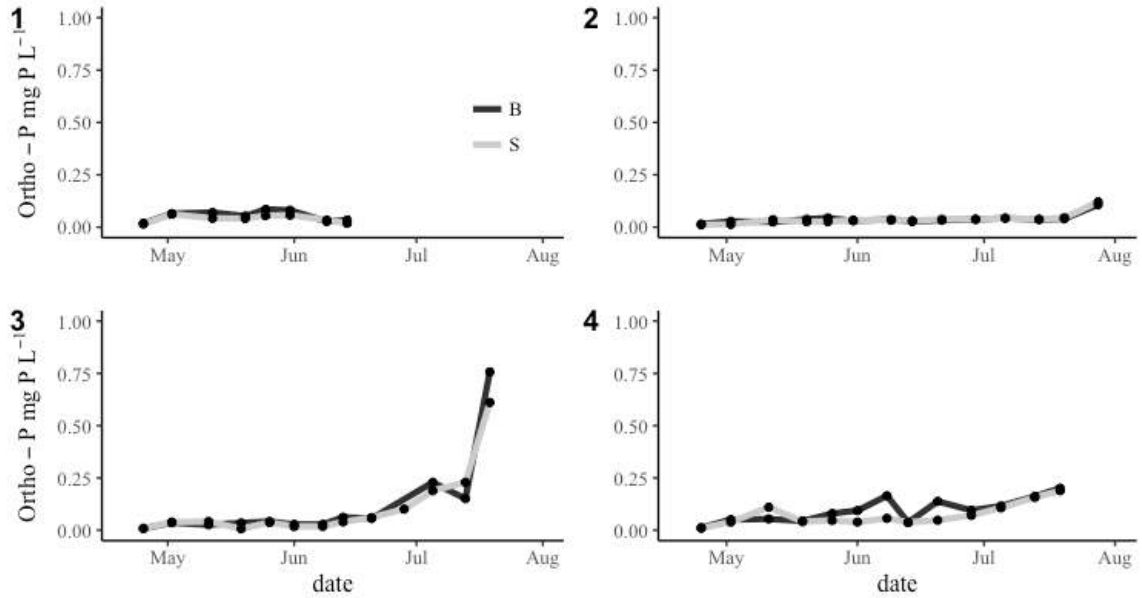


Figure B.2.4. Ortho-P concentrations in four vernal pools. Samples collected from April to August 2016.

B2.2.4.2. Nitrate

Nitrate concentrations in the four pools were near or below the detection limit ($0.002 \text{ mg N L}^{-1}$) for the duration of sampling. Nitrate concentration ranged from 0.0 to 0.05 mg N L^{-1} with an average of $0.01 \pm 0.01 \text{ mg N L}^{-1}$. The NO_3^- concentration was always at or below detection in P1, from below detection to 0.01 mg N L^{-1} in P2, from below detection to 0.05 mg N L^{-1} in P3, and from below detection to 0.04 mg N L^{-1} in P4. These four vernal pools were NO_3^- limited, based on the very low concentrations of NO_3^- . Nitrate had a weak but significant increasing relationship with time ($R^2 = 0.07, p < 0.01$). There were significant variations in NO_3^- among pools ($p < 0.05$).

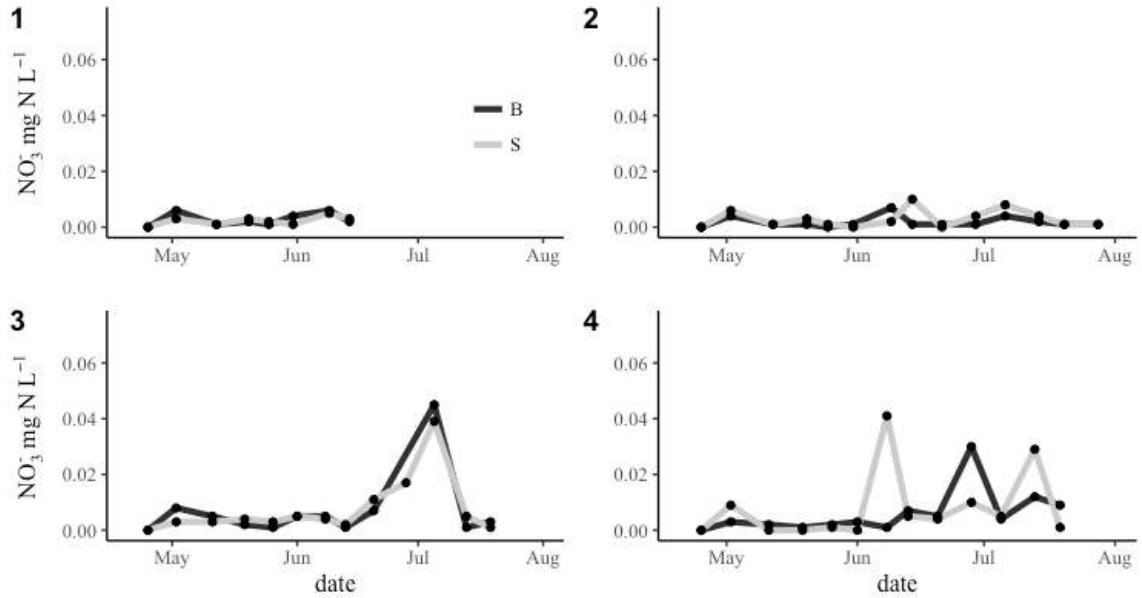


Figure B.2.5. Nitrate concentrations in four vernal pools. Samples collected from April to August 2016.

B2.2.4.3. Ammonium

Ammonium concentrations in the four pools ranged from below the detection limit (0.02 mg N L⁻¹) to 2.9 mg L⁻¹, with an average of 0.14 ± 0.41 mg N L⁻¹. The NH₄⁺ concentration ranged from below detection to 0.63 mg N L⁻¹ in P1, from below detection to 0.31 mg N L⁻¹ in P2, from below detection to 2.94 mg N L⁻¹ in P3, and from below detection to 0.47 mg N L⁻¹ in P4. Concentrations of NH₄⁺ increased during the season ($R^2 = 0.45, p < 0.001$), and did not vary significantly among pools or between benthic and surface samples.

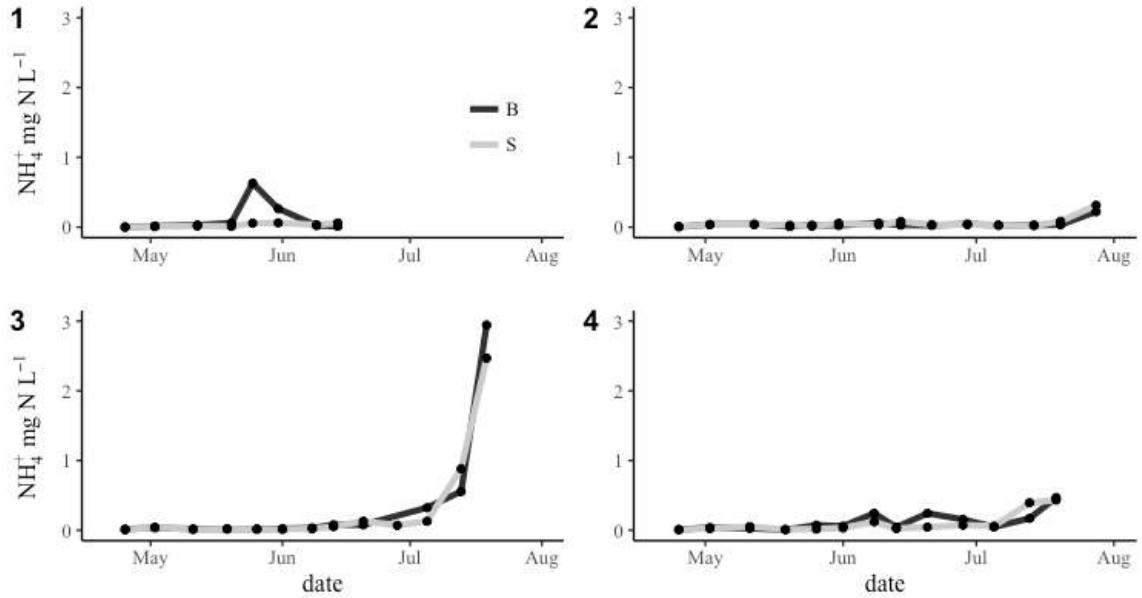


Figure B.2.6. Ammonium concentrations in four vernal pools. Samples collected from April to August 2016.

B2.2.5. Anions and Cations

B2.2.5.1. Chloride

The concentrations of Cl^- in the four pools ranged from 0.83 to 22.45 mg $\text{Cl}^- \text{L}^{-1}$, with an average of 2.42 ± 2.38 mg $\text{Cl}^- \text{L}^{-1}$. The Cl^- concentration ranged from 2.14 to 22.45 mg $\text{Cl}^- \text{L}^{-1}$ in P1, from 0.83 to 3.58 mg $\text{Cl}^- \text{L}^{-1}$ in P2, from 1.73 to 3.78 mg $\text{Cl}^- \text{L}^{-1}$ in P3, and from 1.26 to 1.88 mg $\text{Cl}^- \text{L}^{-1}$ in P4. There was a significant decreasing linear relationship between Cl^- and time ($R^2 = 0.14$, $p < 0.001$). There were significant differences in Cl^- concentrations among pools ($p < 0.001$).

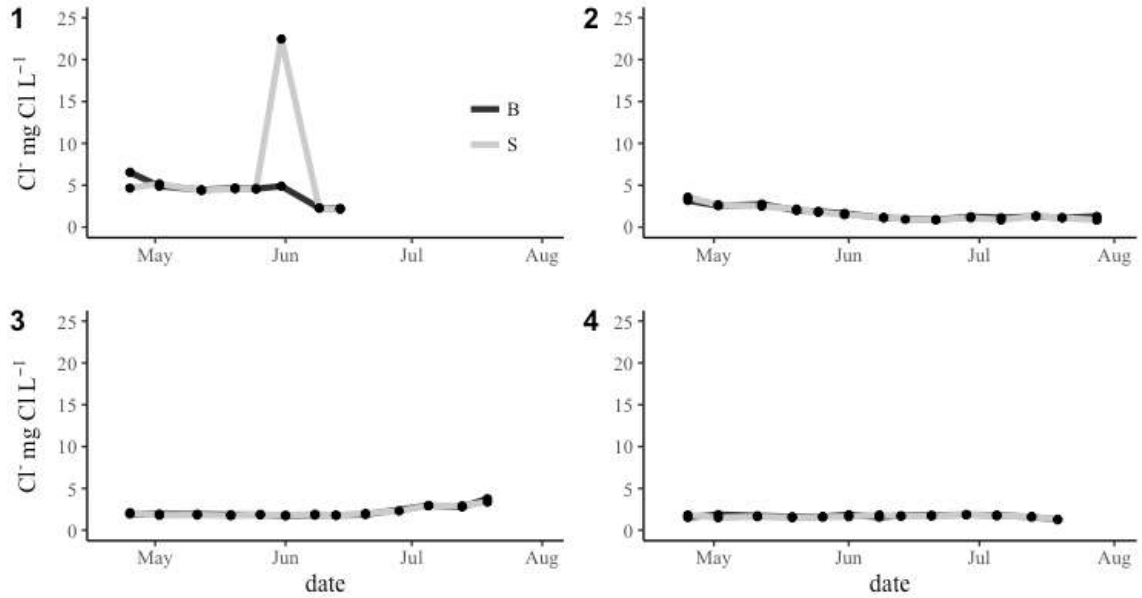


Figure B.2.7. Chloride concentrations in four vernal pools. Samples collected from April to August 2016.

B2.2.5.2. Sulfate

The concentrations of SO_4^{2-} in the four pools ranged from 0.01 to 4.99 mg S L⁻¹, with an average of 0.33 ± 0.82 mg S L⁻¹. The SO_4^{2-} concentration ranged from 0.03 to 4.99 mg S L⁻¹ in P1, from 0.01 to 0.18 mg S L⁻¹ in P2, from 0.03 to 0.33 mg S L⁻¹ in P3, and from 0.04 to 0.49 mg S L⁻² in P4. There was no significant linear relationship between SO_4^{2-} and time. There were significant differences in SO_4^{2-} concentrations among pools ($p < 0.001$).

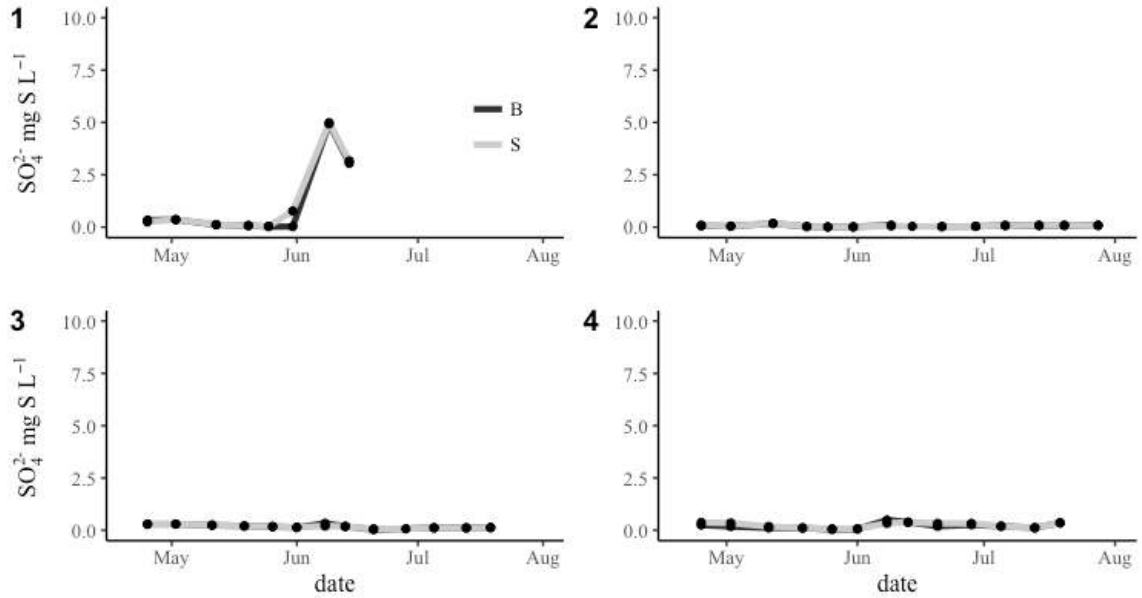


Figure B.2.8. Sulfate concentrations in four vernal pools. Samples collected from April to August 2016.

B2.2.5.3. Sodium

The concentrations of Na^+ in the four pools ranged from 1.04 to 12.99 mg Na L^{-1} , with an average of 1.97 ± 1.32 mg Na L^{-1} . The Na^+ concentration ranged from 1.78 to 12.99 mg Na L^{-1} in P1, from 1.33 to 3.33 mg Na L^{-1} in P2, from 1.21 to 3.02 mg Na L^{-1} in P3, and from 1.04 to 1.99 mg Na L^{-1} in P4. There was a weak but significant negative linear relationship between Na^+ and time ($R^2 = 0.05$, $p < 0.05$). There were significant differences in Na^+ concentrations among pools ($p < 0.001$).

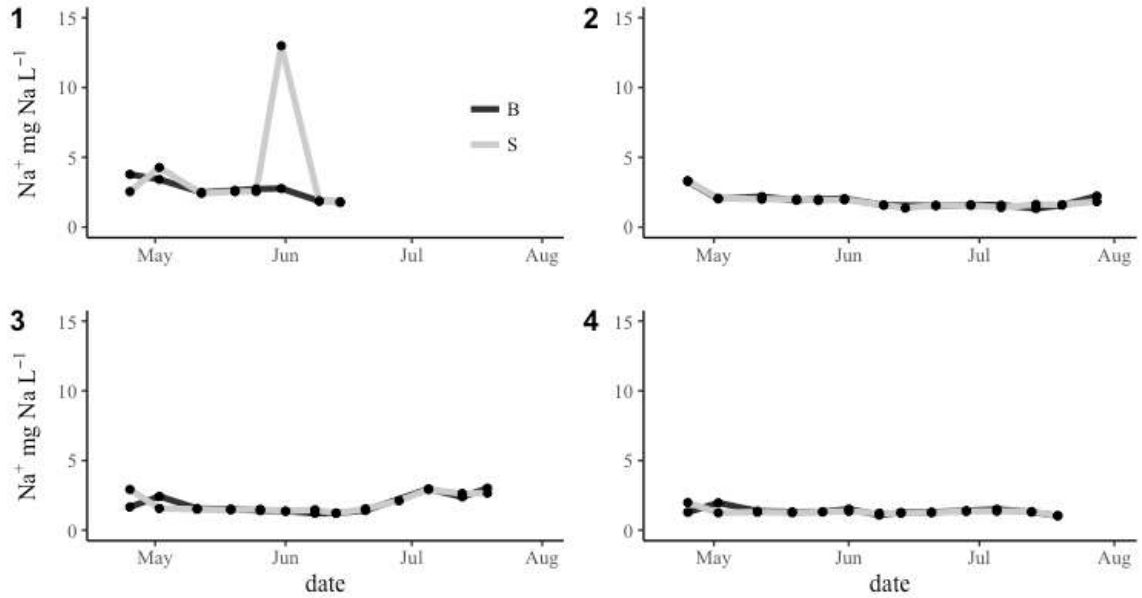


Figure B.2.9. Sodium concentrations in four vernal pools. Samples collected from April to August 2016.

B2.2.5.4. Potassium

The concentrations of K⁺ in the four pools ranged from 0.16 to 4.16 mg K L⁻¹, with an average of 0.84 ± 0.58 mg K L⁻¹. The K⁺ concentration ranged from 0.31 to 1.92 mg K L⁻¹ in P1, from 0.16 to 1.41 mg K L⁻¹ in P2, from 0.23 to 4.16 mg K L⁻¹ in P3, and from 0.41 to 1.17 mg K L⁻² in P4. There was a significant increasing relationship between K⁺ and time ($R^2 = 0.24$, $p < 0.001$). There were significant differences in K⁺ concentrations among pools ($p < 0.001$).

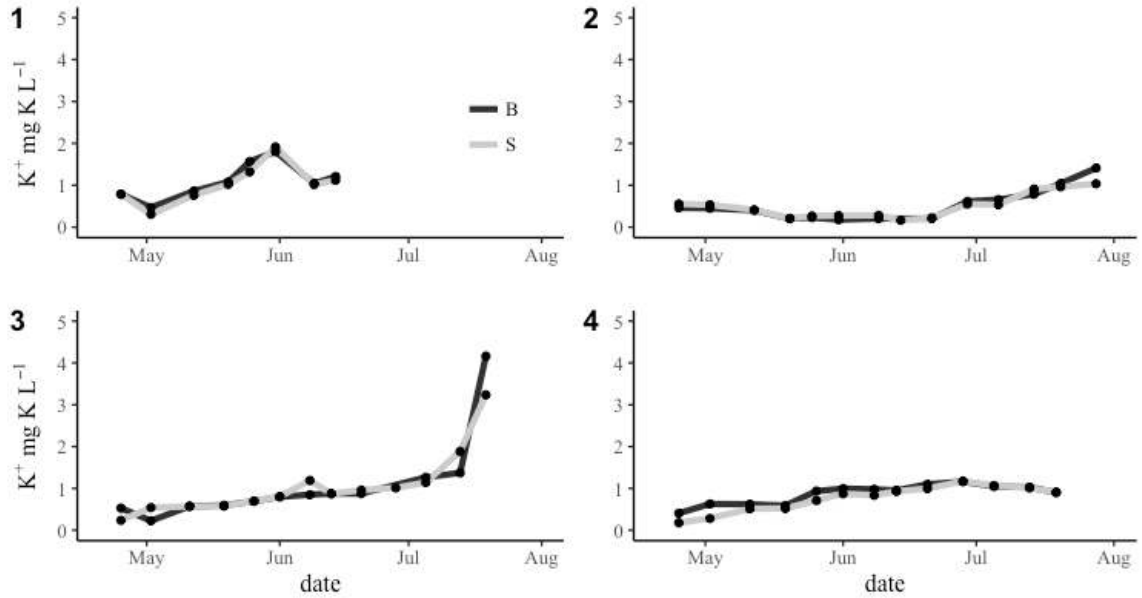


Figure B.2.10. Potassium concentrations in four vernal pools. Samples collected from April to August 2016.

B2.2.5.5. Magnesium

The concentrations of Mg^{2+} in the four pools ranged from 0.21 to 1.90 mg Mg L⁻¹, with an average of 0.96 ± 0.45 mg Mg L⁻¹. The Mg^{2+} concentration ranged from 0.72 to 1.54 mg Mg L⁻¹ in P1, from 0.97 to 1.81 mg Mg L⁻¹ in P2, from 0.21 to 1.69 mg Mg L⁻¹ in P3, and from 0.26 to 1.90 mg Mg L⁻¹ in P4. There was no significant linear relationship between Mg^{2+} and time. There were significant differences in Mg^{2+} concentrations among pools ($p < 0.001$).

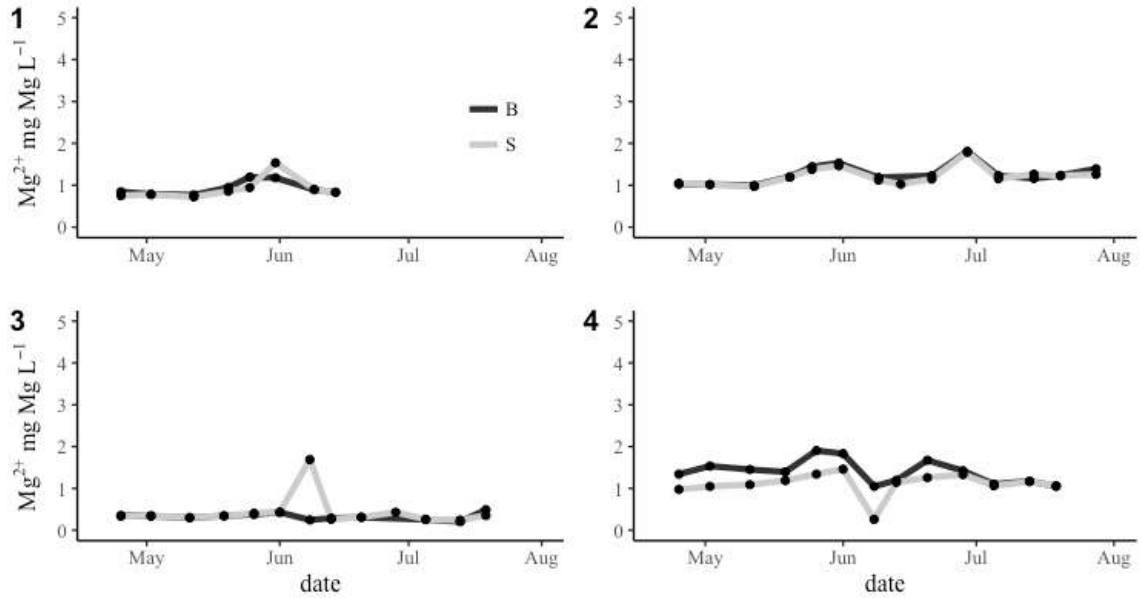


Figure B.2.11. Magnesium concentrations in four vernal pools. Samples collected from April to August 2016.

B2.2.5.6. Calcium

The concentrations of Ca^{2+} in the four pools ranged from 0.58 to 10.78 mg Ca L^{-1} , with an average of $3.55 \pm 2.62 \text{ mg Ca L}^{-1}$. The Ca^{2+} concentration ranged from 1.26 to 4.52 mg Ca L^{-1} in P1, from 2.28 to 5.61 mg Ca L^{-1} in P2, from 0.58 to 10.78 mg Ca L^{-1} in P3, and from 1.03 to 9.89 mg Ca L^{-1} in P4. There was not a significant relationship between Ca^{2+} and time. There were significant differences in Ca^{2+} concentrations among pools ($p < 0.001$).

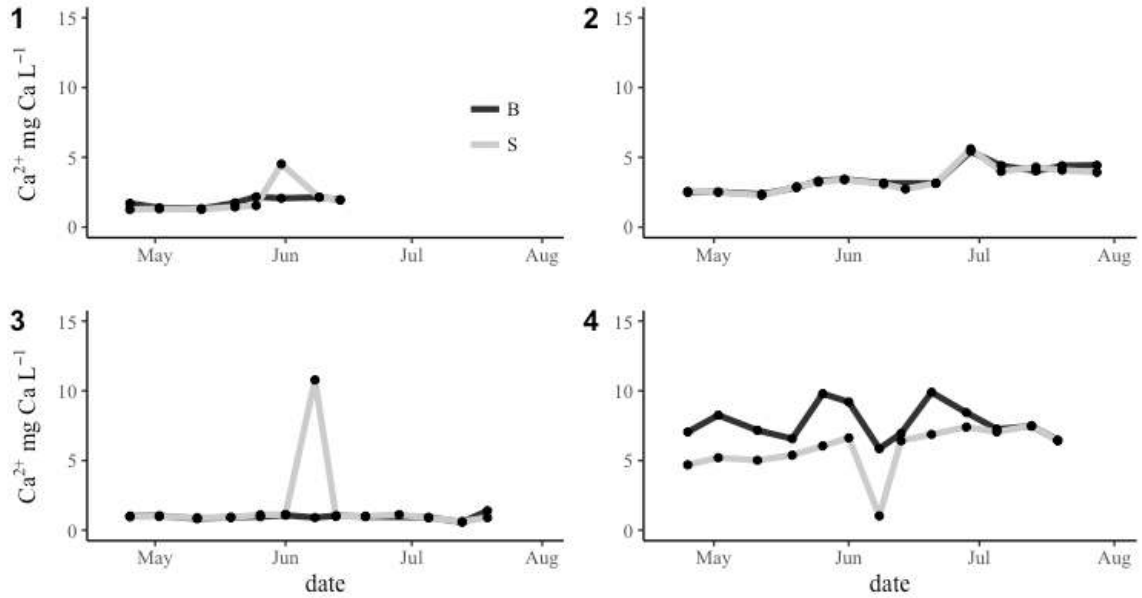


Figure B.2.12. Calcium concentrations in four vernal pools. Samples collected from April to August 2016.

B2.2.6. Dissolved Organic Carbon

The concentrations of DOC in the four pools ranged from 5.82 to 148.35 mg C L⁻¹, with an average of 18.93 ± 14.96 mg C L⁻¹. The DOC concentration ranged from 8.40 to 20.32 mg C L⁻¹ in P1, from 13.20 to 29.12 mg C L⁻¹ in P2, from 5.82 to 28.68 mg C L⁻¹ in P3, and from 9.65 to 148.35 mg C L⁻² in P4. There was a significant increasing linear relationship between DOC and time ($R^2 = 0.22$, $p < 0.001$). There were significant differences in DOC concentrations among pools ($p < 0.001$).

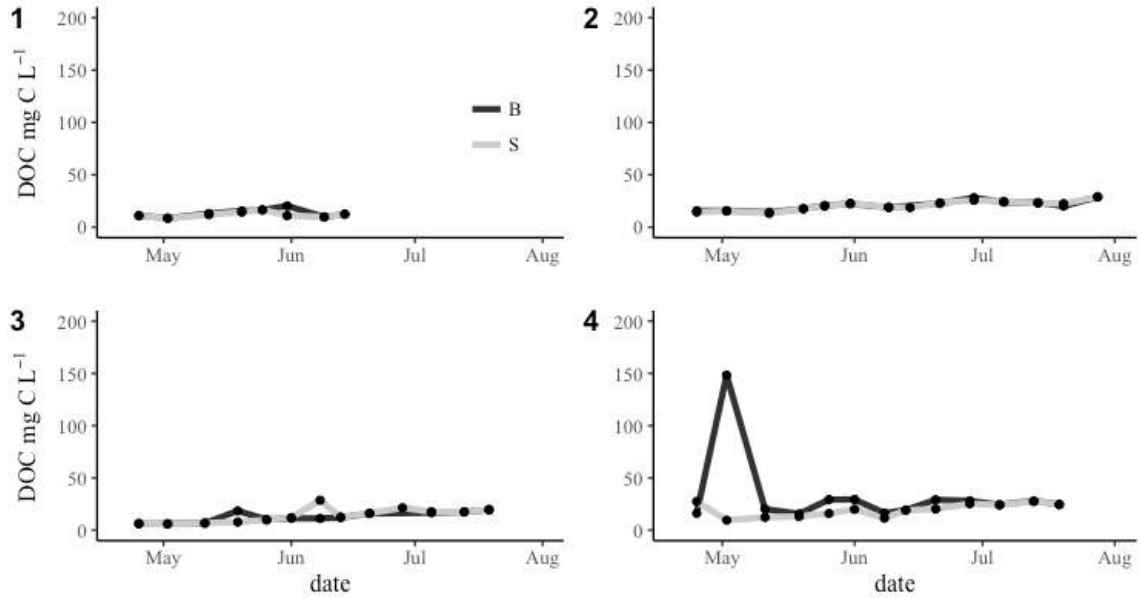


Figure B.2.13. Dissolved organic carbon concentrations in four vernal pools. Samples collected from April to August 2016.

B2.2.7. Alkalinity

Alkalinity ranged from 23.3 to 481.7 $\mu\text{eq L}^{-1}$ in the four pools, with an average of $169.9 \pm 121.2 \mu\text{eq L}^{-1}$. The alkalinity ranged from 35.9 to 169.5 $\mu\text{eq L}^{-1}$ in P1, from 56.3 to 296.1 $\mu\text{eq L}^{-1}$ in P2, from 23.3 to 338.7 $\mu\text{eq L}^{-1}$ in P3, and from 212.4 to 481.7 $\mu\text{eq L}^{-1}$ in P4.

There was a significant increasing relationship between alkalinity and time ($R^2 = 0.11$, $p < 0.001$). There were significant differences in alkalinity among pools ($p < 0.001$).

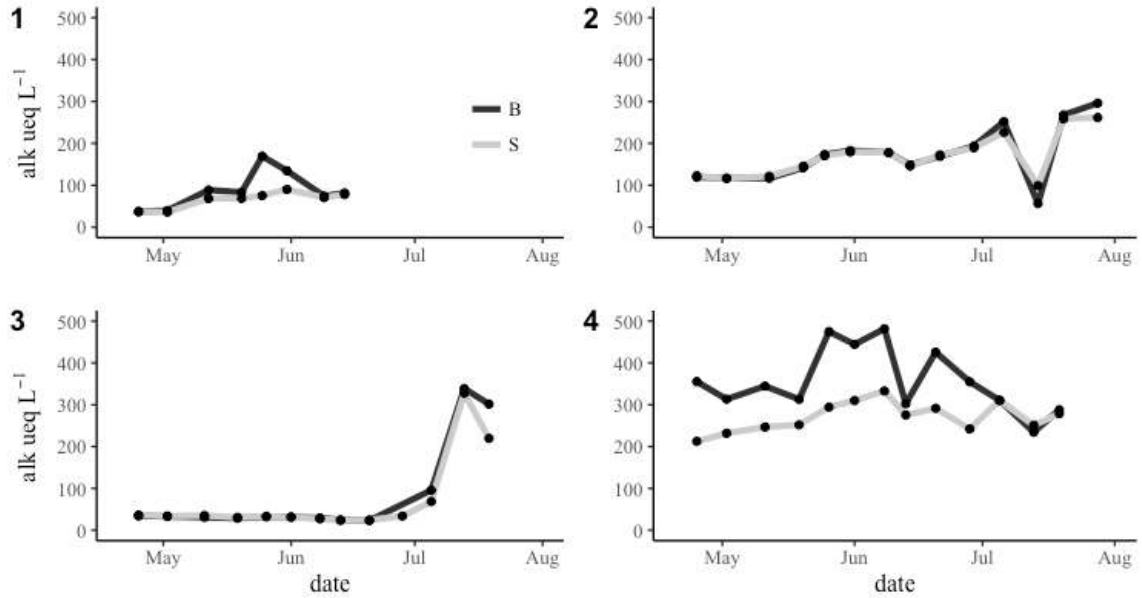


Figure B.2.14. Alkalinity in four vernal pools. Sampled from from April to August 2016.

B2.2.8. Chlorophyll a

Chlorophyll *a* concentrations in the four pools ranged from 0 to 190 $\mu\text{g L}^{-1}$, with an average of $15.3 \pm 31.1 \mu\text{g L}^{-1}$, suggesting trophic level ranging from oligotrophic to hypereutrophic throughout the wet season in 2016. Chlorophyll *a* concentrations ranged from 0 to 43 $\mu\text{g L}^{-1}$ in P1, from 0 to 20 $\mu\text{g L}^{-1}$ in P2, from 0 to 190 $\mu\text{g L}^{-1}$ in P3, and from 0 to 29 $\mu\text{g L}^{-1}$ in P4. There was no significant relationship between chl *a* and time. The chl *a* concentrations varied significantly between pools ($p < 0.001$).

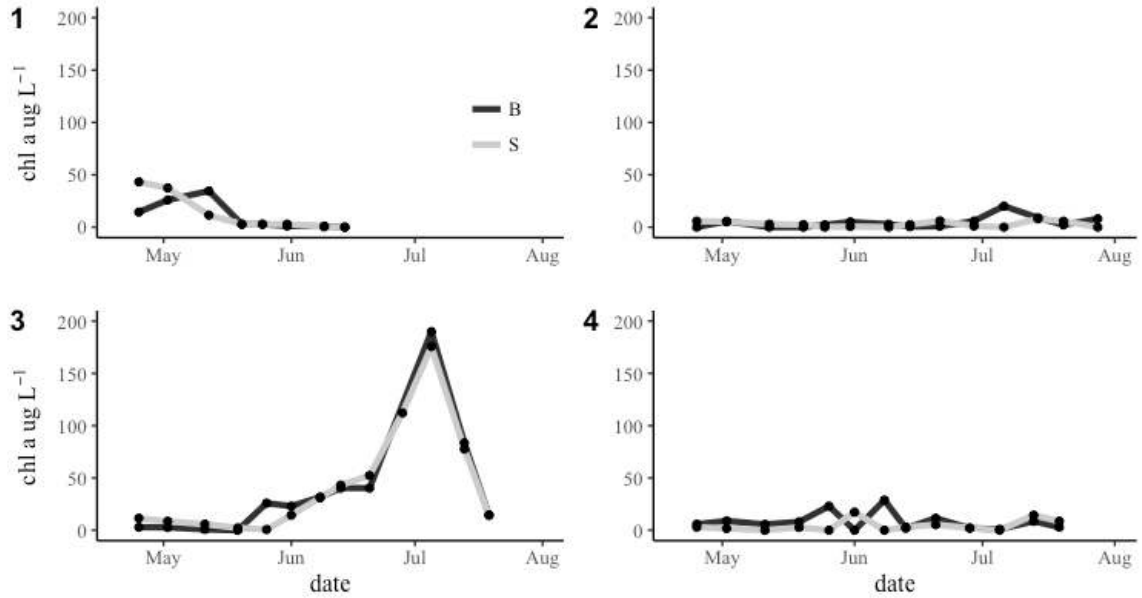


Figure B.2.15. Chlorophyll *a* concentrations in four vernal pools. Samples collected from April to August 2016.

B2.2.9. Metals

B2.2.9.1. Aluminum

The concentrations of total aluminum (Al) ranged from 48 to 375 $\mu\text{g L}^{-1}$, with an overall average of $176 \pm 94 \mu\text{g L}^{-1}$. Total Al concentrations ranged from 111 to 353 $\mu\text{g L}^{-1}$ in P1, from 200 to 375 $\mu\text{g L}^{-1}$ in P2, from 48 to 146 $\mu\text{g L}^{-1}$ in P3, and from 73 to 276 $\mu\text{g L}^{-1}$ in P4. There was a weak, but significant increasing relationship between Al and time ($R^2 = 0.07, p < 0.01$). There were significant differences in total Al concentrations among pools ($p < 0.001$).

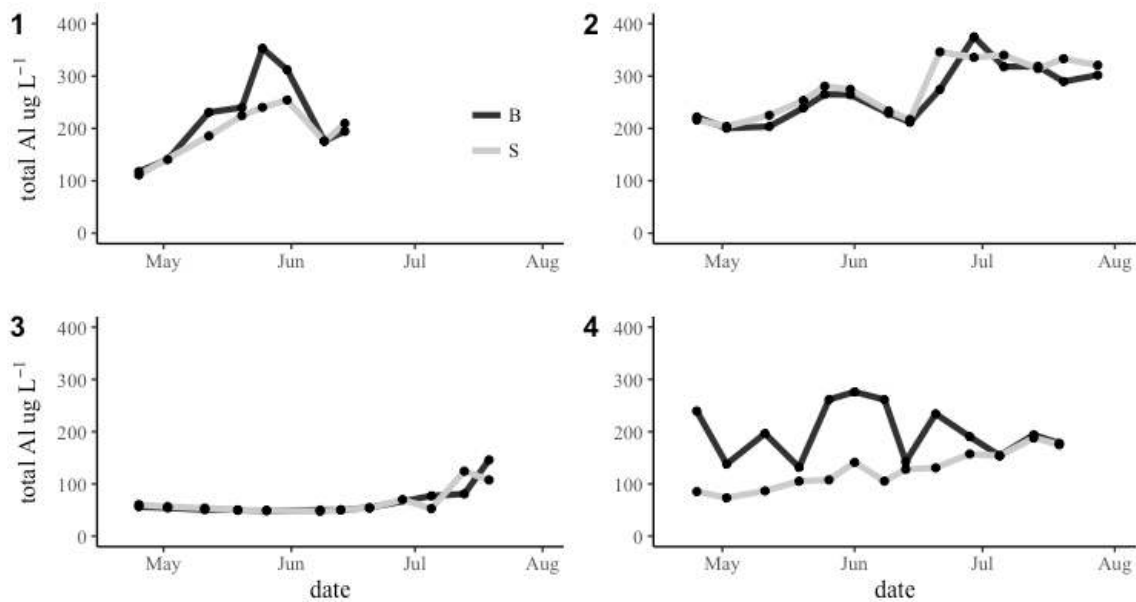


Figure B.2.16. Concentrations of total Al in four vernal pools. Samples collected from April to August 2016.

The concentrations of organically bound Al ranged from 33 to 259 $\mu\text{g L}^{-1}$, with an overall average of $128 \pm 64 \mu\text{g L}^{-1}$. Organically bound Al concentrations ranged from 48 to 243 $\mu\text{g L}^{-1}$ in P1, from 78 to 259 $\mu\text{g L}^{-1}$ in P2, from 33 to 49 $\mu\text{g L}^{-1}$ in P3, and from 62 to 227 $\mu\text{g L}^{-1}$ in P4. There was a weak, but significant increasing relationship between DOC bound Al concentrations and time ($R^2 = 0.05$, $p < 0.05$). There were significant differences in organically bound Al concentrations among pools ($p < 0.001$).

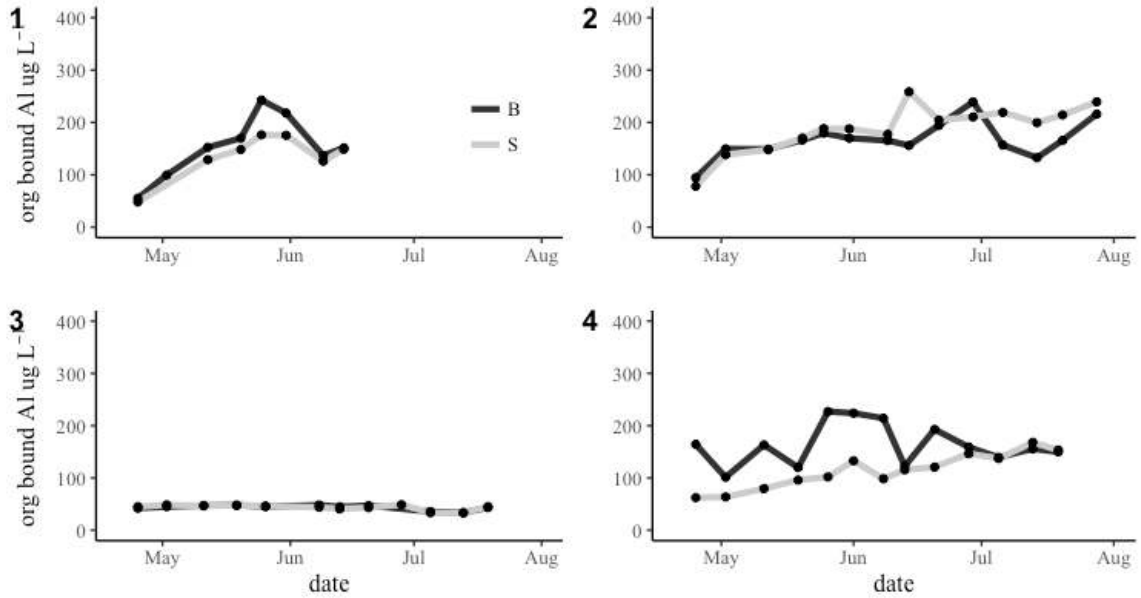


Figure B.2.17. Concentrations of organically bound Al in four vernal pools. Samples collected from April to August 2016.

The concentrations of ionic Al ranged from 0 to $120 \mu\text{g L}^{-1}$, with an overall average of $30 \pm 25 \mu\text{g L}^{-1}$. Ionic Al concentrations ranged from 10 to $93 \mu\text{g L}^{-1}$ in P1, from 0 to $120 \mu\text{g L}^{-1}$ in P2, from 0 to $9 \mu\text{g L}^{-1}$ in P3, and from 0 to $68 \mu\text{g L}^{-1}$ in P4. There was not a significant relationship between ionic Al concentrations and time. There were significant differences in ionic Al concentrations among pools ($p < 0.001$).

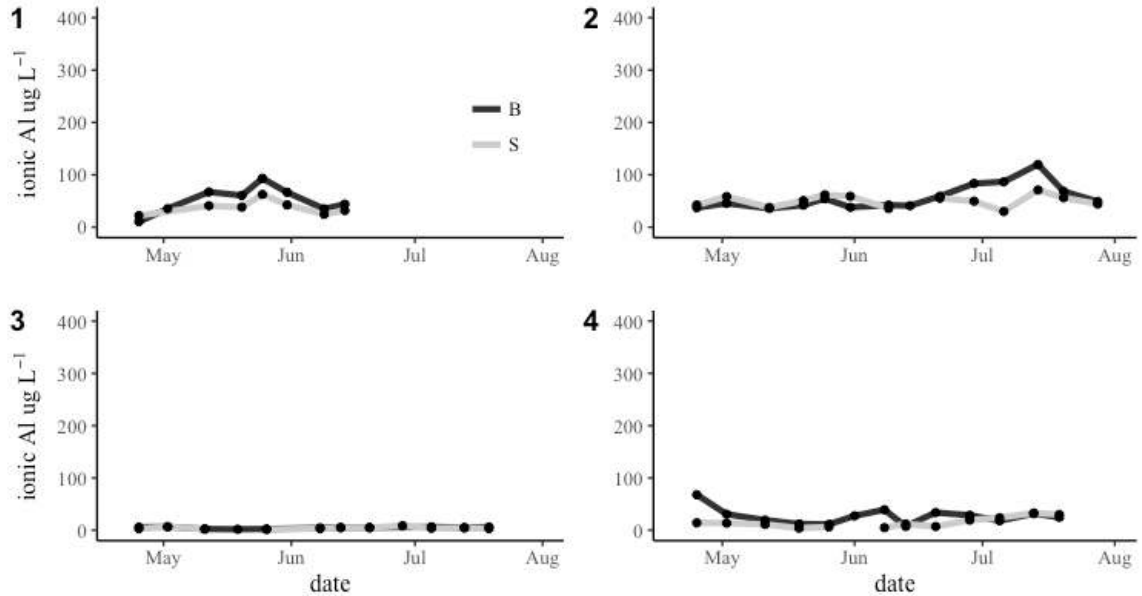


Figure B.2.18. Concentrations of ionic Al in four vernal pools. Samples collected from April to August 2016.

B2.2.9.2. Iron

Concentrations of total iron (Fe) ranged from 33 to 5664 $\mu\text{g L}^{-1}$, with an overall average of $1252 \pm 1567 \mu\text{g L}^{-1}$. Concentrations of total Fe ranged from 607 to 4578 $\mu\text{g L}^{-1}$ in P1, from 706 to 5664 $\mu\text{g L}^{-1}$ in P2, from 32 to 120 $\mu\text{g L}^{-1}$ in P3, and from 94 to 1027 $\mu\text{g L}^{-1}$ in P4. There was a weak but significant increasing relationship between total Fe and time ($R^2 = 0.04, p < 0.05$). There were significant differences in concentrations of total Fe among pools ($p < 0.001$).

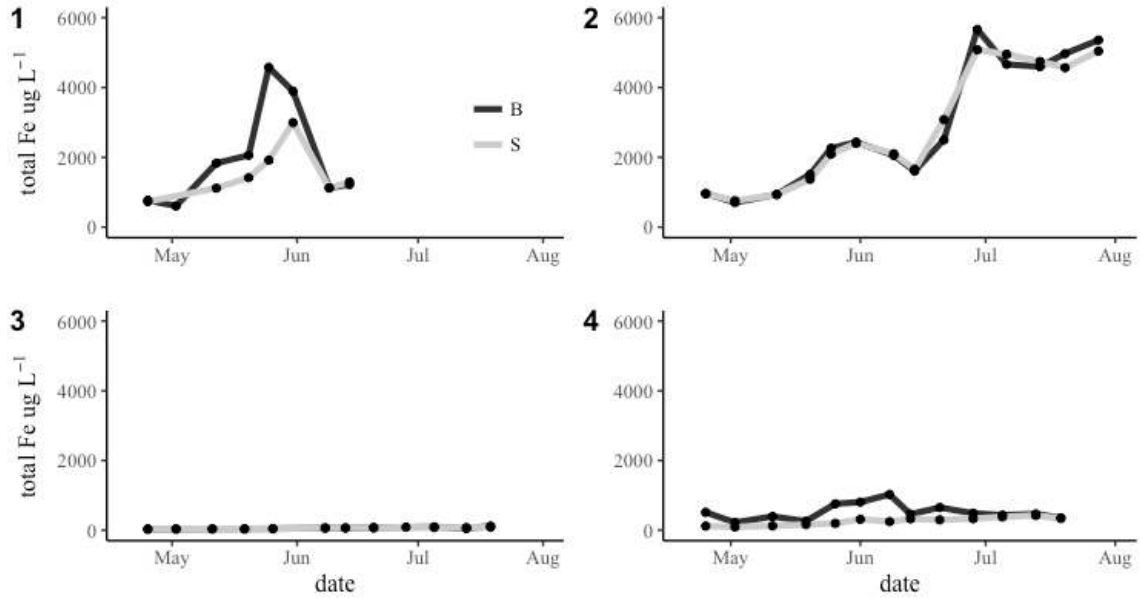


Figure B.2.19. Concentrations of total Fe in four vernal pools. Samples collected from April to August 2016.

The concentrations of organically bound Fe ranged from 32 to 4107 $\mu\text{g L}^{-1}$, with an overall average of $726 \pm 888 \mu\text{g L}^{-1}$. Concentrations of organically bound Fe ranged from 324 to 2190 $\mu\text{g L}^{-1}$ in P1, from 415 to 4107 $\mu\text{g L}^{-1}$ in P2, from 32 to 80 $\mu\text{g L}^{-1}$ in P3, and from 71 to 465 $\mu\text{g L}^{-1}$ in P4. There was a weak but significant increasing relationship between organically bound Fe concentrations and time ($R^2 = 0.06$, $p = 0.01$). There were significant differences in concentrations of organically bound Fe among pools ($p < 0.001$).

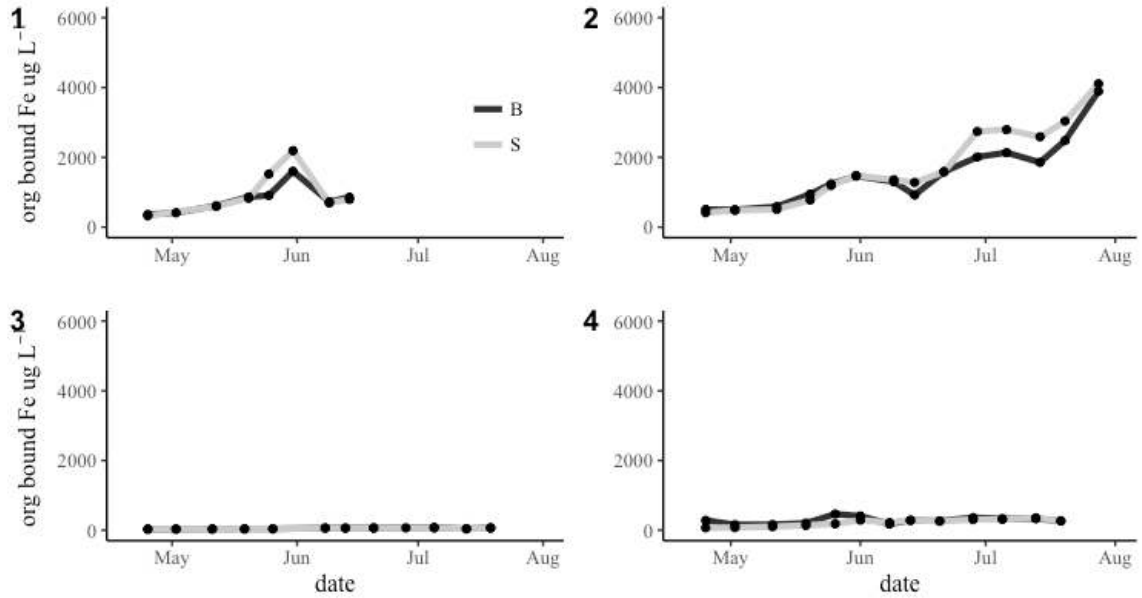


Figure B.2.20. Concentrations of organically bound Fe in four vernal pools. Samples collected from April to August 2016.

The concentrations of ionic Fe ranged from 0 to 3480 $\mu\text{g L}^{-1}$, with an overall average of $250 \pm 525 \mu\text{g L}^{-1}$. Ionic Fe concentrations ranged from 73 to 3480 $\mu\text{g L}^{-1}$ in P1, from 0 to 2415 $\mu\text{g L}^{-1}$ in P2, from 0 to 29 $\mu\text{g L}^{-1}$ in P3, and from 0 to 541 $\mu\text{g L}^{-1}$ in P4. There was a weak but significant increasing relationship between ionic Fe concentrations and time ($R^2 = 0.064$ $p < 0.05$). There were significant differences in ionic Fe concentrations among pools ($p < 0.001$).

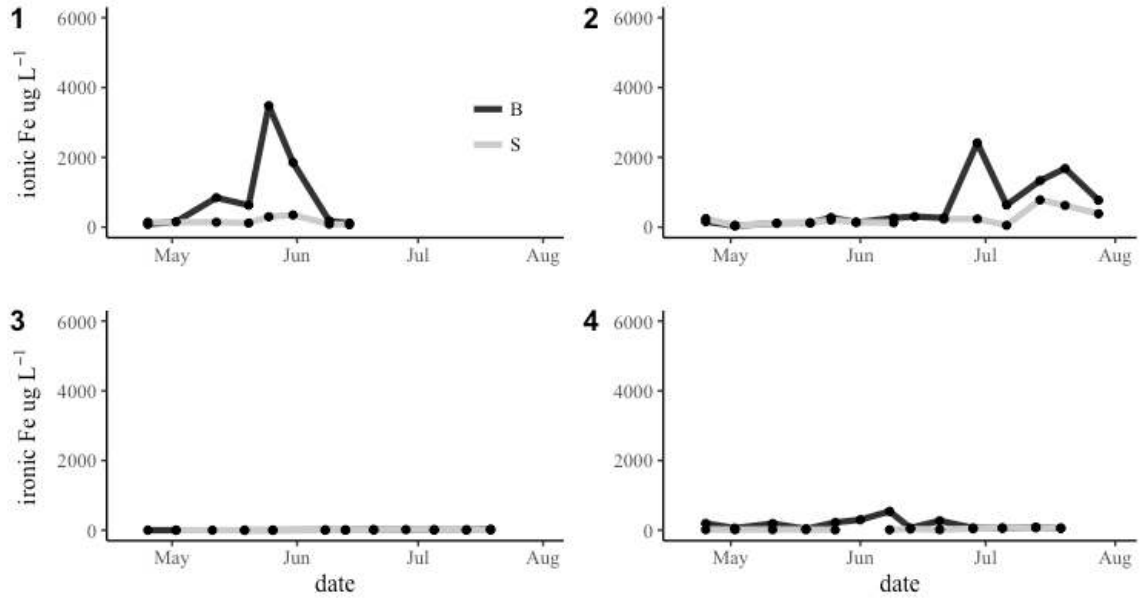


Figure B.2.21. Concentrations of ionic Fe in four vernal pools. Samples collected from April to August 2016.

B2.2.9.3. Manganese

The concentrations of total manganese (Mn) ranged from 18 to 675 $\mu\text{g L}^{-1}$, with an overall average of $89 \pm 98 \mu\text{g L}^{-1}$. Concentrations of total Mn ranged from 63 to 165 $\mu\text{g L}^{-1}$ in P1, from 38 to 675 $\mu\text{g L}^{-1}$ in P2, from 20 to 41 $\mu\text{g L}^{-1}$ in P3, and from 18 to 112 $\mu\text{g L}^{-1}$ in P4. There was a significant increasing relationship between total Mn and time ($R^2 = 0.10, p < 0.01$). There were significant differences in total Mn concentrations among pools ($p < 0.001$).

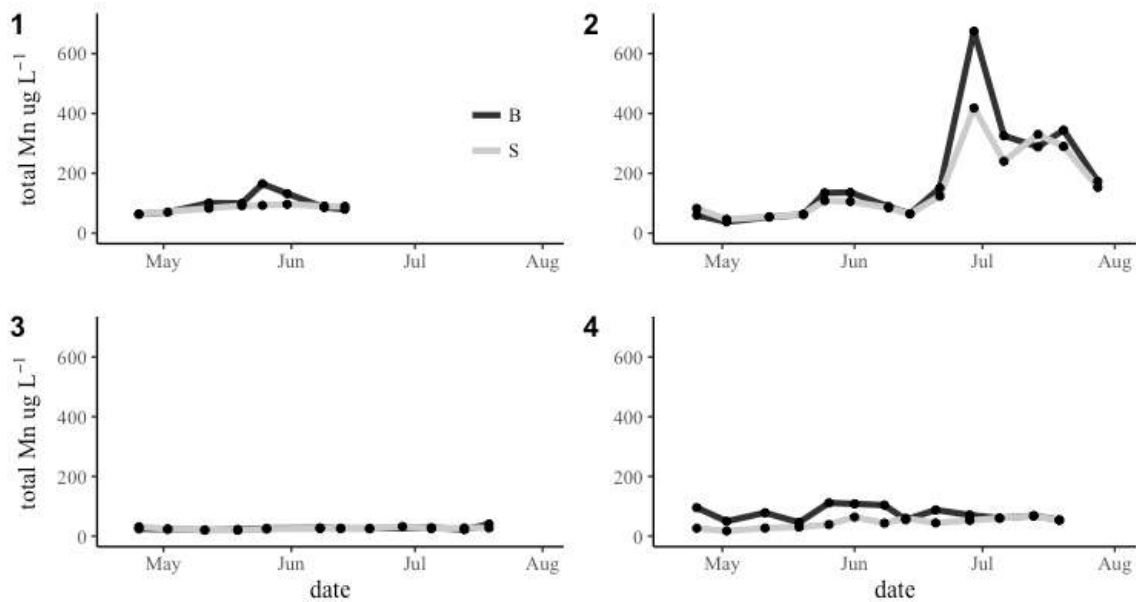


Figure B.2.22. Concentrations of total Mn in four vernal pools. Samples collected from April to August 2016.

The concentrations of organically bound Mn ranged from 0 to 18 $\mu\text{g L}^{-1}$, with an overall average of $2 \pm 3 \mu\text{g L}^{-1}$. Organically bound Mn ranged from 0 to 2 $\mu\text{g L}^{-1}$ in P1, from 0 to 18 $\mu\text{g L}^{-1}$ in P2, from 0 to 1 $\mu\text{g L}^{-1}$ in P3, and from 0 to 3 $\mu\text{g L}^{-1}$ in P4. There was a significant increasing relationship between organically bound Mn concentrations and time ($R^2 = 0.38, p < 0.001$). There were significant differences in organically bound Mn concentrations among pools ($p < 0.001$).

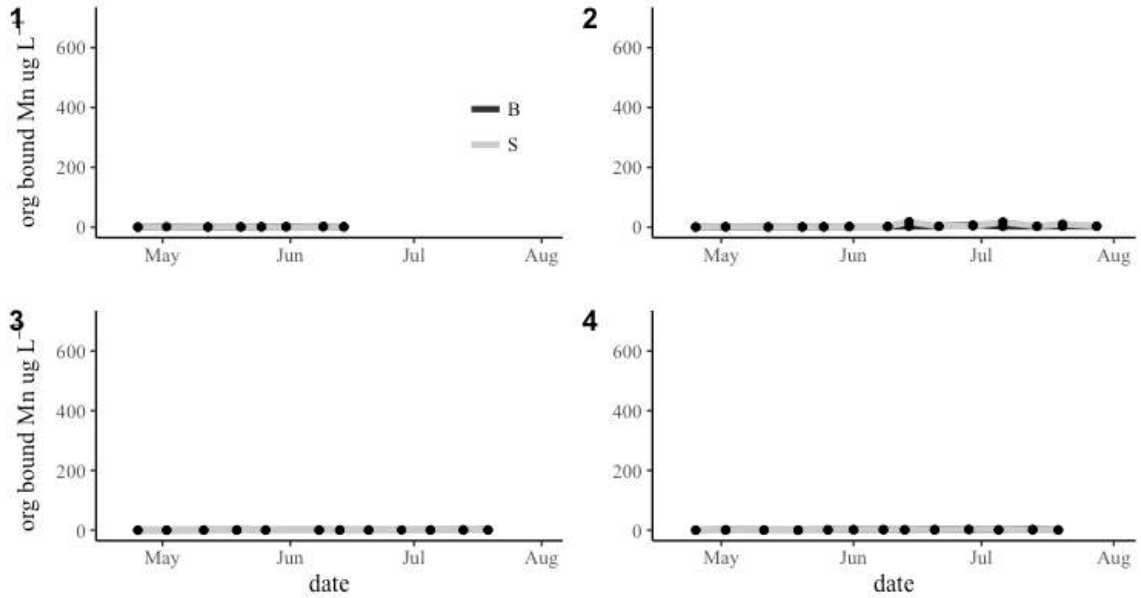


Figure B.2.23. Concentrations of organically bound Mn in four vernal pools. Samples collected from April to August 2016.

The concentrations of ionic Mn ranged from 16 to 651 $\mu\text{g L}^{-1}$, with an overall average of $85 \pm 94 \mu\text{g L}^{-1}$. Ionic Mn concentrations ranged from 53 to 157 $\mu\text{g L}^{-1}$ in P1, from 35 to 651 $\mu\text{g L}^{-1}$ in P2, from 17 to 31 $\mu\text{g L}^{-1}$ in P3, and from 16 to 101 $\mu\text{g L}^{-1}$ in P4. There was a significant increasing relationship between ionic Mn concentrations and time ($R^2 = 0.09, p < 0.01$). There were significant differences in ionic Mn concentrations among pools ($p < 0.001$).

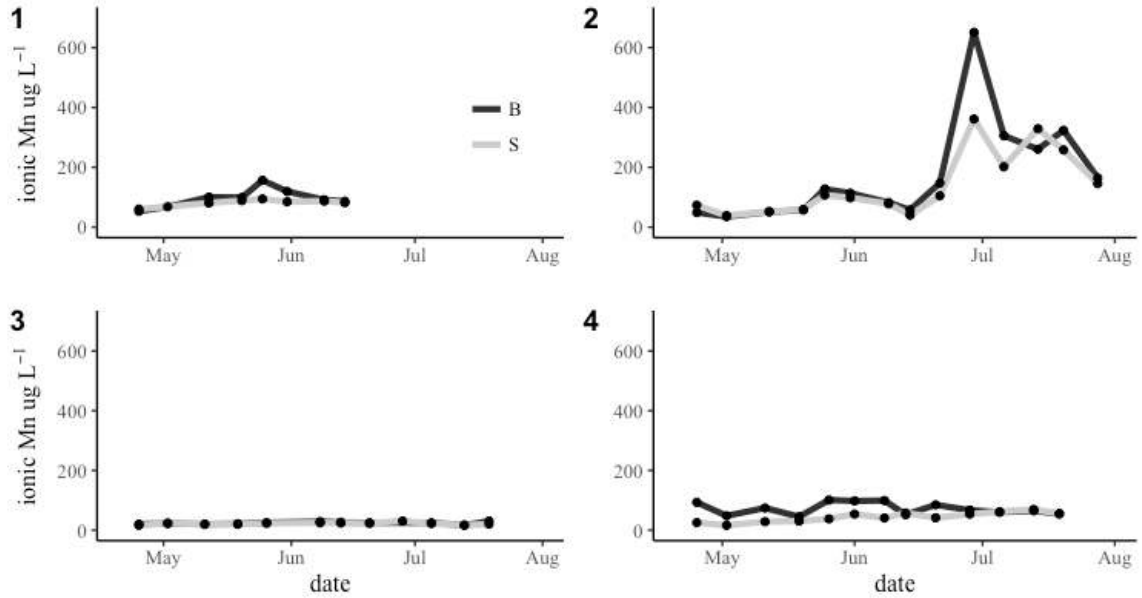


Figure B.2.24. Concentrations of ionic in four vernal pools. Samples collected from April to August 2016.

B2.2.9.4. Silicon

The concentrations of total silicon (Si) ranged from 63 to 5207 $\mu\text{g L}^{-1}$, with an overall average of $2173 \pm 1285 \mu\text{g L}^{-1}$. Concentrations of total Si ranged from 2402 to 4707 $\mu\text{g L}^{-1}$ in P1, from 63 to 1701 $\mu\text{g L}^{-1}$ in P2, from 1467 to 3945 $\mu\text{g L}^{-1}$ in P3, and from 2027 to 5207 $\mu\text{g L}^{-1}$ in P4. There was no significant relationship between total Si and time. There were significant differences in total Si among pools ($p < 0.001$).

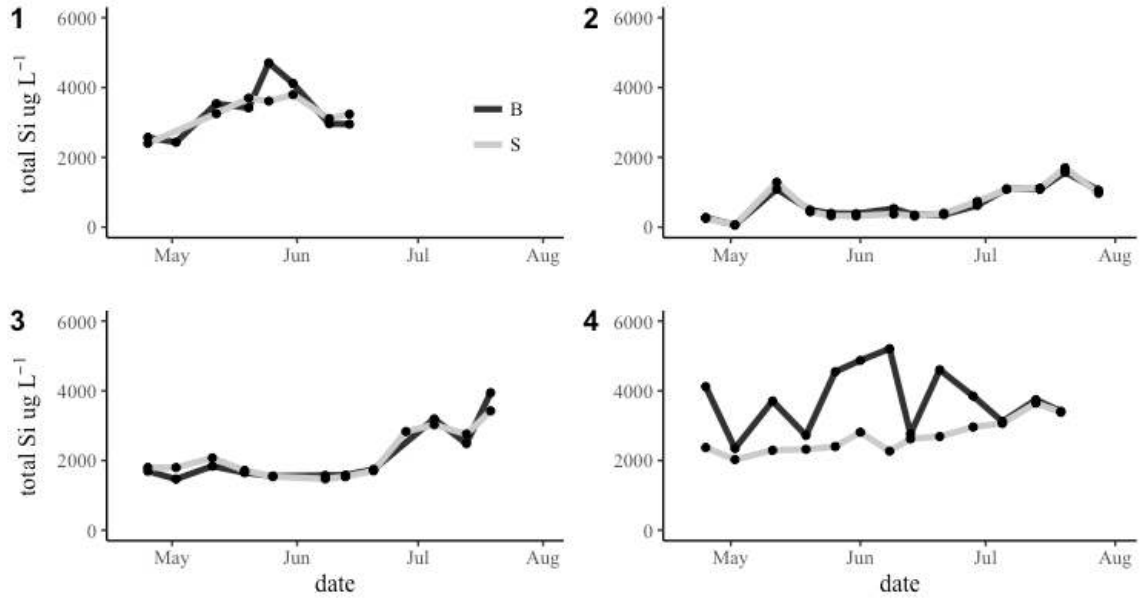


Figure B.2.25. Concentrations of total Si in four vernal pools. Samples collected from April to August 2016.

The concentrations of organically bound Si ranged from 45 to 4537 $\mu\text{g L}^{-1}$, with an overall average of $2017 \pm 1191 \mu\text{g L}^{-1}$. Organically bound Si concentrations ranged from 2203 to 3953 $\mu\text{g L}^{-1}$ in P1, from 45 to 1441 $\mu\text{g L}^{-1}$ in P2, from 1250 to 3730 $\mu\text{g L}^{-1}$ in P3, and from 2002 to 4537 $\mu\text{g L}^{-1}$ in P4. There was no significant relationship between organically bound Si and time. There were significant differences in concentrations of organically bound Si among pools ($p < 0.001$).

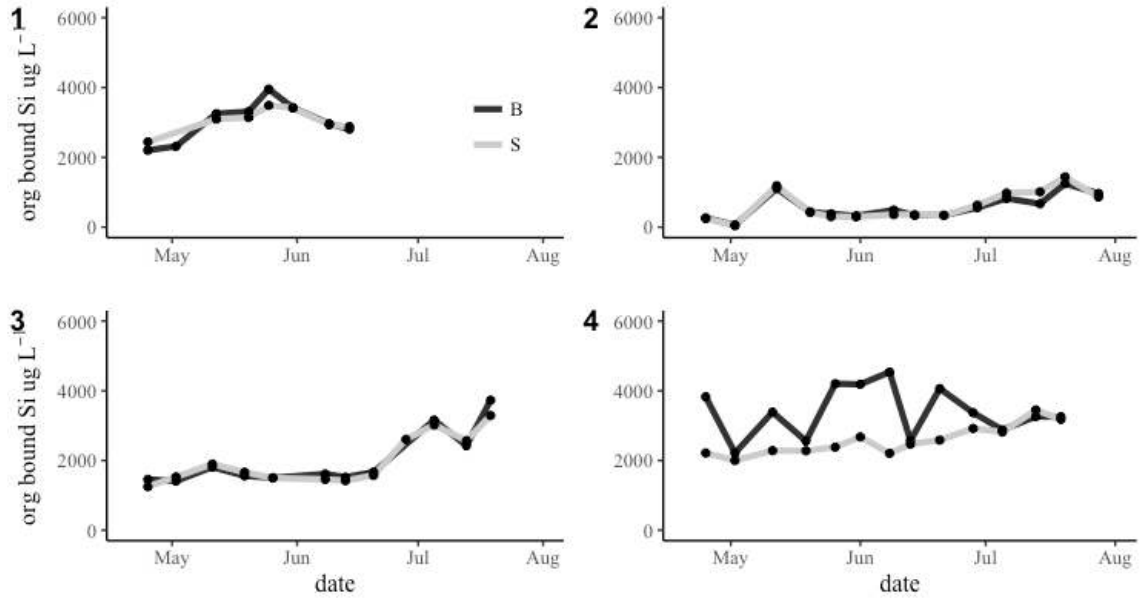


Figure B.2.26. Concentrations of organically bound Si in four vernal pools. Samples collected from April to August 2016.

The ionic concentrations of Si ranged from 0 to $678 \mu\text{g L}^{-1}$, with an overall average of $149 \pm 157 \mu\text{g L}^{-1}$. Ionic Si concentrations ranged from 0 to $678 \mu\text{g L}^{-1}$ in P1, from 0 to $336 \mu\text{g L}^{-1}$ in P2, from 23 to $489 \mu\text{g L}^{-1}$ in P3, and from 0 to $543 \mu\text{g L}^{-1}$ in P4. There was a weak but significant increasing relationship between ionic Si and time ($R^2 = 0.07, p < 0.01$). There were significant differences in concentrations of ionic Si among pools ($p < 0.001$).

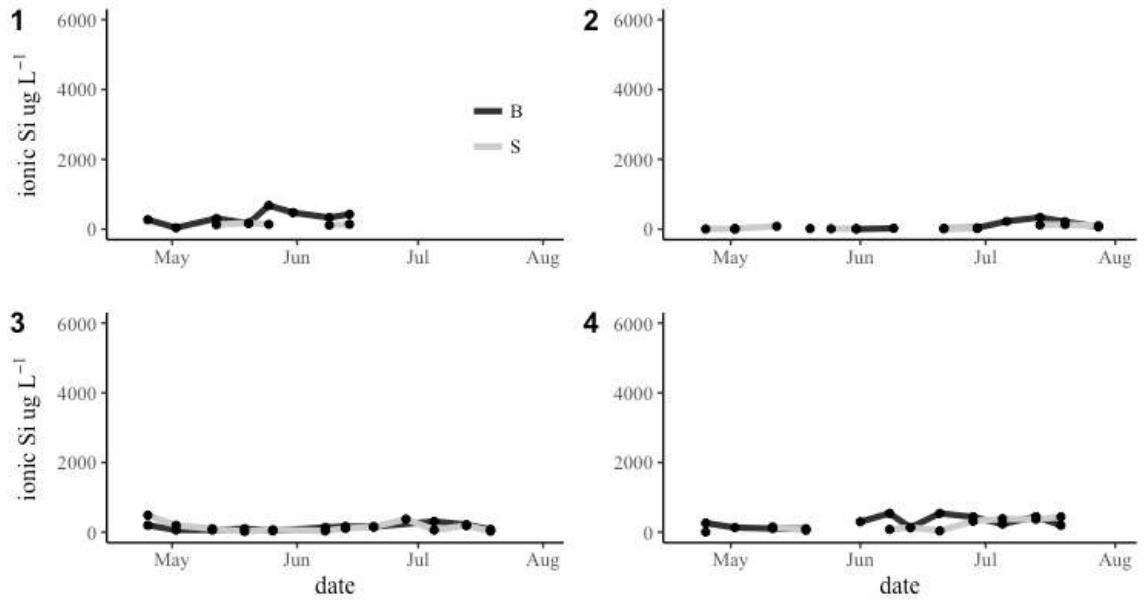


Figure B.2.27. Concentrations of ionic Si in four vernal pools. Samples collected from April to August 2016.

BIOGRAPHY OF THE AUTHOR

Lydia Kifner was born on September 1st, 1993. She was raised in Strafford, Vermont, and graduated from Thetford Academy in 2011. She attended the University of New Mexico and graduated in 2015 with a Bachelor of Science in Environmental Science. She returned to the northeast and entered the University of Maine's Civil and Environmental Engineering Department in 2015. Lydia is a candidate for the Master of Science degree in Civil Engineering from the University of Maine in December 2017.